



LUND UNIVERSITY

Linear Drum Boiler-Turbine Models

Eklund, Karl

1971

Document Version:

Publisher's PDF, also known as Version of record

[Link to publication](#)

Citation for published version (APA):

Eklund, K. (1971). *Linear Drum Boiler-Turbine Models*. [Doctoral Thesis (monograph), Department of Automatic Control]. Department of Automatic Control, Lund Institute of Technology (LTH).

Total number of authors:

1

General rights

Unless other specific re-use rights are stated the following general rights apply:

Copyright and moral rights for the publications made accessible in the public portal are retained by the authors and/or other copyright owners and it is a condition of accessing publications that users recognise and abide by the legal requirements associated with these rights.

- Users may download and print one copy of any publication from the public portal for the purpose of private study or research.
- You may not further distribute the material or use it for any profit-making activity or commercial gain
- You may freely distribute the URL identifying the publication in the public portal

Read more about Creative commons licenses: <https://creativecommons.org/licenses/>

Take down policy

If you believe that this document breaches copyright please contact us providing details, and we will remove access to the work immediately and investigate your claim.

LUND UNIVERSITY

PO Box 117
221 00 Lund
+46 46-222 00 00

REPORT 7117
NOVEMBER 1971

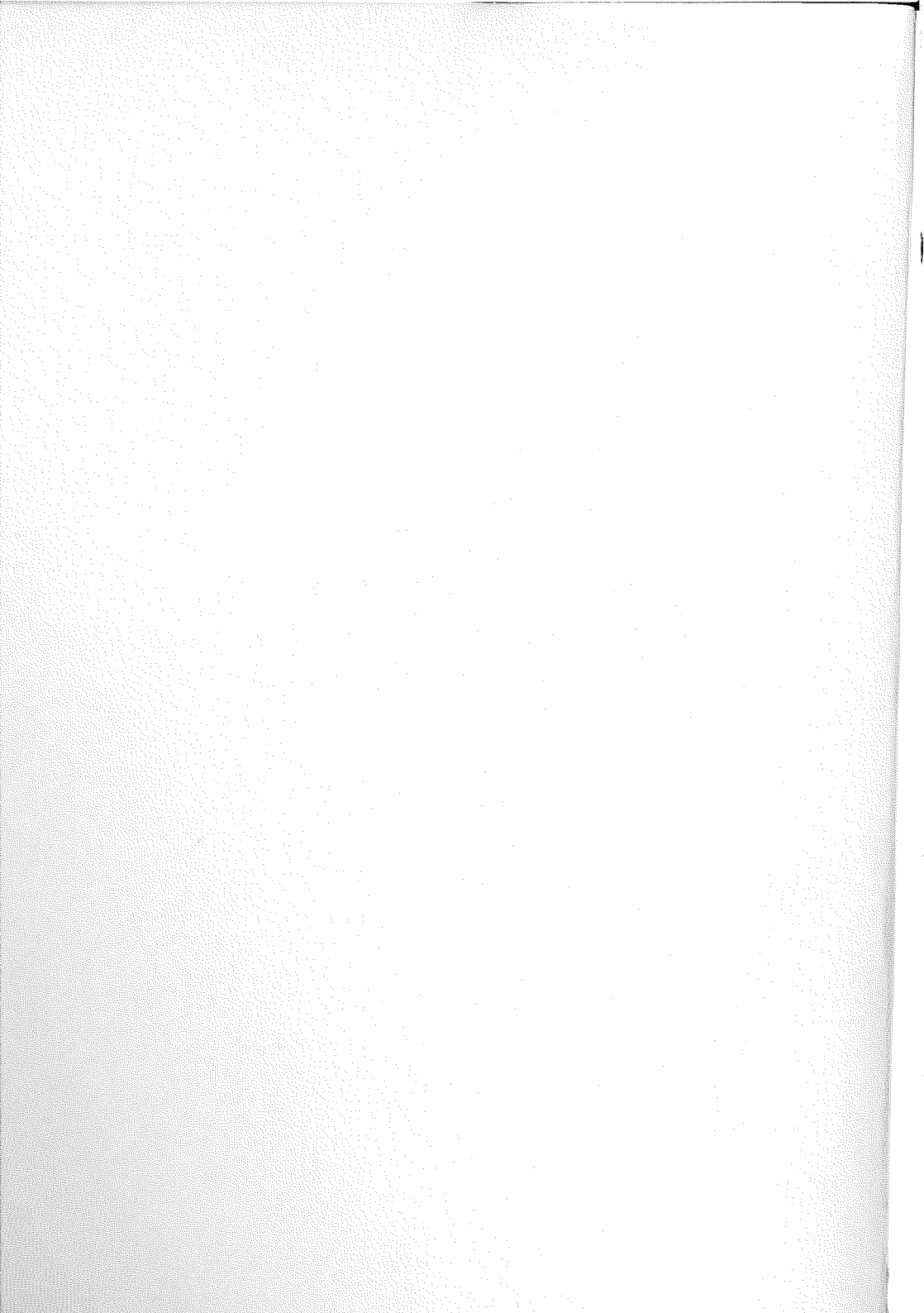
Linear drum boiler -turbine models

KARL EKLUND

TILLHÖR REFERENSBIBLIOTEKET

UTLÄNAS EJ

LTH



Karl Eklund

Linear Drum Boiler-Turbine Models

Lund 1971

Printed in Sweden
Studentlitteratur
Lund 1971

TABLE OF CONTENTS

CHAPTER 1 - INTRODUCTION 7

1. BACKGROUND 7
2. MODEL BUILDING 9
 - 2.1 Construction Data Models 10
3. CONTROL 10
4. CONTENT 11
5. ACKNOWLEDGEMENTS 13

CHAPTER 2 - NUMERICAL MODEL BUILDING 14

1. INTRODUCTION 14
2. A SYSTEMATIC MODEL REDUCTION TECHNIQUE 15
3. REDUCTION TO STATE SPACE FORM. A GENERAL APPROACH 17
 - 3.1 Pseudo-Inverse 17
 - 3.2 Main Result 20
 - 3.3 Check of Conditions 24
 - 3.4 Choice of State Variables 24
 - 3.5 Application to a Boiler Model 27
4. REDUCTION TO STATE SPACE FORM. AN ALTERNATIVE APPROACH 31

CHAPTER 3 - FIELD MEASUREMENTS 34

1. INTRODUCTION 34
2. POWER PLANT UNIT P16-G16 35
 - 2.1 Plant Configuration 35
 - 2.2 The Boiler 37
 - 2.3 The Turbines 38
 - 2.4 Control Equipment 39
3. MEASURING PROGRAM AND EQUIPMENT 40
 - 3.1 Experiments 40
 - 3.2 Measured Variables 41
 - 3.3 Measuring Devices 42
 - 3.4 Recording Equipment 42

- 4. CHARACTERISTICS OF MEASUREMENTS 43
 - 4.1 Choice of Sampling Rate 43
 - 4.2 Choice of Input Signal 44
 - 4.3 Experiment Conditions 49
- 5. RESULTS 49

CHAPTER 4 - CONSTRUCTION DATA MODELS 65

- 1. INTRODUCTION 65
- 2. MODEL PROGRAMME 68
 - 2.1 Model Main Programme 68
 - 2.2 Model Subroutines 70
- 3. DERIVATION OF EQUATIONS 70
 - 3.1 Drum System 71
 - 3.2 Superheater 87
 - 3.3 Attemperator 94
 - 3.4 Control Valve 96
 - 3.5 Turbine 97
- 4. COMPARISON OF DRUM SYSTEM MODELS 101
 - 4.1 Model Order 101
 - 4.2 Numerical Example 103
 - 4.3 Conclusions 109
- 5. APPLICATION TO ÖRESUNDSVERKET POWER PLANT 109
 - 5.1 Simplified Configuration 109
 - 5.2 Model Order 111
 - 5.3 Model Main Programme 112
 - 5.4 Input Data 113
 - 5.5 Complete Model 114

CHAPTER 5 - IDENTIFICATION OF DIFFERENCE EQUATION MODELS 118

- 1. INTRODUCTION 118
- 2. RESUMÉ OF THE MAXIMUM LIKELIHOOD METHOD 119
- 3. RESULTS OF IDENTIFICATION 122
 - 3.1 Drum Pressure 122
 - 3.2 Active Power 136
- 4. CONCLUSIONS 144

CHAPTER 6 - IDENTIFICATION OF STATE SPACE MODELS 147

- 1. INTRODUCTION 147
- 2. RESUMÉ OF THE IDENTIFICATION METHOD 148
- 3. RESULTS OF IDENTIFICATION 152

- 3.1 Closed Loop Models 153
- 3.2 Open Loop Models 162
- 3.3 Computational Aspects 164
- 4. CONCLUSIONS 167

CHAPTER 7 - EVALUATION OF MODEL FROM CONSTRUCTION
DATA 169

- 1. INTRODUCTION 169
- 2. COMPARISON TO FIELD MEASUREMENTS 170
 - 2.1 Fuel Flow Perturbations 170
 - 2.2 Feedwater Flow Perturbations 174
 - 2.3 Attemperator Flow Perturbations 174
 - 2.4 Control Valve Position Perturbations 178
- 3. COMPARISON TO RESULTS OF IDENTIFICATION 181
 - 3.1 Transfer Functions 182
 - 3.2 One-Step Ahead Prediction Errors 187
- 4. CONCLUSIONS AND RECOMMENDATIONS 189

REFERENCES 191

APPENDIX 196



CHAPTER 1 - INTRODUCTION

1. Background

The Swedish interest for the characteristics of thermal power plants has grown considerably during the last years. The reason is a change of the structure of the Swedish power system. Up till now power generation has been dominated by hydro-electric power plants. The installed power of these plants is roughly 80 percent of the total installed power in the current system. The major part of these plants are connected to the consumers by very long transmission lines. The majority of the thermal power plants are close to the consumers.

In the present system, the control of mains frequency and the net stabilization have been performed using the hydro-electric power plants. The thermal power plants have essentially been running at a scheduled constant load.

A drastic change of these conditions is predicted in the future [36], [37]. This is mainly due to the fact that nearly all available water power has now been utilized. The demand for power will however continue to increase and the installed power must be doubled roughly each ten years. Consequently, the dominating role of hydro-electric power plants in the power system will rapidly diminish.

In [36] the new operating conditions for different types of power plants are predicted. It is concluded that a number of thermal power plants must

- participate in control of mains frequency
- participate in control of net stability after failures, that is, large load changes
- make a large number of start up and shut down.

To be able to judge the possible contribution of thermal power plants to the first two items the dynamic properties of these plants must be known. Furthermore, possible control strategies should be studied and evaluated.

The changed operating conditions thus motivate the study of models valid for both small and large load changes. For small load changes it is usually

sufficient with linear models. Different models may however be required for different operating points. For large load changes, it is known that the dynamics of the boiler-turbine unit varies to such an extent, that nonlinear models must be used.

This work deals with dynamic models of thermal power plants with drum-type boilers, since the majority of existing and projected boilers in Sweden are of this type. The scope of the work is further limited to the problem of small disturbances that is, only linear models are considered. However, as a by-product of this study a simple nonlinear model for a drum-type boiler-turbine unit was developed [53]. This model is well suited for studies of large load changes.

The scope of this work thus is to derive linear models for a drum-type boiler-turbine unit. The models may be used for

- design of regulators for steady state control
- redesign of the process itself by improved knowledge of the dynamic properties
- further studies of nonlinear models

The boiler-turbine unit is a multi-variable system and as such an interesting application from a control point of view. Both the design of control strategies and process identification include principal difficulties. In this work only the problems associated with process identification are discussed.

A good model will also clearly indicate the limitations of the existing plants, from the point of view of the new operating requirements. It can thus be used to investigate the need for a redesign of the plant.

This work clearly shows that the linear models obtained are different for different stationary points. The knowledge of the physical parameters causing the major part of these differences may suggest the nonlinearities to be preserved in a nonlinear model.

There was the opportunity to perform a series of dynamical experiments on a large thermal power plant. The results are used to evaluate the theoretically derived models. Certainly such experiments also improve the general knowledge of the dynamics of the process.

2. Model Building

There are two different approaches to the modelbuilding problem

- physical equations
- process identification

In the sequel we will call models based on the first approach for construction data models. In this work, models based on both approaches are presented. Certainly both methods can be combined to improve either type of model.

The choice of method depends on several things e.g.

- the knowledge of the process
- the available results of identification experiments or the possibilities to do such experiments
- the purpose of the model

In the last item we have included the question of e.g. linear or nonlinear models and desired representation of the model.

The major advantages of construction data models are that, the model can be built before the real process, the influence of different physical parameters can be investigated and the model can have any form (linear-nonlinear, discrete or continuous time, ordinary or partial differential equations, time variant or time invariant, single input-single output or multivariable). Methods for process identification are well developed for multiple input-single output linear systems. In other cases it is usually necessary to have some a priori information to reduce the computational effort involved. For example, algorithms to identify parameters in a given multivariable or nonlinear structure are available. A comparison between the total effort for developing a model from physical equations and from measurements is, for complex processes, usually advantageous for the later type of models. Also process identification usually produces more accurate models since the parameters are adjusted to the plant under consideration. The models obtained by identification are however strictly limited to a particular plant and to the particular operating conditions under which they were obtained.

2.1 Construction Data Models

Often the dynamic model of a process can be regarded as an extension of a static model. Such models can often be supplied by the manufacturer and will ease the modelling task. Especially the gathering of construction data can be essentially reduced.

As mentioned earlier the building of a construction data model requires a good knowledge of the physical phenomena involved. Further, even if the physical phenomena are known, they might be very complex and the resulting model not feasible for e.g. control purposes. This creates the important problem of approximating process behaviour or process equations in a proper way. Consider for example a heat exchanger, which is described by partial differential equations but might, for most control purposes, be approximated by a low order set of ordinary differential equations. The approximating problem for this application is extensively discussed in Chapter 4.

The steady state control problem requires a linear model. A construction data model usually directly leads to a state space representation which is a useful form for further calculations. However, the amount of numerical calculations to establish the matrices A , B , C and D of the state space model $S(A, B, C, D)$ is very large. The natural way to handle this problem is to use a computer. The model will thus exist as a computer programme which as input has construction data from the process and as output has the matrices of $S(A, B, C, D)$. This, in a sense, makes the model independent of the process under consideration and increase the model applicability.

A severe problem, when modelling large and complex processes, is to decide if the final result is right or wrong. Using a computer, the entire task is divided into a number of smaller tasks, which can be programmed as subroutines and tested separately.

3. Control

The two major control tasks of a thermal power plant are

- steady state control
- control of large load changes

In this work none of these problems are studied. In control literature most papers have dealt with the steady state control problem. The essential difficulty of this problem is that the boiler-turbine unit represents a multivariable system. The disturbance on the system is the changing demand for power. This disturbance has been modelled, by process identification, by the author in [15], using data from the Swedish power system. The report also includes a multivariable regulator based on linear quadratic optimal control theory. The process considered is the drum system of the boiler. The process and regulator was simulated on a hybrid computer. Other authors e.g. [2], [35] have reported similar and more complete studies. The results obtained indicate that there are no great problems associated with such an approach to multivariable control of thermal power plants. However, none of the authors presents any results from implementation on the real process.

The control of large changes which usually leads to an optimization problem has not been treated in literature as extensively as the steady state control problem. The reason is probably that the modelling appears more difficult. The simple nonlinear model in [53] may represent a first step to overcome this problem.

4. Content

A systematic approach to the numerical modelbuilding problem is outlined in Chapter 2. A straight-forward linearization of the physical equations does not directly give a state model on standard form. Instead a model of the following form is obtained

$$E \frac{dv}{dt} + Fv + Gu = 0 \quad (1.1)$$

$$Py + Qv + Ru = 0$$

where the vectors u and y are the input and output vectors respectively, vector v contains all other variables introduced and E , F , G , P , Q and R are matrices of proper order. It is then a crucial problem to assign a minimal number of state variables to eq. (1.1) and reduce this equation to state space form. This problem is solved both in a general case and in a special case. Both methods are applied to boiler models in this work.

All significant facts about the measurements and the Öresundsverket power plant, which is used as an application, are accounted for in Chapter 3. Since the experiments were designed for identification, the choice of input sequences, sampling rate etc are also discussed. Experiments were made at two different load levels, 90 % and 50 % of full load respectively and the perturbed inputs were fuel flow, feedwater flow, control valve position, and two attemperator flows. This gives ten different experiments and a selection of recorded variables is shown at the end of Chapter 3.

In Chapter 4 all model equations are derived. Both the assumptions and the equations are presented in detail. The model for the drum system is especially treated and one section deals with the comparison of such models of different order. A 5th order model is found to be best suited. Data from Öresundsverket power plant is used to derive numerical results. Models of 9th and 15th order are discussed. The approach taken in this section is similar to earlier works. However, the systematic approach taken to the drum system model and the general effort to keep model order low, give a model of essentially lower order than others presented. The model has the form of a computer programme built on subroutines, which generate the models for power plant components such as drum system, superheater and turbines. In Appendix A the drum system subroutine is listed as an example.

Chapters 5 and 6 deal both with models from measurements. The maximum likelihood method is used throughout. In Chapter 5, single input - single output linear difference equation models are identified. The considered input-output relations are those connecting fuel flow and control valve position to the outputs, drum pressure and active power. Models at both load levels are computed and compared. The results show that low order models are obtained and that there is a significant difference between the models obtained at half load and those obtained at full load. The boiler has marked nonlinear characteristics. In Chapter 6 the theoretically derived multivariable model is improved using the measurements. A number of parameters of the A and B matrices of the state space form is estimated.

The representation is not canonical and we have the problem of identifiability. In this case it is found that the model

$$x(t + 1) = \Phi x(t) + \Gamma u(t) + K \epsilon(t) \quad (1.2a)$$

$$y(t) = Cx(t) + Du(t) + \epsilon(t) \quad (1.2b)$$

where $\hat{\Theta}$ and $\hat{\Gamma}$ are the sampled model A and B matrices and the matrix K can be interpreted as the Kalman filter gains, yields essentially better results than a model of type (1.2) but not including the third term on the right hand side of eq. (1.2 a). However, compared to the initial construction data model, an improvement is achieved in all cases. To the best of authors knowledge this type of measurements and identification has not been reported earlier.

The last chapter is concerned with the evaluation of the construction data model. The evaluation is based on a comparison of recorded and simulated responses. Further, the models obtained in Chapter 5 are compared to those calculated from the construction data model. The one-step ahead prediction errors for all models are also given and discussed. From this material we establish the validity of the assumptions and approximations used to derive the construction model. Even if this evaluation is based only on one application to the model programme, a significant amount of general conclusions may be drawn and a set of initial approximations recommended.

5. Acknowledgements

This work has been supported by the Swedish board for Technical Development under Contract no. 70-337-U270.

The work has been supervised by Prof K J Åström to whom the author wish to express his gratitude for invaluable help and guidance throughout this work.

A significant part of the results presented here is based on the experiments on Öresundsverket power plant. The experiments were made in cooperation with Sydsvenska Kraft AB. The author wish to thank this company, the staff of Öresundsverket power plant and especially Civ ing B Ahlman who was responsible for the plant during the experiment but never hesitated to remove the regulators.

The author has experienced the team work at the Division for Automatic Control as very valuable. Tekn lic I Gustavson has let me share some of his knowledge of identification of industrial data. Tekn lic Per Hagander and Tekn lic K Mårtenson has read the manuscript and contributed by valuable comments. Civ ing Lars-Erik Ohlson run part of the identification programs. The first manuscript was typed by Mrs. Gudrun Christensen and the drawings were made by Miss Marianne Steinertz, Mrs. Carina Bolinder and Mr Bengt Lander.

1. Introduction

It is very tedious to establish a linearized mathematical model of an industrial process of some complexity. Even if basic physical laws are applicable it can be extremely laborious to compute the steady-state values and to linearize the equations. In particular we must take into account that it is often highly desirable to develop linearized models for different operating conditions and to investigate the sensitivity of the model to physical parameters. It is also very difficult to check the linearized equations even if the basic equations themselves are often quite easy to check.

It thus seems attractive to develop an algorithm which enables a digital computer to perform all the tedious work. Such an algorithm is proposed in this chapter. We start with the basic non-linear equations and proceed to compute steady-state values and linearize. The final result is a system description in state space form. The state space form is convenient because a large amount of control theory uses this representation of the system as a starting point and since important physical variables can be retained as state variables in the final model. The procedure is based on well-known methods for solving non-linear equations and numerical differentiation. One crucial difficulty is to assign the smallest number of state variables to the linearized model. A method for solving this problem is the main result of this chapter. It has been published in [16].

The procedure is outlined in Section 2. The main result is given in Section 3 as a theorem. The assignment of state variables is not unique. It is discussed how this non-uniqueness can be exploited to choose state variables which are physically significant. Section 3 also contains an application to a boiler drum system model. In Section 4 an alternative approach to the reduction problem is given. The problem considered is a special case of that stated and solved in Section 3 but the computational effort involved is less.

2. A systematic model reduction technique

To establish a mathematical model of an industrial process it is often convenient to divide the process into a number of components. These components are treated separately. A set of equations which describes the dynamic and static relations between the inputs and outputs for each component is derived. The components are coupled through a number of internal variables which might be of secondary interest. This technique simplifies the derivation of the basic equations but introduces a number of auxiliary variables, see e.g. [30]. The resulting mathematical model is usually a set of non-linear equations which includes both ordinary and partial differential equations. Partial differential equations are approximated by finite differences in the space coordinates. We also assume that the system has constant coefficients. The system behaviour for small disturbances around an equilibrium state is often of great interest. This behaviour might be described by the linearized system equations. Thus, if we require the resulting model to be a set of linear ordinary differential equations, the following systematic approach is proposed.

The process is described by basic physical laws such as the laws of conservation of mass, energy and momentum. Let the resulting set of equations be

$$f(\dot{v}, v, u) = 0 \quad (2.1a)$$

$$g(y, v, u) = 0 \quad (2.1b)$$

where f is an ℓ vector whose components are non-linear functions of the variables v_i , their time derivatives and the process input variables u_i ; g is a k vector whose components are non-linear functions of the variables v_i , u_i and the process output variables y_i . The input vector u and the output vector y are identified and treated separately already at this stage. All other variables are included in v . The set of equations is consistent if the number of variables v_i equals ℓ and if y is a k vector. We can always assume that the vector f does not depend on du/dt because we can then introduce a new input variable $u^{*i} = du/dt$.

The steady-state values are obtained if we put time derivatives equal to zero in eq. (2.1), viz.

$$f(0, v, u) = 0 \quad (2.2a)$$

$$g(y, v, u) = 0 \quad (2.2b)$$

Given the steady-state values u^0 of u , eqs. (2.2a) and (2.2b) determine the steady-state values v^0 and y^0 of v and y respectively. The zero solutions of the non-linear eq. (2.2) are obtained by standard techniques, e.g. a Newton-Raphson method or as given in [39].

Linearize eq. (2.1). We get

$$E\dot{v} + Fv + Gu = 0 \quad (2.3a)$$

$$Py + Qv + Ru = 0 \quad (2.3b)$$

where

$$\begin{aligned} E &= f_v(0, v^0, u^0) && \{l \times l\}, \\ F &= f_v(0, v^0, u^0) && \{l \times l\}, \\ G &= f_u(0, v^0, u^0) && \{l \times l\}, \\ P &= g_y(y^0, v^0, u^0) && \{k \times k\}, \\ Q &= g_v(y^0, v^0, u^0) && \{k \times l\}, \\ R &= g_u(y^0, v^0, u^0) && \{k \times m\}. \end{aligned}$$

To avoid new symbols the perturbed variables, that is the differences $v - v^0$, $y - y^0$ and $u - u^0$, are denoted as the variables themselves. The matrices of first partial derivatives of the vectors f and g with respect to \dot{v} , v and u and y , v and u respectively are obtained by numerical differences.

The linearized set of eqs. (2.3) is reduced to state space form $S(A, B, C, D)$

$$\begin{aligned} \frac{dx}{dt} &= Ax + Bu, \\ y &= Cx + Du, \end{aligned} \quad (2.4)$$

where x is the state n vector, u is the input m vector and y is the output k vector, A , B , C and D are matrices of proper order.

The problem of reducing eqs. (2.3) to state space form is to find the smallest possible number of state variables and to assign these to the model. A method which solves this problem is the main result of the paper and is presented in the following section.

If the transfer function representations are needed, these are easily obtained from eq. (2.4) using standard methods, see e.g., [49].

3. Reduction to state space form. A general approach

Since the proof of the theorem given below requires knowledge of the concept of pseudo-inverses some relevant properties are given as an introduction.

A detailed presentation of the pseudo-inverse and its properties can be found in e.g. [13].

3.1 Pseudo-Inverse

Every matrix $A^{\{m \times r\}}$ of rank $n > 0$ has a rank factorization of the form

$$A^{\{m \times r\}} = B^{\{m \times n\}} C^{\{n \times r\}} \quad (3.1)$$

where both B and C have rank n. The pair of matrices B and C are not unique. The requirements are that the columns of B form a basis for the column space generated by the columns of A. C is then chosen to satisfy (3.1). The pseudo-inverse of A is now defined as

$$A^+ = C^T (CC^T)^{-1} (B^T B)^{-1} B^T \quad (3.2)$$

Some of the properties are

- (1) For any matrix A there always exists a unique pseudo-inverse.
- (2) The rank of A^+ equals the rank of A.
- (3) If A is quadratic and non-singular $A^+ = A^{-1}$.
- (4) $(A^+)^+ = A$
- (5) $AA^+A = A$ and $A^+AA^+ = A^+$.
- (6) $(AA^+)^2 = AA^+$ and $(A^+A)^2 = A^+A$, that is AA^+ and A^+A are projections.
- (7) AA^+ and A^+A are symmetric matrices.

Further we have

$$B^+ = (B^T B)^{-1} B^T$$

$$C^+ = C^T (C C^T)^{-1}$$

where B and C are the same matrices as in (3.1).

We will also use the following rank properties of the pseudo-inverse. Let T be an $m \times n$ matrix, where n is the rank of T and $m \geq n$

Lemma 1

The rank of the matrix TT^+ is n .

Proof

The rank of T and T^+ equals n . We have according to (5) above

$$(TT^+)T = T$$

Then

$$\rho(T) = n \leq \min\{\rho(TT^+), \rho(T)\}$$

where $\rho(T)$ denotes the rank of T . We also have

$$\rho(TT^+) \leq \min\{\rho(T), \rho(T^+)\}$$

Thus

$$\rho(TT^+) = n$$

□

Lemma 2

The rank of the matrix $(I - TT^+)$ is $m - n$.

Proof

We have

$$\rho\{(I-TT^+) + TT^+\} \leq \rho(I-TT^+) + \rho(TT^+)$$

or

$$\rho(I-TT^+) \geq \rho(I) - \rho(TT^+) = m - n$$

and

$$(I-TT^+)T = 0$$

The last equation implies that the dimensions of the range space of $(I-TT^+)$ is less than or equal to $m-n$. Thus

$$\rho(I-TT^+) = m - n \quad \square$$

Introduce the notations $R(T)$ and $N(T)$ which stand for the range space and the null space of the matrix T respectively. Then we also have

Lemma 3

The range space of T equals the null space of $(I-TT^+)$.

Proof

We have

$$(I-TT^+)T = 0$$

Hence

$$t_i \in N(I-TT^+), \quad i = 1, \dots, n, \quad (3.3)$$

where t_i is the i :th column vector of T . According to Lemma 2 we have

$$\rho(I-TT^+) = m - n$$

The dimension of the null space of $(I-TT^+)$ is then n . The vectors t_i ($i = 1, \dots, n$) are linearly independent and span the range space of T . Thus

$$R(T) = N(I-TT^+) \quad \square$$

3.2 Main Result

Before stating the theorem it is convenient to consider the structure of eq. (2.3). It is clear that the number of state variables in a minimal representation can at most equal the rank of E. If the rank of E equals ℓ the number of state variables is ℓ and eq. (2.3a) can be solved directly using the inverse of E. The reduction to standard form is, in this case, trivial. However, in general the rank of E is less than ℓ and greater than zero. This is a consequence of two facts. Static equations in the variables v_i and u_i create rows of zeros in E. The number of time derivatives introduced might exceed the rank of E. That is we have additional static equations in the variables v_i and u_i which are not quite apparent.

If the inverse of P in eq. (2.3b) does not exist, one or several of the outputs are a linear combination of the others. The linearly dependent outputs may be excluded by computation of the linearly independent rows of P. However, physical insight usually permits us to avoid this problem and there is no loss of generality to assume that the inverse of P exists.

Theorem 1

Given a linear dynamic system with constant coefficients described by

$$E\dot{v}(t) + Fv(t) + Gu(t) = 0 \quad (3.4a)$$

$$Py(t) + Qv(t) + Ru(t) = 0 \quad (3.4b)$$

where $v(t)$ is an ℓ vector, $u(t)$ is an m vector, $y(t)$ is a k vector and E, F, G, P, Q, R are matrices of proper order. Assume that the rank of E is n , $0 < n \leq \ell$. Let a rank factorization of E be

$$E \begin{Bmatrix} \ell \times \ell \end{Bmatrix} = K \begin{Bmatrix} \ell \times n \end{Bmatrix} L \begin{Bmatrix} n \times \ell \end{Bmatrix} \quad (3.5)$$

where the matrices K and L both have rank n . If

$$(i) \rho\{(I - KK^+)F\} = \ell - n$$

$$(ii) R\{(I - KK^+)F\} \cap R(L) = 0$$

then the state space form of the linear system (3.4) is

$$\left. \begin{aligned} \dot{\mathbf{x}}(t) &= \mathbf{A}\mathbf{x}(t) + \mathbf{B}u(t) \\ y(t) &= \mathbf{C}\mathbf{x}(t) + \mathbf{D}u(t) \end{aligned} \right\} \quad (3.6)$$

where the state n vector is

$$\mathbf{x}(t) = \mathbf{L}v(t)$$

and

$$\begin{aligned} \mathbf{A} &= -\mathbf{K}^+ \mathbf{F} \left\{ \mathbf{L}^T \mathbf{L} + \mathbf{F}^T (\mathbf{I} - \mathbf{K}\mathbf{K}^+) \mathbf{F} \right\}^{-1} \mathbf{L}^T \\ \mathbf{B} &= \mathbf{K}^+ \left[\mathbf{F} \left\{ \mathbf{L}^T \mathbf{L} + \mathbf{F}^T (\mathbf{I} - \mathbf{K}\mathbf{K}^+) \mathbf{F} \right\}^{-1} \mathbf{F}^T (\mathbf{I} - \mathbf{K}\mathbf{K}^+) - \mathbf{I} \right] \mathbf{G} \\ \mathbf{C} &= -\mathbf{P}^{-1} \mathbf{Q} \left\{ \mathbf{L}^T \mathbf{L} + \mathbf{F}^T (\mathbf{I} - \mathbf{K}\mathbf{K}^+) \mathbf{F} \right\}^{-1} \mathbf{L}^T \\ \mathbf{D} &= \mathbf{P}^{-1} \left[\mathbf{Q} \left\{ \mathbf{L}^T \mathbf{L} + \mathbf{F}^T (\mathbf{I} - \mathbf{K}\mathbf{K}^+) \mathbf{F} \right\}^{-1} \mathbf{F}^T (\mathbf{I} - \mathbf{K}\mathbf{K}^+) \mathbf{G} - \mathbf{R} \right] \end{aligned}$$

Proof

It is sufficient to prove that there exists a unique solution to eq. (3.4) and that this solution is given by eq. (3.6).

The proof consists of three steps. First eq. (3.4a) is formally rewritten, as two equations, one representing the dynamic relations and the other the static relations of eq. (3.4a). This manipulations also give an equation relating v to x and u . Second it is shown that there exists a solution to eq. (3.4a) and finally that this solution is unique.

Combining eqs. (3.4a) and (3.5) we get

$$\mathbf{K}\mathbf{L}\dot{v} + \mathbf{F}v + \mathbf{G}u = 0 \quad (3.7)$$

Introduce the n vector x defined by

$$\mathbf{x} = \mathbf{L}v \quad (3.8)$$

Eqs. (3.7) and (3.8) then give

$$\mathbf{K}\dot{\mathbf{x}} = -(\mathbf{F}v + \mathbf{G}u) \quad (3.9)$$

We will thus show that the dynamic relations of the original eq. (3.4a) can be represented by a differential equation for x . There exists a solution to eq. (3.9) if

$$Fv + Gu \in R(K) \quad (3.10)$$

Using Lemma 3, eq. (3.10) can be replaced with

$$Fv + Gu \in N(I - KK^+) \quad (3.11)$$

where

$$K^+ = (K^T K)^{-1} K^T$$

By definition eq. (3.11) is equivalent to

$$(I - KK^+)(Fv + Gu) = 0 \quad (3.12)$$

or

$$(I - KK^+)Fv = - (I - KK^+)Gu \quad (3.13)$$

The solution of eq. (3.13) gives the static equation in the vectors u and v . If condition (i) holds then

$$R(I - KK^+) = R\{(I - KK^+)F\} \quad (3.14)$$

Hence

$$(I - KK^+)Gu \in R\{(I - KK^+)F\} \quad (3.15)$$

and eq. (3.13) has a solution for every given u . Then a solution of eq. (3.9) exists.

Rewriting eqs. (3.8) and (3.13) as

$$\begin{pmatrix} L \\ (I - KK^+)F \end{pmatrix} v = \begin{pmatrix} x \\ - (I - KK^+)Gu \end{pmatrix} \quad (3.16)$$

or

$$Tv = z \quad (3.17)$$

A solution to eq. (3.16) exists since the vector z belongs to the range space of T according to eq. (3.15). If condition (ii) holds then

$$\rho(T) = \ell \quad (3.18)$$

and the solution is unique. Eq. (3.16) thus relates the vector v to the vectors x and u .

Solving (3.16) using the pseudo-inverse of T and the fact that $(I-KK^+)$ is a symmetric projection we get.

$$v = T_1 x + T_2 u \quad (3.19)$$

where

$$T_1 = \{L^T L + F^T (I-KK^+) F\}^{-1} L^T$$

$$T_2 = \{L^T L + F^T (I-KK^+) F\}^{-1} F^T (I-KK^+) G$$

Combining eqs. (3.9) and (3.19) we get

$$\dot{x}(t) = -K^+ F T_1 x(t) - (K^+ F T_2 + K^+ G) u(t) \quad (3.20)$$

This differential equation has a unique solution for every given initial condition $x(t_0)$ and input $u(t)$.

Now the existence of a solution to (3.4a) for every initial condition $v(t_0)$ and every input $u(t)$ in the interval $[t_0, t_1]$ follows from the fact that, the solution to eq. (3.20), with the initial condition $x(t_0) = L v(t_0)$, in the interval $[t_0, t_1]$ satisfy eq. (3.4a). This follows from the construction of eq. (3.20) and is proved by substituting eqs. (3.19) and (3.20) into the original differential equation and using eq. (3.13). Notice that both conditions of the theorem are necessary since they guarantee the existence of a solution to eq. (3.13) and the existence of a unique solution to (3.16).

The uniqueness of a solution to (3.4a) follows from eq. (3.16) since, for every given vector $v(t)$ and input $u(t)$, which satisfy eq. (3.13), then eq. (3.16) uniquely determines the vector $x(t)$. Again this requires both conditions of the theorem.

It is thus proved that there exists a unique solution to eq. (3.4a) and that this solution is given by eq. (3.20). All static equations in the variables v_i and u_i are given by eq. (3.13). When eqs. (3.4b), (3.19) and (3.20) are combined, the state space form of the original set of equations is obtained and the theorem is proved. \square

Notice that the theorem only supplies a solution to the reduction problem when the number of state variables equals the rank of E .

3.3 Check of Conditions

An algorithm which performs the rank factorization of the matrix E is a necessary subroutine of the reduction programme. It is then convenient to formulate the conditions as rank conditions. Condition (i) is already in a suitable form. If condition (i) holds, condition (ii) is equivalent to that the rank of T equals ℓ . Hence

$$(i) \quad \rho\{(I - KK^+)F\} = \ell - n$$

$$(ii) \quad \rho(T) = \ell$$

where the matrix T is defined by eq. (3.17). The conditions should be checked in the listed order.

3.4 Choice of State Variables

The state variables are given by

$$x = Lv$$

The matrix L is not uniquely determined but L is chosen to satisfy

$$E = KL$$

where the column vectors of K form a basis for the vector space generated by the column vectors of E. In this subsection we will investigate if this non-uniqueness of L could be exploited to get a simple physical interpretation of the state variables.

The variables v_i often have a simple physical interpretation. It seems attractive then to retain these variables as state variables. Let E be arranged so that the n first columns of E are linearly independent. Assume that s is the largest number of variables v_i which can be retained as state variables, viz.

$$\begin{aligned} x_1 &= v_1, \\ x_2 &= v_2, \\ &\vdots \\ x_s &= v_s, \quad s \leq n \end{aligned}$$

The matrix L can then be partitioned as

$$L = \left[\begin{array}{c|c} L_{11} & L_{12} \\ \hline L_{21} & L_{22} \end{array} \right]$$

where

$$L_{11} = I \quad \{s \times s\}$$

$$L_{12} = 0 \quad \{s \times (\ell - s)\}$$

$$L_{21} \quad \{(n-s) \times s\}$$

$$L_{22} \quad \{(n-s) \times (\ell - s)\}$$

However, in general, the number s will equal zero. To show this let

$$E = [e_1 \ e_2 \ \dots \ e_n \ e_{n+1} \ \dots \ e_\ell]$$

where e_i is the i :th column vector of E . The vectors e_1, \dots, e_n are linearly independent and e_{n+1}, \dots, e_ℓ are linearly dependent. Let k_1, \dots, k_n be an arbitrary basis for the column space generated by e_1, \dots, e_n . Then the rank factorization of E may be written as

$$\begin{aligned} & [e_1 \dots e_n \ e_{n+1} \dots e_\ell] = \\ & = [k_1 \dots k_n] \left[\begin{array}{c|c} I & 0 \\ \hline L_{21} & L_{22} \end{array} \right] = \\ & = \left[\begin{array}{c|c} K_{11} & K_{12} \\ \hline K_{21} & K_{22} \end{array} \right] \left[\begin{array}{c|c} I & 0 \\ \hline L_{21} & L_{22} \end{array} \right] \end{aligned} \quad (3.22)$$

where the sub-matrices of the partitioned matrix K have the dimensions

$$K_{11} \quad \{s \times s\},$$

$$K_{12} \quad \{s \times (n-s)\},$$

$$K_{21} \quad \{(\ell-s) \times s\},$$

$$K_{22} \quad \{(\ell-s) \times (n-s)\}.$$

Evaluating eq. (3.22) we get

$$\begin{aligned}
 & [e_1 \dots e_s \quad e_{s+1} \dots e_n \quad e_{n+1} \dots e_\ell] = \\
 & = \begin{bmatrix} K_{11} + K_{12}L_{21} & | & K_{12}L_{22} \\ K_{21} + K_{22}L_{21} & | & K_{22}L_{22} \end{bmatrix}
 \end{aligned}$$

The identity above implies

$$[e_{s+1} \dots e_n \quad e_{n+1} \dots e_\ell] = [k_{s+1} \dots k_n] L_{22} \quad (3.23)$$

There might still be n linearly independent column vectors in the left-hand matrix in (3.23). The right-hand matrix has maximally $n-s$ linearly independent column vectors. Equation (3.23) thus gives $s = 0$. This means that there is, in general, no especially favourable choice of the state variables available.

A natural way to obtain a basis for the column space of E is to choose the linearly independent columns of E as a basis. The rank factorization of E then is

$$E = K \left[L_1 \quad \left| \quad L_2 \right. \right] \quad (3.24)$$

where

$$K = [e_1 \dots e_n],$$

$$L_1 = I \{n \times n\},$$

$$L_2 \quad \{n \times (\ell - n)\}.$$

The sub-matrix L_2 gives the coefficients of the expressions which constitute the $\ell - n$ linearly dependent column vectors e_{n+1}, \dots, e_ℓ of E . That is, if

$$e_{n+i} = \sum_{j=1}^n \lambda_{ji} e_j, \quad i = 1, 2, \dots, \ell - n$$

then

$$(\ell)_i = [\lambda_{1i} \dots \lambda_{ni}]^T, \quad i = 1, 2, \dots, \ell - n$$

where $(\ell_2)_i$ denotes the i :th column vector of L_2 . If only one of the vectors e_1, \dots, e_n , say e_1 , is needed to establish e_{n+1}, \dots, e_ℓ , then the choice (3.24) creates rows of zeros in the sub-matrix L_2 except in the row corresponding to e_1 . Considering that we have no especially favourable choice of state variables available it seems attractive to use the choice of (3.24).

Note that if the rank n of E equals the number ℓ of derivatives of variables v_i then L_2 will equal zero and we get

$$x_i = v_i, \quad i = 1, \dots, n$$

3.5 Application to a Boiler Drum System Model

In this sub-section we will give an application of the reduction procedure to a practical problem. We will consider the drum system (drum-down-comer-riser) of a drum boiler for a 150 MW power station unit. The drum pressure is 140 bar and the outlet steam temperature 530°C. The derivation of the basic non-linear equations, computation of steady-state values and linearization result in the matrices E, F, G, P, Q, R . The derivation of these results as well as a FORTRAN programme for the computations are documented in [17]. The complete output of the FORTRAN programme which computes the matrices of the state space form given the matrices E, F, G, P, Q, R is presented in Table 3.1. This table also includes some intermediate results. The matrix K^+K which should equal the unit matrix is used to check the accuracy of K^+ .

The components of the vector v correspond to the following physical quantities

$v =$	p_d	drum pressure
	y	drum liquid level
	T_w	drum liquid temperature
	T_r	riser tube temperature
	x_m	steam quality
	m_0	riser outlet flow
	m_w	downcomer flow
	m_e	evaporation flow
	Q_r	heat flow from the risers to the steam water mixture

MATRIX E

Table with 10 columns and 10 rows of numerical values, representing Matrix E.

MATRIX F

Table with 10 columns and 10 rows of numerical values, representing Matrix F.

MATRIX G

Table with 10 columns and 10 rows of numerical values, representing Matrix G.

MATRIX P

Table with 10 columns and 10 rows of numerical values, representing Matrix P.

MATRIX Q

Table with 10 columns and 10 rows of numerical values, representing Matrix Q.

MATRIX R

Table with 10 columns and 10 rows of numerical values, representing Matrix R.

THE RANK OF MATRIX E = 0

THE LINEAR INDEPENDENT ROWS OF E

1 2 8 0 5 6 7 0 0

THE LINEAR INDEPENDENT COLUMNS OF E

1 2 3 4 5 6 0 0 0

THE RESULT OF THE RANK FACTORIZATION E=KL

MATRIX K

Table with 10 columns and 10 rows of numerical values, representing Matrix K.

MATRIX L

Table with 10 columns and 10 rows of numerical values, representing Matrix L.

THE PSEUDOINVERSE OF K

Table with 10 columns and 10 rows of numerical values, representing the pseudoinverse of Matrix K.

MATRIX K(PSEUDO)*K SHOULD EQUAL THE UNIT MATRIX

Table with 10 columns and 10 rows of numerical values, representing the product of Matrix K and its pseudoinverse.

MATRIX (I-K*(PSEUDO))*F

4.756+008	7.000+000	-1.060-017	0.000+000	2.744+004	6.592+000	-3.240-018	1.767-017	-2.377-011
-1.771+001	6.000+000	6.066+000	0.000+000	0.000+000	0.000+000	0.000+000	0.000+000	0.000+000
7.323+005	9.000+000	-1.632-004	0.000+000	4.223+001	1.701+004	-4.996-005	2.719+004	-3.658-006
1.653+003	0.000+000	0.000+000	-3.305+003	0.000+000	0.000+000	0.000+000	0.000+000	0.000+000
7.000+000	0.000+000	0.000+000	7.000+000	0.000+000	0.000+000	0.000+000	0.000+000	0.000+000
9.956+020	0.600+000	-2.220-019	0.000+000	2.857+006	-1.703-011	2.104+011	-2.103-011	-4.975-023
-5.277+009	0.000+000	7.297+009	0.000+000	-1.870+005	-4.442+009	2.224+009	-1.202+008	1.621+012
-3.070+007	0.000+000	6.844+007	0.000+000	-1.771+003	-4.197+007	2.006+007	-1.141+006	1.534+010
3.416+001	0.000+000	-6.837-001	0.000+000	0.000+000	0.000+000	0.000+000	0.000+000	0.000+000

MATRIX (I-K*(PSEUDO))*G

0.000+000	2.879+008	-2.055-007
0.000+000	0.000+000	0.000+000
0.000+000	4.431+005	-3.162-004
0.000+000	0.000+000	0.000+000
0.000+000	0.000+000	0.000+000
0.000+000	-2.104+011	9.215+015
0.000+000	-1.965+009	1.401+008
0.000+000	-1.658+007	1.326+006
0.000+000	0.000+000	0.000+000

MATRIX L*I+L*(I-K*(PSEUDO))*F

2.731+006	-4.729+009	-2.117-001	-5.443+006	3.086+005	7.351+009	-3.693+004	3.418+001	1.653+003
-4.729+009	1.000+000	6.281+009	0.000+000	-2.573+012	0.000+000	0.000+000	0.000+000	0.000+000
-2.117+001	6.281+009	1.467+000	0.000+000	-7.403+005	-1.638+008	3.219+009	-6.837+001	5.969+012
-5.443+006	0.000+000	3.086+005	1.093+007	0.000+000	0.000+000	0.000+000	0.000+000	-1.305+003
3.086+005	-2.933+012	-6.883+005	0.000+000	1.178+000	4.222+005	-2.107+005	1.149+004	-1.545+008
7.351+009	0.000+000	-1.638+008	0.000+000	4.222+005	1.000+000	2.656+000	2.717+003	-3.660+012
-3.693+004	0.000+000	6.223+009	0.000+000	-2.107+005	2.656+000	7.054+000	-1.354+000	1.825+012
3.418+001	0.000+000	-6.937+001	0.000+000	1.149+004	2.717+000	-1.355+000	1.000+000	-9.947+012
1.653+003	0.000+000	5.969+012	-3.305+003	-1.545+008	-3.660+012	1.826+012	-9.947+012	1.000+000

MATRIX P(INVERSE)

1.000+000	0.000+000
0.000+000	1.600+000

SYSTEM MATRICES

MATRIX A

-3.061+002	-3.913+010	3.985+002	2.481+002	1.484+000	-1.078+004
-7.622+005	-7.654+013	-7.282+005	9.987+005	-4.978+001	-1.467+005
4.996+007	5.518+010	-1.004+001	1.144+003	-5.747+000	1.793+004
4.113+002	1.945+010	-9.056+012	-8.229+002	-5.180+009	-8.541+013
-1.506+005	-5.319+013	3.584+005	3.972+005	-5.311+002	-1.878+006
-1.337+001	-1.643+008	4.363+001	-2.473+000	1.872+004	-1.708+000

MATRIX B

0.000+000	1.422+003	-1.051+002
0.000+000	4.365+005	2.613+004
0.000+000	-9.989+003	2.994+003
2.488+005	6.663+013	2.336+012
0.000+000	-4.389+006	3.071+005
0.000+000	9.139+001	-6.469+000

MATRIX C

1.000+000	4.729+009	3.599+011	3.689+006	2.243+007	7.620+013
1.958+013	1.000+000	6.327+014	1.744+014	-6.960+014	8.611+020

MATRIX D

0.000+000	-1.736+011	-1.240+010
0.000+000	-2.065+019	-1.448+018

The input variables are

$$u = \begin{bmatrix} Q_g & \text{heat flow to risers} \\ m_{fw} & \text{feedwater flow} \\ m_s & \text{steam outlet flow} \end{bmatrix}$$

and the output variables are

$$y = \begin{bmatrix} p_d & \text{drum pressure} \\ y_1 & \text{drum liquid level} \end{bmatrix}$$

The two last columns of E equal zero. All other columns have non-zero elements. The column vectors 6 and 7 of E have non-zero elements only in the second row and consequently they are linearly dependent. The rank of E is at most 6 and the number of time derivatives of the variables v_i exceeds the rank of E. The time derivatives of the riser outlet flow and the downcomer flow which correspond to the non-zero elements in columns 6 and 7 arise from momentum equations for the riser and the downcomer.

Both conditions of Theorem 1 are satisfied in this case and the reduction is successful. The computed rank of E equals 6. Previously we found that the non-uniqueness of the rank factorization could not always be exploited for a favourable choice of the state variables. However, in special cases K could be chosen as the linearly independent columns of E and a simple form of L is obtained. This choice is used in the reduction programme. For the drum system K equals the first six columns of E. Using the pseudo-inverse of K the matrix L is computed to satisfy the equation $E = KL$. The state variables are given by the matrix L. We get

$$\begin{aligned} x_1 &= v_1, \\ x_2 &= v_2, \\ x_3 &= v_3, \\ x_4 &= v_4, \\ x_5 &= v_5, \\ x_6 &= v_6 + 2.656v_7, \end{aligned}$$

and the state variables have simple physical interpretation.

Equation (3.13) gives all static equations in the variables v_i and u_i .

A successful reduction requires $\rho\{(I-KK^+)F\} = \ell-n$. This rank equals 3 and consequently the number of static equations in the variables u_i and v_i is 3. These equations are given by the matrices $(I-KK^+)F$ and $(I-KK^+)G$ in Table 3.1. The original linearized equation contains two apparent static equations in the variables v_i and u_i which are found in the fourth and ninth rows of F and G . These equations are re-found in the fourth and ninth rows of $(I-KK^+)F$ and $(I-KK^+)G$. The third static equation is given by any of the rows 1, 3, 7, 8 of $(I-KK^+)F$ and $(I-KK^+)G$. These four rows are in pairs linearly dependent. The existence of the third static equation is a consequence of the fact that the number of time derivatives of the variables v_i exceeds the rank of E and primarily of the assumptions made when basic physical laws were applied to the process.

Inspecting the system matrices A , B , C and D we find that D equals zero and that the two outputs equal the first two state variables as expected.

Several elements of A and B also approximately equal zero. However, some caution must be observed when interpreting a number as small since the numerical value of the elements depend on the chosen units.

If the reduction is made manually it is indeed very tedious work. It is therefore believed that this algorithm represents a very attractive solution to the reduction problem.

4. Reduction to state space form. An alternative approach.

In the case when the number of state variables equals the number of derivatives of physical variables an alternative and simpler expression for the matrices of $S(A, B, C, D)$ can be derived. This method will be used frequently as a complement to the more elaborate method described in Section 3.

Rewriting eq. (3.4) as

$$E\dot{x}(t) + Fx(t) + Gu(t) + Hv(t) = 0 \quad (4.1a)$$

$$Py(t) + Qx(t) + Ru(t) + Sv(t) = 0 \quad (4.1b)$$

where the input and output vectors u and y are defined as before. All

physical variables which appear differentiated are included in the n-vector x and the remaining variables in the r-vector v . Coefficient matrices are constant. As before the inverse of P is assumed to exist. Stating the result as a theorem we get

Theorem 2

Consider a linear time invariant dynamical system given by eqs. (4.1). Define the order of the variables v_i in a way such that, if the rank of H equals r then the rank of H_2 equals r . Matrix H_2 is given by the partitioning of eq. (4.1a).

$$\begin{bmatrix} E_1 \\ \text{---} \\ E_2 \end{bmatrix} \dot{x}(t) + \begin{bmatrix} F_1 \\ \text{---} \\ F_2 \end{bmatrix} x(t) + \begin{bmatrix} G_1 \\ \text{---} \\ G_2 \end{bmatrix} u(t) + \begin{bmatrix} H_1 \\ \text{---} \\ H_2 \end{bmatrix} v(t) = 0 \quad (4.2)$$

where matrices indexed by 2 have r rows. If

(i) $\rho(H) = r$ and thus $\rho(H_2) = r$

(ii) $\rho(E_1 - H_1 H_2^{-1} E_2) = n$

then the state space form of eqs. (4.1) is

$$\dot{x}(t) = Ax(t) + Bu(t)$$

$$y(t) = Cx(t) + Du(t)$$

where

$$A = - (E_1 - H_1 H_2^{-1} E_2)^{-1} (F_1 - H_1 H_2^{-1} F_2)$$

$$B = - (E_1 - H_1 H_2^{-1} E_2)^{-1} (G_1 - H_1 H_2^{-1} G_2)$$

$$C = - P^{-1} \left\{ Q + S H_2^{-1} \left[E_2 (E_1 - H_1 H_2^{-1} E_2)^{-1} (F_1 - H_1 H_2^{-1} F_2) - F_2 \right] \right\}$$

$$D = - P^{-1} \left\{ R + S H_2^{-1} \left[E_2 (E_1 - H_1 H_2^{-1} E_2)^{-1} (G_1 - H_1 H_2^{-1} G_2) - G_2 \right] \right\}$$

Proof

Evaluate eq. (4.2)

$$E_1 \dot{x} + F_1 x + G_1 u + H_1 v = 0 \quad (4.3)$$

$$E_2 \dot{x} + F_2 x + G_2 u + H_2 v = 0 \quad (4.4)$$

If condition (i) holds then eq (4.4) gives

$$v = -H_2^{-1} E_2 \dot{x} - H_2^{-1} F_2 x - H_2^{-1} G_2 u \quad (4.5)$$

Substitute eq. (4.5) into eq. (4.3) and solve for \dot{x} . We get

$$\begin{aligned} \dot{x} = & - (E_1 - H_1 H_2^{-1} E_2)^{-1} (F_1 - H_1 H_2^{-1} F_2) x - \\ & - (E_1 - H_1 H_2^{-1} E_2)^{-1} (G_1 - H_1 H_2^{-1} G_2) u \end{aligned} \quad (4.6)$$

The above equation has a unique solution if condition (ii) of the theorem holds. Using an argument similar to the one used in Theorem 1 it is easily shown that a unique solution satisfying the original differential equation exists for every initial condition $x(t_0)$. Combining eq. (4.1b), eq. (4.5) and eq. (4.6) the state space form of eqs. (4.1) is obtained and the proof is completed. \square

If the reduction method presented above applies, the state variables have a nice physical interpretation since they will simply equal the physical variables which appear differentiated in the equations.

Eq. (4.1) can be written as

$$E' \dot{x}(t) + F' x(t) + G' u(t) + H' v_1(t) = 0 \quad (4.7a)$$

$$P' y(t) + Q' x(t) + R' u(t) + S' v_2(t) = 0 \quad (4.7b)$$

where the vector v has been expressed as two vectors v_1 and v_2 with as few common elements as possible. Both eqs. (4.7) are consistent. This procedure reduces the dimensions of coefficient matrices and the reduction programme used for eq. (4.7a) can also be applied to eq. (4.7b) if the conditions of Theorem 2 are fulfilled. From a computational point of view this later approach is usually advantageous and has been used in the boiler application.

CHAPTER 3 - FIELD MEASUREMENTS

1. Introduction

The field measurements were performed in June 1969, in cooperation with Sydsvenska Kraft AB on the power plant Öresundsverket situated in Malmö, Sweden.

Experiments were designed for two purposes:

- to understand the behaviour of the boiler during large load transients,
- to give a basis for identification of parameters in linear models valid for small perturbations around a steady state.

Engineers from Sydsvenska Kraft AB designed the first set of experiments. The second set of experiments were designed by the author. Only these experiments are analysed in detail.

Measured responses of the power plant are used for identification in Chapters 5 and 6 as well as for comparison with responses of models from construction data in Chapter 7.

Section 2 gives a description of the power plant unit P16-G16. Especially the boiler and the turbines are treated. In Section 3 the measuring program is presented in more detail. Also measuring points and equipment are presented. Properties of measuring devices are discussed. It is essential in a dynamical experiment that the input signal which excites the process is carefully chosen. The choice of input signals as well as sampling rate and other measurement characteristics is accounted for in Section 4. In the last section the results of the experiments are shown and commented.

2. Power plant unit P16-G16

The considered unit is the largest of five units of the Öresundsverket power plant. It was taken into operation in 1964. The drum type boiler was built by Steinmüller and the turbine by Stal-Laval AB. Alternators were delivered by ASEA. Fig 2.1 shows a reduced drawing from an aerial photograph of the entire power plant.

2.1 Plant Configuration

The size and characteristics of the power plant are well defined by the maximum figures given below:

- active power	160 MW
- steam flow	500 t/h
- drum pressure	150 kg/cm ²
- turbine inlet temperatures	535°C
- feedwater temperature	300°C

A complex process as a boiler includes a large number of auxiliary equipment and machinery. A schematic diagram is given in Fig 2.2 where some essential systems and components are included. In the boiler (1) steam of up to 150 kg/cm² is produced by oil-firing. The temperature rises to 535°C in the superheaters. In the high pressure turbine (2) the steam expands to about 32 kg/cm² thereby developing maximally 45 MW. The steam temperature drops and the steam is returned to the boiler and temperature rises to 535°C. After expansion in the intermediate and low pressure turbine which maximally gives 115 MW the steam is condensed to water in the condenser (4). The condensate is pumped through the preheater (6) to the feedwater tank (7). From the tank the water goes to the feed pumps (8) and is pumped through the preheaters (9) and through the economisers and back to the boiler which completes the cycle. The make-up water is produced by an equipment for demineralisation. When modelling this process only the boiler and turbines will be considered.

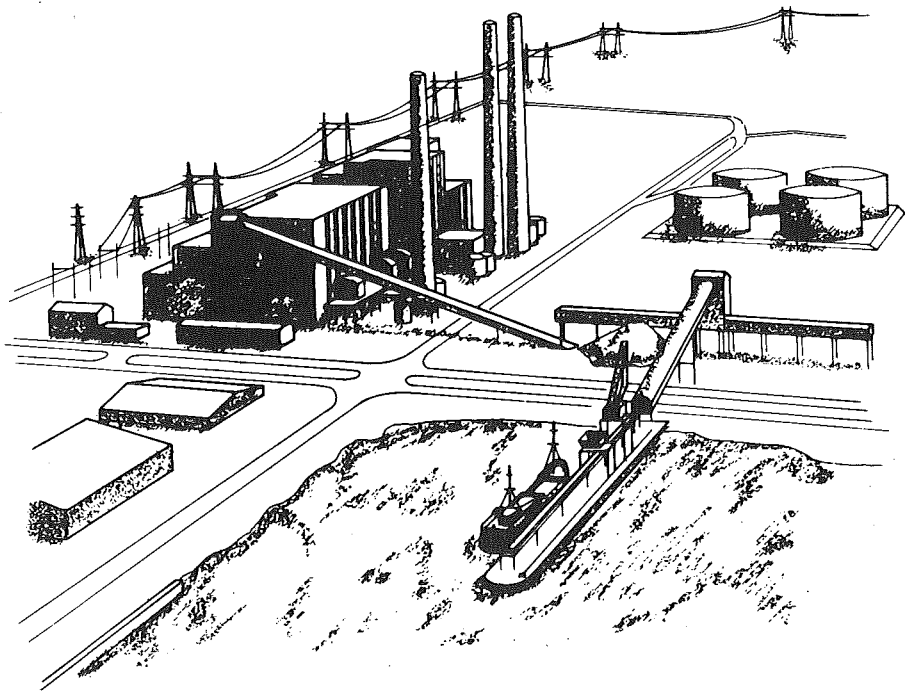


Fig 2.1 - A drawing from a photograph of the Öresundsverket power plant.

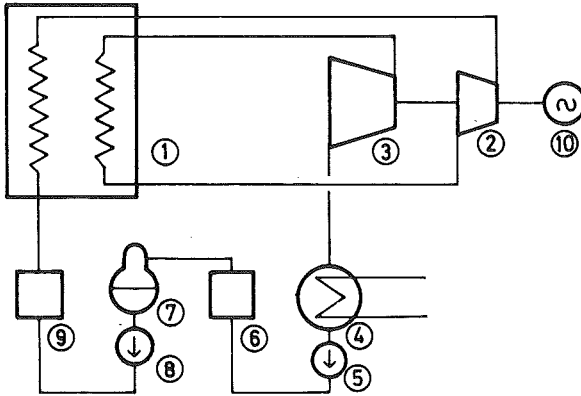


Fig 2.2 - A schematic diagram of Öresundsverket power plant unit P16-G16.

- | | |
|----------------------------|--------------------|
| 1. Boiler | 6. L. P. preheater |
| 2. H. P. turbine | 7. Feed tank |
| 3. I. P. and L. P. turbine | 8. Feed pump |
| 4. Condenser | 9. H. P. preheater |
| 5. Extraction pump | 10. Alternator |

2.2 The Boiler

A schematic picture of the boiler is shown in Fig 2.3. Steam is separated from water in the drum (1) and splits on two equal steam paths. After passing three superheaters (5), (7) and (9) the steam from both paths are mixed and transported to high pressure turbine (10). Steam expands in H. P. turbine and is returned to the reheater (11). The final expansion takes place in the L. P. turbine (12).

The three superheaters are thus divided into two parts each. Under normal operating conditions the thermal state of steam in the two paths is roughly equal.

The two spray attemperators separating superheaters are also split into two parts each. The attemperator flows are used to control the steam temperature after the following superheater or the temperature before H. P. turbine but also to trim the symmetry of the steam paths.

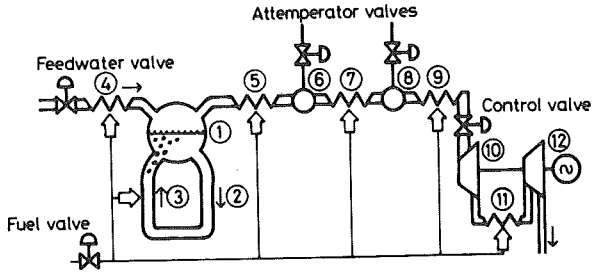


Fig 2.3 - A simplified diagram of the boiler of Öresundsverket.

- | | |
|-------------------|---------------------------|
| 1. Drum | 8. Attemperator 2 |
| 2. Downcomers | 9. Superheater 3 |
| 3. Risers | 10. High pressure turbine |
| 4. Economiser | 11. Reheater |
| 5. Superheater 1 | 12. Low pressure turbine |
| 6. Attemperator 1 | |
| 7. Superheater 2 | |

The economiser (4) is situated in the later parts of the combustion gas channel and is also divided into two parts. The air needed for combustion first passes an air-preheater. The fans for air and combustion gases have movable blades which give these actuators a fast response to control actions.

There are twelve burners. The number of burners in action depends essentially on the load but could be varied to a certain extent.

2.3 The Turbines

There are two turbines in the plant unit since the steam is reheated. The H. P. turbine is a radial flow turbine and the L. P. turbine of the axial flow type. Steam inlet data are $T = 535^{\circ}\text{C}$, $p = 130 \text{ kg/cm}^2$ and $T = 535^{\circ}\text{C}$, $p = 32 \text{ kg/cm}^2$ respectively.

At full load the H. P. turbine gives 45 MW and the L. P. turbine 115 MW. The major part of output power is thus generated by the L. P. turbine.

2.4 Control Equipment

The controlling equipment of the boiler is named Conronic and produced by Schoppe & Faeser.

The main controlled variables are given in Table 2.1. The inputs which cause the intended control action are also given. The boiler model

Controlled variable	Regulator acts on:
Boiler pressure	Fuel flow
Drum level	Feedwater flow
Steam temperature before H. P. turbine	Attemperator flows
Steam temperature before L. P. turbine	Combustion gas flow
Fuel-air ratio	Air flow
Active power	Control valve position

Table 2.1 - Main control loops of boiler P16.

discussed in this work makes it possible to study all control loops except for the one associated with the regulator acting on combustion gas flow. The regulator for this loop is seldom needed since high temperatures are rare.

The control of active power and drum pressure requires some comments. There are two different ways to operate the boiler-turbine unit so as to produce a given power. If the control valve is fully open, active power is changed by changing the drum pressure. Keeping drum pressure constant, active power is altered by changing control valve position. Certainly fuel flow must be adapted to active power. For small perturbations around a steady state the so called turbine regulator controls active power using the control valve. The initiated variations of drum pressure is handled by the drum pressure regulator using the fuel flow. Table 2.1 thus does not give a complete description of the whole control system.

Properties of the regulators such as used measured variables and signal treatment are not discussed since the regulators were disabled during the experiments.

3. Measuring program and equipment

In this section only experiments concerned with small perturbations around a steady state will be treated. Some results from the large load transients have been used and presented in [53].

3.1 Experiments

The experiments were designed for identification of parameters in linear models. The basis for the identification algorithms is a set of recorded data of process input and output signals. Efficient algorithms are available to identify systems with several inputs and one output. The identification of multivariable systems is more complicated since the coupling between inputs and outputs might not be known a priori. The numerical algorithm thus has to seek for the correct structure, which for large systems is very time consuming, or has to assume this structure known.

The boiler is a typical multivariable process. It was intended to perform experiments where only one input variable at a time is perturbed and also experiments where all input variables are perturbed simultaneously. Unfortunately the power situation at the time for the experiments was such that the economic consequences of a failure would be large. The more complicated multivariable experiments were then inhibited.

The intended purpose of the measurements requires that the process is in open loop. All main regulators listed in Table 2.1 except for the fuel-air ratio regulator were then disconnected. This is of no consequence since air flow could be changed rather fast and when modelling the boiler fuel flow and heat flow can be considered equivalent.

The experiments are listed in Table 3.1. The steady state in the first five experiments is about 90 % of full load. This point was chosen in order not to get too high values of any variable. Load level is then decreased to roughly 50 % of full load and the experiments are repeated. As seen from the table the steady state was approximately the same within each set of five experiments. However, to be able to perturb control valve position Exp. E slightly differs from the other four at 90 % load level.

By choosing two different load levels for experiments the influence of non-linearities can be investigated. When designing control strategies for processes based on linear models it is essential to have an estimate of the validity range.

Attemperator flows in Exps. C, D, H and I were only perturbed in one of the two steam paths.

Exp.	Perturbed input variable	Active power MW	Drum pressure kg/cm ²
A	Fuel flow	140	125
B	Feedwater flow	140	125
C	Attemperator flow 1	140	125
D	Attemperator flow 2	140	125
E	Control valve position	135	135
F	Fuel flow	68	110
G	Feedwater flow	68	110
H	Attemperator flow 1	68	110
I	Attemperator flow 2	68	110
J	Control valve position	70	110

Table 3.1 - Some characteristics of experiments.

3.2 Measured Variables

Twentythree variables as listed below were recorded during the measurements

- active power
- drum level
- flow of fuel
 - feedwater
 - attemperator 1 (both paths)
 - attemperator 2 (" ")
 - steam (" ")
- steam temperature before attemperator 1
 - after attemperator 1
 - before attemperatur 2
 - after attemperator 2
 - before control valve
 - before reheater
 - after reheater
- feedwater temperature (both paths)
- steam pressure in drum
 - before control valve
 - after control valve
 - before L. P. turbine

The position of the measuring points are indicated in Fig 2.3

The only significant variable which was not automatically recorded was control valve position. Approximate values were recorded manually.

3.3 Measuring Devices

For all measuring points the ordinary measuring equipment of the boiler-turbine unit was used. The equipment was of the standard industrial type. All recorded temperatures were measured by thermocouples, all flows and drum level by difference pressure gauges. For the recording the signal was taken from the ordinary transducers and amplifiers.

Calibrating curves for recorded flows and temperatures were available. The drum level measurement was also calibrated according to the drum pressure.

Except for the temperature transmitters all measuring equipment can be considered fast compared to the boiler dynamics.

3.4 Recording Equipment

A data-logger was used to record measured quantities. Measured values were punched on paper tape.

Maximum scanning and punching rate is 10 values in 1.8 seconds. Accuracy is approximately 0.01 % of maximum recordable value. Disturbances of net frequency are eliminated by integrating the input signal over one period of this frequency.

Input signals are scanned sequentially. No sample and hold features were available. Recorded time series of different variables are thus shifted in time. This must be taken into account when identifying if the shift is a considerable fraction of the sampling interval.

4. Characteristics of Measurements

The choice of sampling rate and input signal are two important problems when making an identification experiment. These problems have been treated in literature [20], [23], [54]. In the general case no solution has been given. Since the choices heavily depend on process dynamics the ideal identification experiment requires repeated measurements.

4.1 Choice of Sampling Rate

The choice of sampling interval for parametric identification is treated in [27] for some special systems. It is shown that there often exists an optimal sampling rate. This rate depends on e.g. the criterion and noise characteristics. The calculation of the optimal sampling rate requires that the system is known. However, the following rules of thumb for the choice of the sampling interval T_s often apply

$$T_s = \min \begin{cases} (0.5 \div 1.5) T_{\min} \\ \frac{\pi}{2 \div 5} \cdot \frac{1}{\omega_{\max}} \end{cases} \quad (4.1)$$

where

T_{\min} smallest time constant

ω_{\max} largest resonant frequency

associated with the process dynamics.

In the boiler case the process dynamics was estimated using rough models from first principles and measured step responses. This information indicated that the smallest time constant of interest was about 10 seconds. The data-logger was capable to scan the twentythree measuring points in 4.8 seconds. This reduced the possible sampling intervals to 5 - 15 seconds. Finally trivial practical limitations restricted the choice to $T_s \geq 10$ seconds. Thus we choose

$$T_s = 10 \text{ sec.}$$

4.2 Choice of Input Signal

The properties of different identification schemes have been discussed in literature [54], [26].

It was decided to use the maximum likelihood method mainly for two reasons. Efficient computer programs utilizing this method were available [25] and the disturbances are modelled.

The identification method do not impose any restriction on a persistent exciting input signal other than, it must be constant over the sampling interval. But this restriction can be avoided, if necessary. Since the input signal had to be generated manually, a square wave type of signal was used. Such an input sequence also take maximum advantage of the permitted amplitude range, which is favourable, when experiments has to be made during normal operating conditions.

The input signal should excite all the essential modes of the process. In the general case, the process dynamics is only known to be bounded to a certain frequency interval. For this reason, it is desirable that the power spectrum of the input signal is approximately constant in this interval.

One type of input signal which satisfy the demands discussed above is the PRBS (Pseudo Random Binary Sequence). The properties of the PRBS are well known and a detailed presentation is found in e.g. [8]. This type of input has been used frequently [5], [46]. However, some significant properties are

- the amplitude is $+a$ or $-a$,
- the sign shifts at time points that are integer multiples of the basic interval T_p ,
- it is periodic with period $N \cdot T_p$ where N is the maximum length
- the normalized autocovariance function is

$$r(\tau) = \begin{cases} 1 & \text{if } \tau = k \cdot N, k=0, 1, -1, \dots \\ -1/N & \text{elsewhere} \end{cases}$$

As an example a PRBS of length $N = 7$ is shown in Fig 4.1.

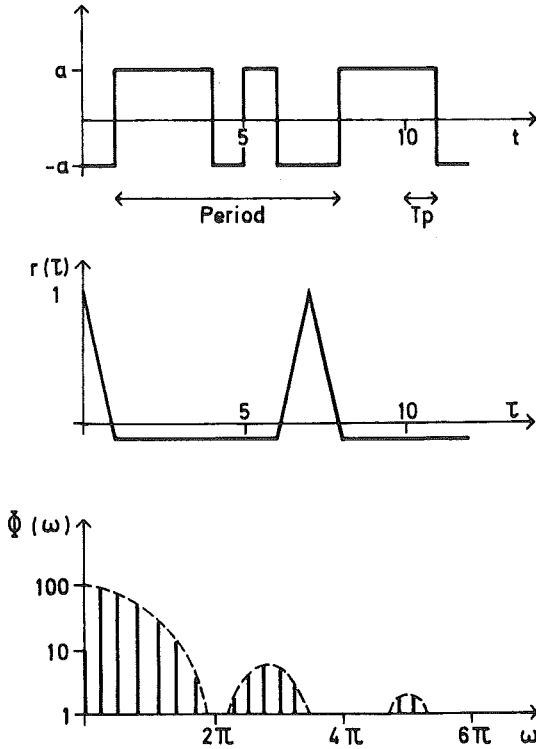


Fig 4.1 - Time series, covariance function and spectral density for a PRBS of length $N = 7$. The sampling interval is normalized to 1.

The PRBS was chosen as the starting point for deriving the input signal to be used. Then, it remains to choose the interval T_p , the length N and the amplitude a .

To choose the interval T_p and the length N the following rules may be used

- choose $N \cdot T_p = 5 T_{\max}$
- choose $r \cdot T_p = 3 T_{\max}$

where r is the longest run of $+a$ or $-a$ and T_{\max} the maximum time constant associated with the process dynamics. The first rule has been given in [8]. The second rule is based on the argument that, the estimates of the gain and largest time constant are improved, if the process is allowed to approach a new steady state during the experiment. The measurement time T_m should in both cases be at least $N \cdot T_p$. The second rule above leads to significantly larger length N and thus to larger measurement time.

In the boiler case the measurement time was limited to one hour for each experiment and thus $T_m = 1$ hour. The maximum time constant of the boiler was estimated to $300 \leq T_{\max} \leq 500$ seconds. According to the first rule above it is possible to identify a maximum time constant of 720 seconds, which seems satisfactory.

The most common PRBS are the m - and QR -sequences with period length $N = 2^n - 1$ (n integer) and $N = N_{QR}$ where N_{QR} is a prime number of the form $4k - 1$ (k integer). In the m -sequence the longest run of $+a$ or $-a$ equals n . According to the second rule above we should choose, for the m -sequence, $nT_p = 3$ ($300 \div 500$) seconds. If we also consider the measurement time given as $(2^n - 1)T_p = 3600$ seconds, we get a small value of n ($n \sim 4$) and thus a large value of T_p . However, the value of the spectral density function of an m -sequence will be small above $\omega_1 = 2\pi/T_p$, see Fig 4.1 where $T_p = 1$. This requires that T_p is chosen in such a way that, the spectral density function of the input covers the interesting frequency range, which approximately equals $0 - 0.3$ rad/sec. The upper bound is given by the Nyquist frequency $f_c = \pi/T_s \approx 0.3$ rad/sec. This situation certainly requires a compromise and we choose

$$T_p = 60 \text{ sec} \quad (4.2)$$

which gives $\omega_1 \approx 0.1$ rad/sec if the sampling interval $T_s = T_p$. The value of T_p is also long enough to reduce the influence of the positioning time of the actuators. That is, the input signal will be approximately constant over most sampling intervals of length 10 seconds.

Now the preliminary choice of input signal was a QR -sequence of length $N=59$. The longest run of $+a$ or $-a$ in this sequence is 5. However, this sequence was manually modified to contain more long runs of $+a$ or $-a$ and thus more power at low frequencies. The final choice was the sequence

$$\begin{array}{l}
 - - + + + + - - - - + + - - - - + - - - + + + + - + - + - - - + - - - + \\
 + + + + - + - - + - - - + + + + +
 \end{array} \quad (4.3)$$

with

$$N = 60 \quad (4.4)$$

where the + and - signs indicate positive and negative deviations of amplitude a from the mean value. The composed input sequence has zero mean value and the covariance and spectral density functions are shown in Fig 4.2. The spectral density function has been computed from the input sequence used in Exp. I. Fig 4.2 shows that we have $\omega_1 \approx 0.1$ rad/sec for the constructed input sequence.

The sequence (4.3) was used in all experiments. Since the dynamics of a superheater is faster than that of drum and reheater a signal with more power at high frequencies might be preferred for e.g. Exps. C and D. However, the sampling interval is short enough to ensure these dynamics to be detected.

Still the amplitude of the input signals remains to be determined. The choice of amplitude must be a compromise between the demand for a large amplitude to keep signal to noise ratio high and the demand for a low amplitude to avoid the influence of non-linearities. Normal operating records and pre-experiments guided the choice which is shown in Table 4.1. The given amplitudes were used for both load level experiments.

| Input | Amplitude |
|------------------------|--------------------------|
| Fuel flow | $\pm 2 \cdot 10^3$ kg/h |
| Feedwater flow | $\pm 20 \cdot 10^3$ kg/h |
| Attemperator flows | $\pm 2 \cdot 10^3$ kg/h |
| Control valve position | ± 3 % |

Table 4.1 - Amplitude of deviations from mean value for input signals.

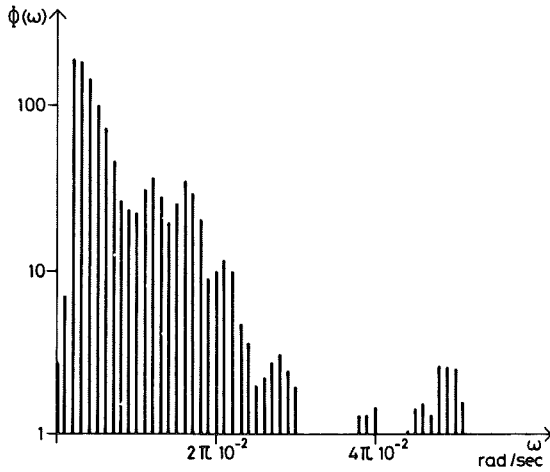
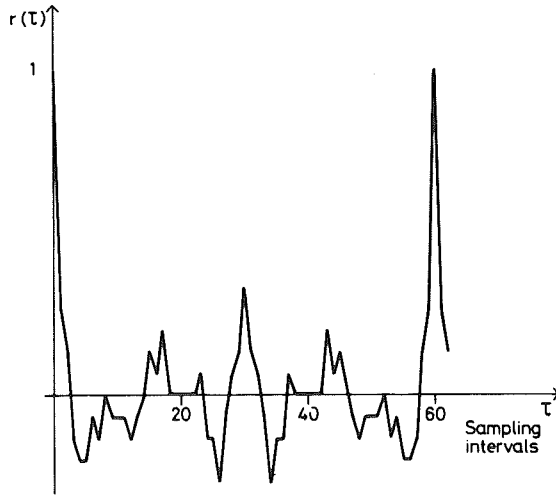


Fig 4.2 - Covariance function $r(\tau)$ and spectral density function $\phi(\omega)$ for the input sequence (4.4) used in experiments.

4.3 Conditions of Experiments

Although most conditions already have been stated in this chapter the significant conditions of experiments will be summarized.

The experiments were made on the open loop process, that is the regulators for drum pressure, drum level, steam temperatures and active power were disconnected. Only the regulator controlling the ratio between fuel and air was intact. The regulators for auxiliary machinery were still in operation.

With the process in open loop the actuators could be manoeuvred from the control room of the power plant. No equipment for automatic generation of the input sequences was installed but the changes were made manually. Most actuators were driven by electrical motors but the maximum settling time for a change was measured to be about 5 seconds. Compared to the basic interval of the input sequence which equals 60 sec. this settling time is acceptable small.

Some precautions were taken in order not to cause failure or damage. The steam temperatures at the inlet of turbines are not allowed to exceed 540°C . Since in all experiments, the inputs will cause variations of these temperatures, the steady state temperatures were decreased to about 510°C using the attemperator flows. The drum level must be kept within certain limits in order not to cause disturbed circulation in the drum system (low level) and to prevent moisture from entering the superheaters (high level). By acting on the feedwater valve these requirements were satisfied.

5. Results

Not all measured variables could be included in this presentation of results. The number of variables has been limited to ten for Exps. A, E, F and J, and to five for Exps. B, C, D, G, H and I. The whole material given will not be used later but already an inspection of the responses from the dynamical tests gives valuable information. Boiler dynamics will not be discussed in detail here. This is accounted for in the following four chapters. Some peculiarities are, however, pointed out.

In Exps. A, E, F and J where the fuel flow and control valve position are the main inputs also the feedwater flow has been changed in order to

avoid extreme high or low drum levels (see Figs. 5.1, 5.5, 5.6 and 5.10). Ideal conditions for a single input experiment is therefore not established.

In these experiments also the attemperator flows vary. This is shown in Figs. 5.1 and 5.6 where the flow in attemperator 1 in the right steam path is included. The reason is that the pressure drop over the attemperator valve changes according to drum pressure variations. Also in the other experiments drum pressure is affected, but the fluctuations are considerably less.

Inspecting temperature responses of Exp. A in Fig 5.1 we find that the amplitude of responses are larger in the first half of the experiment than in the second half. The cause is an asymmetrical heat flow distribution between the left and right steam paths of the boiler. This transient in heat flow distribution was initiated by the changes in fuel flow and the symmetric distribution was reestablished without any aid from the working staff. In fact the asymmetry was not recognized until all tests were finished.

Feedwater flow is the main input variable in Exp. B, Fig 5.2. As a consequence of flow changes and a constant heat flow to the economiser, feedwater temperature is greatly influenced.

Previously we have seen that drum pressure affects attemperator flows. Also the reverse is true. In Exps. C, D, H and I drum pressure is changed according to the changing coolant flows. Thus the response of superheater outlet temperature is caused by the two variables attemperator flow and drum pressure.

In both experiments using attemperator flow 1 the response of steam temperature before attemperator 2 show a non-minimum phase characteristic. This can be caused by a fast pressure transient in the superheater when changing the injected water flow.

A non-minimum phase response is also a property of dynamics relating drum level to control valve position. In this case the phenomenon is caused by fast changes of the volume of steam bubbles in the drum water since a changing drum pressure affects the saturation state in the drum.

In Exp. H where attemperator flow 1 is the main input variable the response of drum pressure is also due to significant changes of feedwater flow.

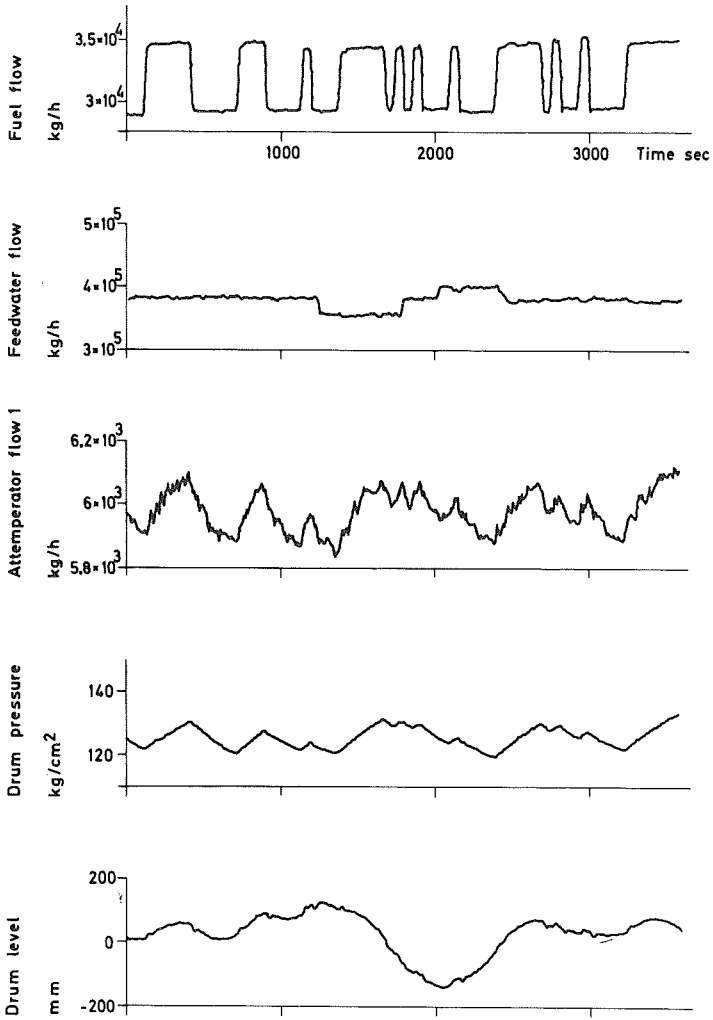


Fig 5.1 - Results of Exp. A.
Main input is fuel flow.

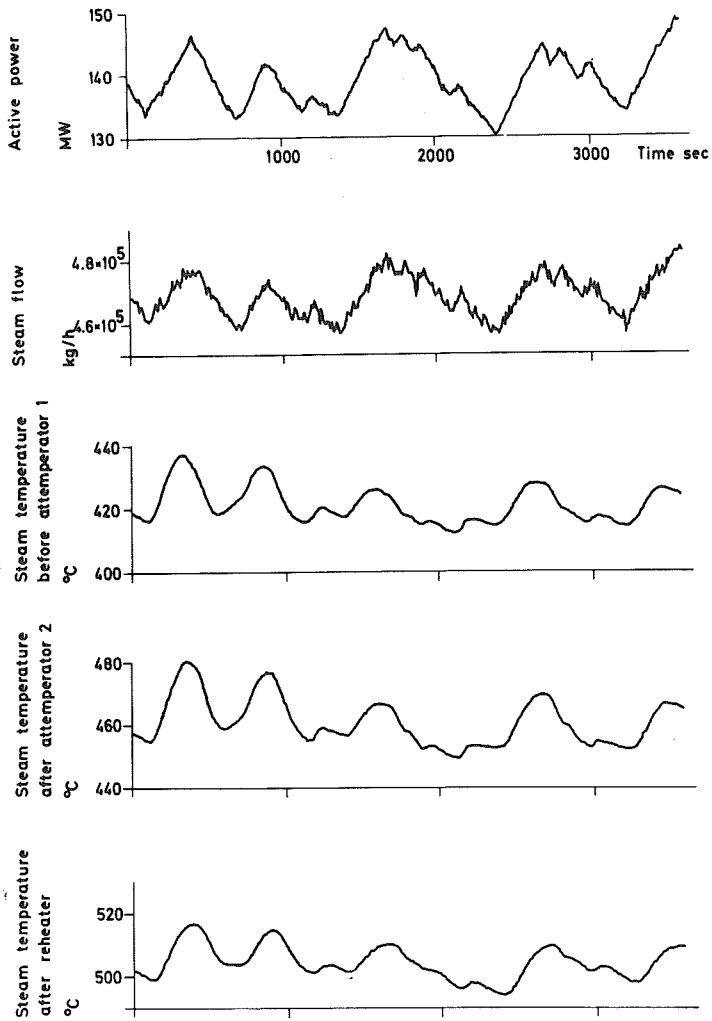


Fig 5.1 - Contd.

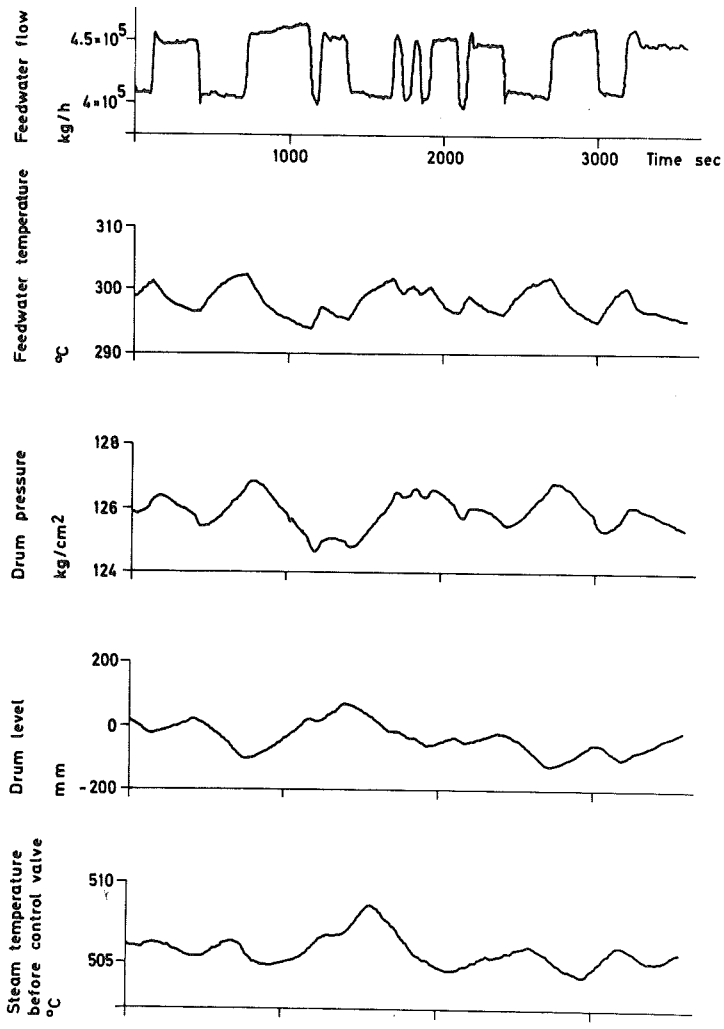


Fig 5.2 - Results of Exp. B.
Main input is feedwater flow.

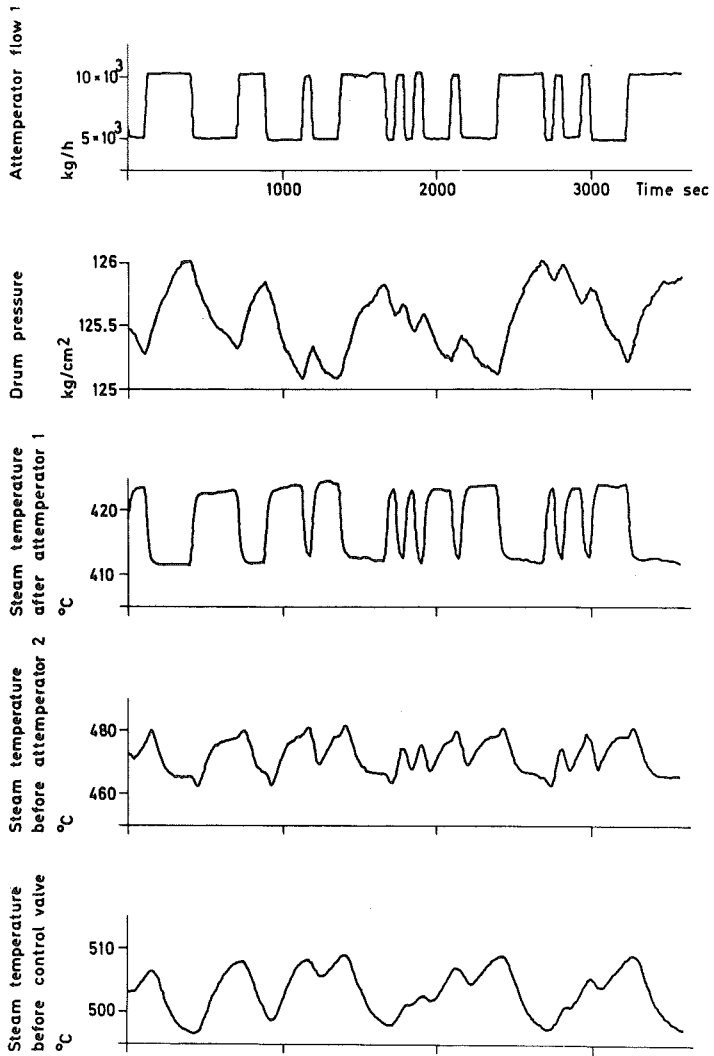


Fig 5.3 - Results of Exp. C.
Main input is attemperator flow 1.

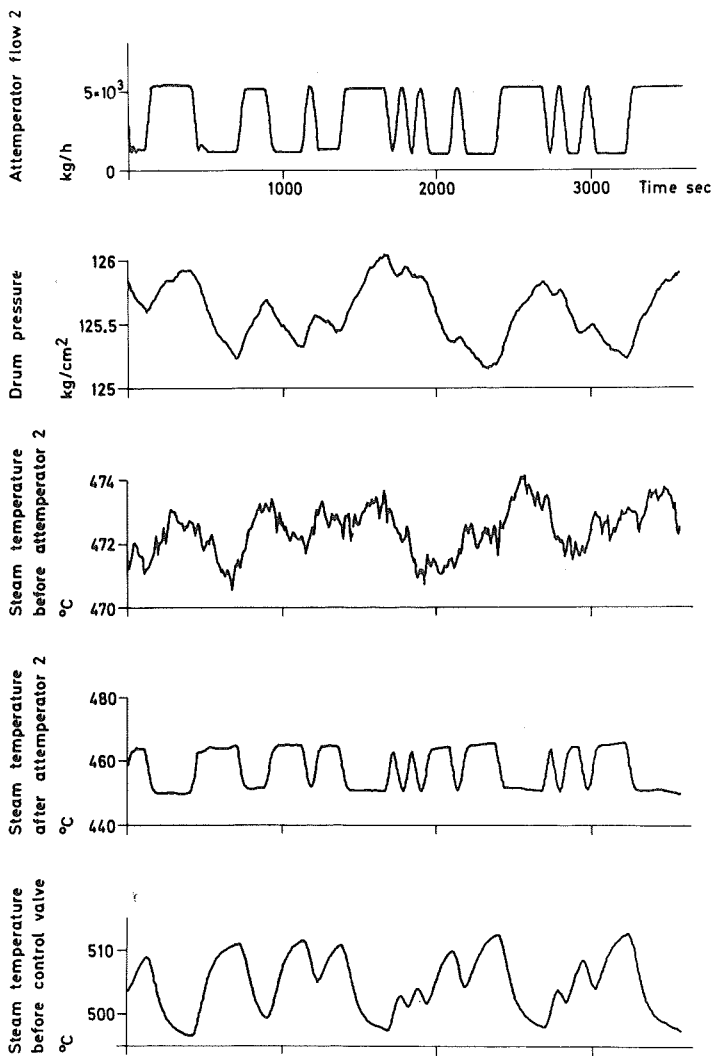


Fig 5.4 - Results of Exp. D.
Main input is attemperator flow 2.

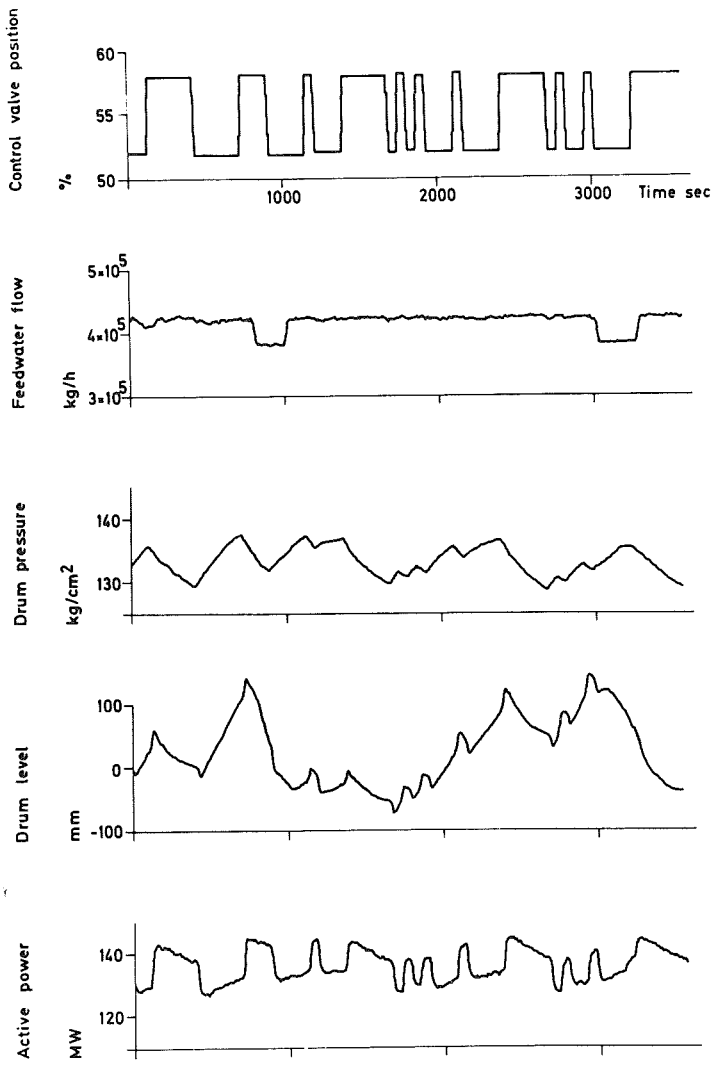


Fig 5.5 - Results of Exp. E.
Main input is control valve position.

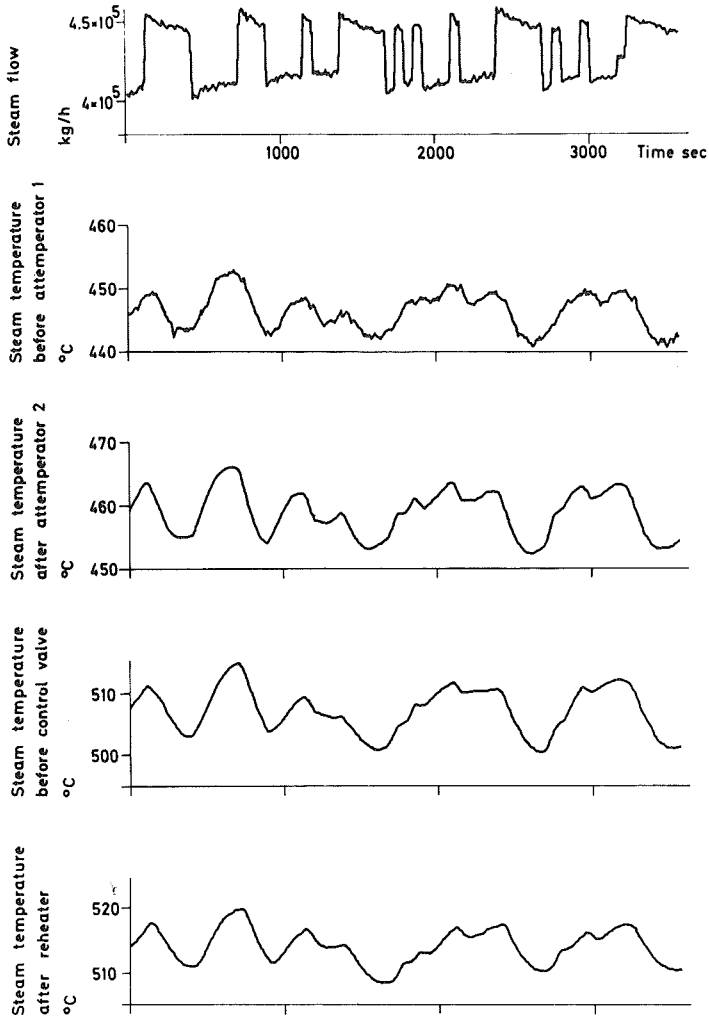


Fig 5.5 - Contd.

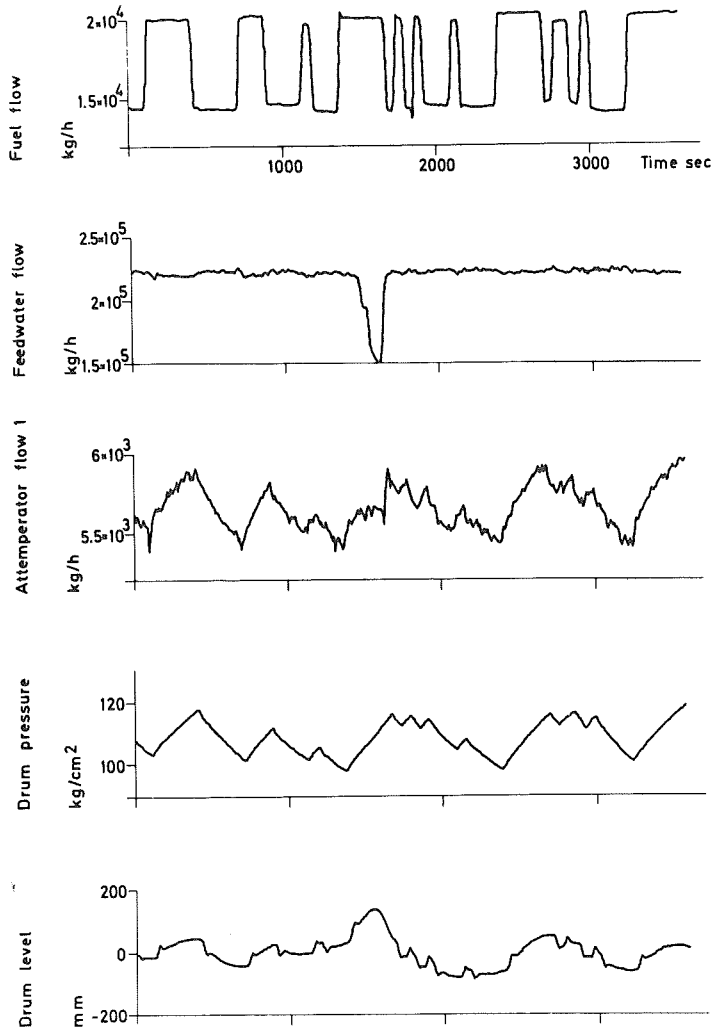


Fig 5.6 - Results of Exp. F.
Main input is fuel flow.

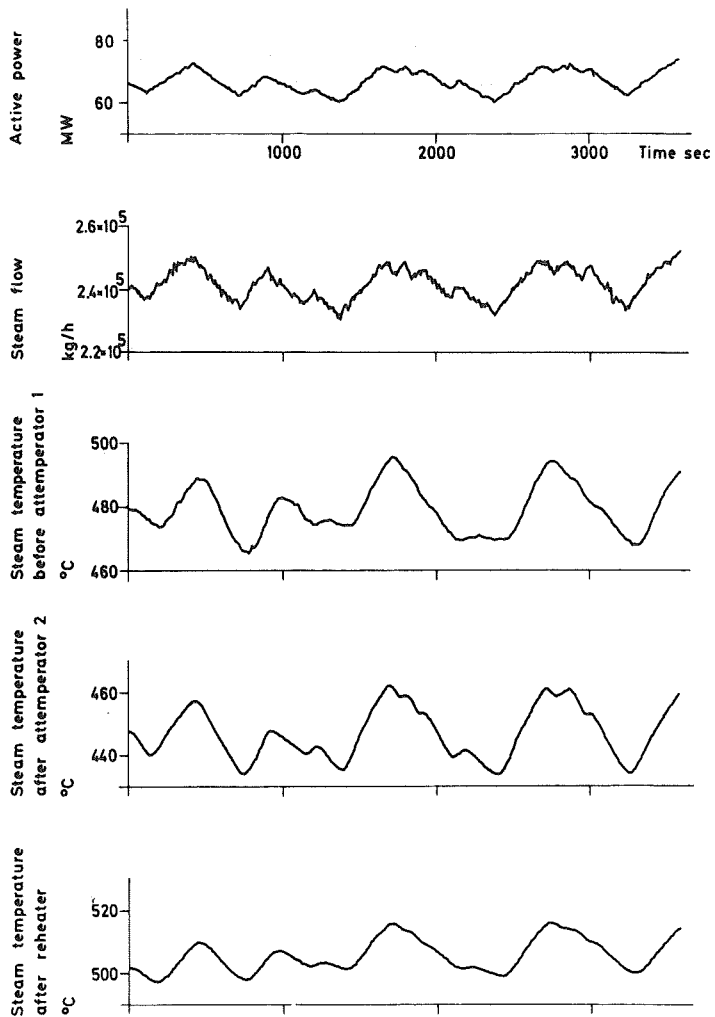


Fig 5.6 - Contd.

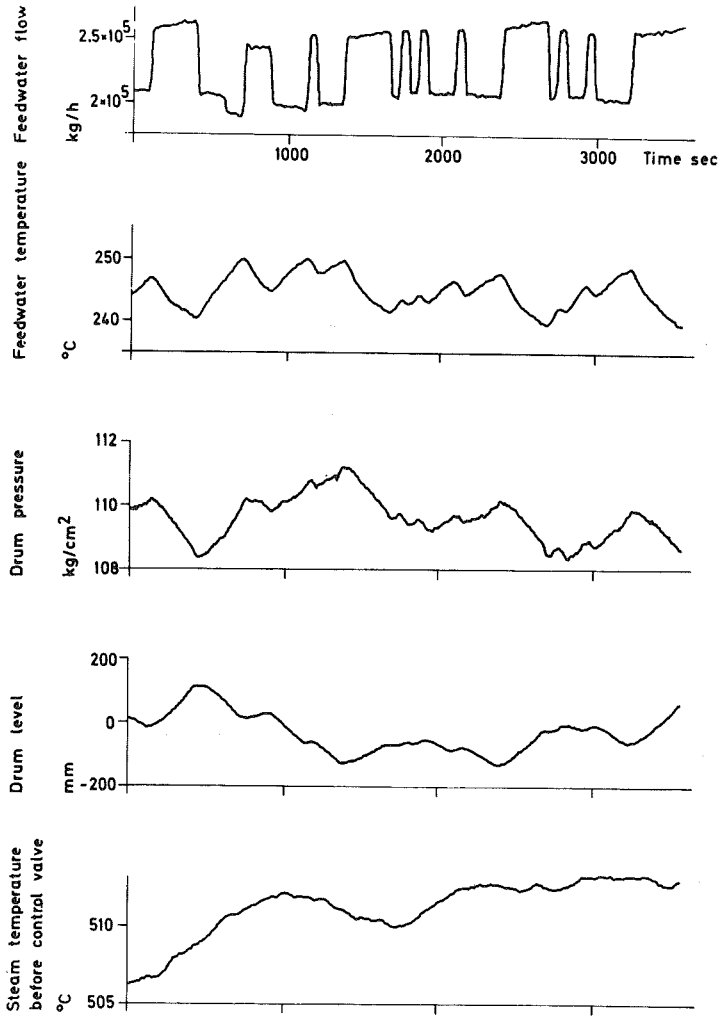


Fig 5.7 - Results of Exp. G.
Main input is feedwater flow.

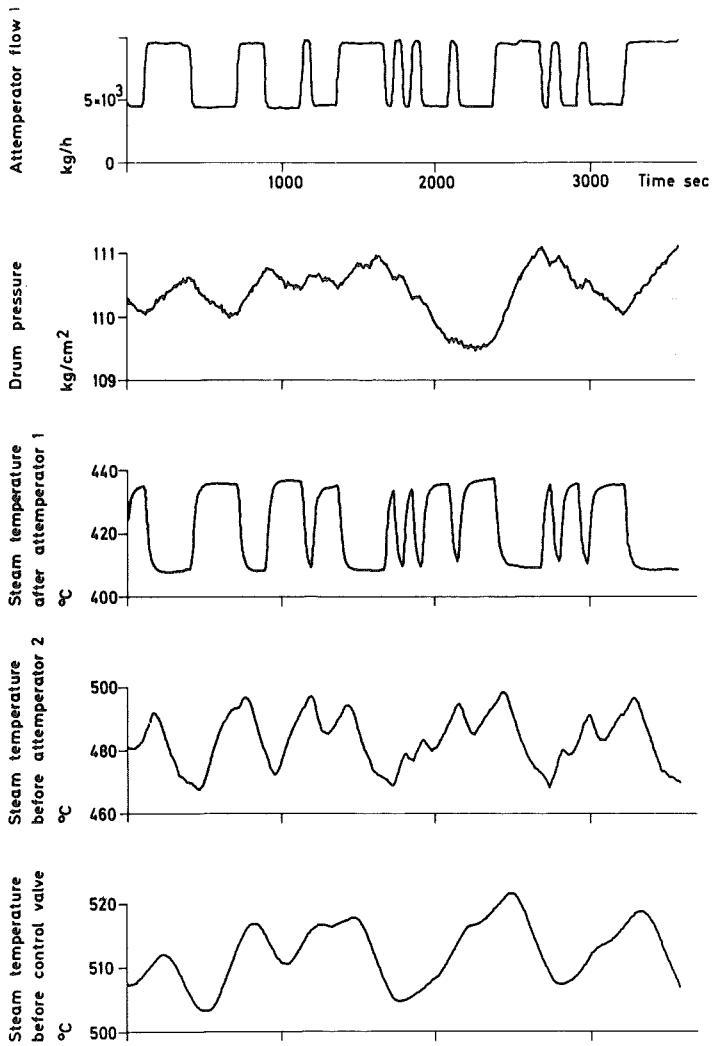


Fig 5.8 - Results of Exp. H.
Main input is attemperator flow 1.

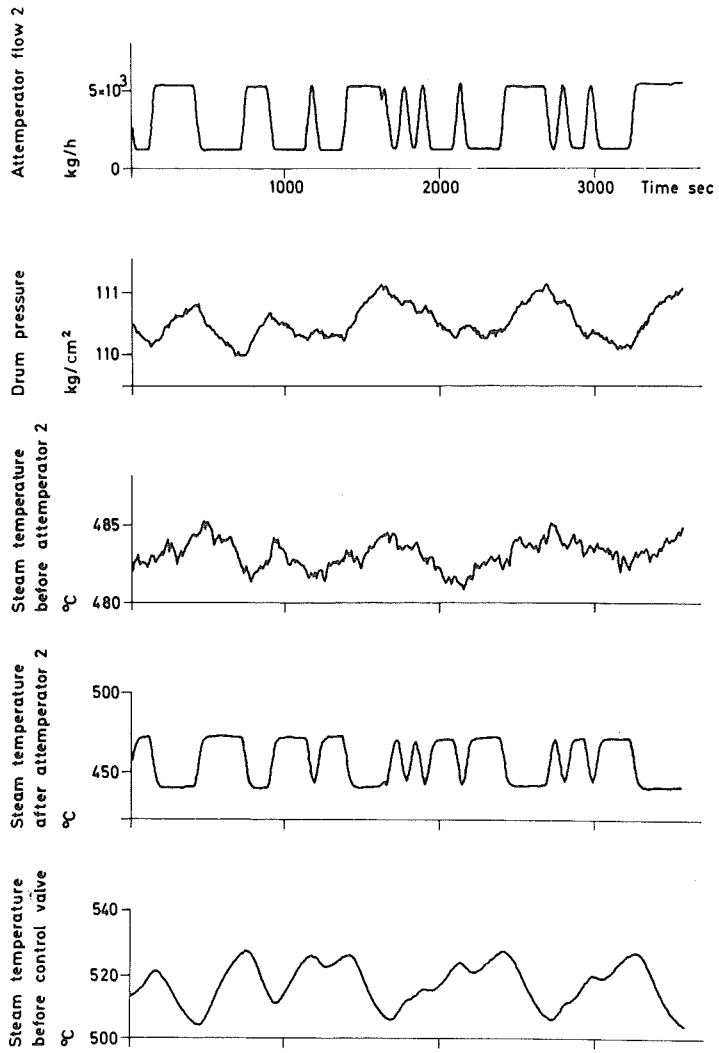


Fig 5.9 - Results of Exp. I.
Main input is attemperator flow 2.

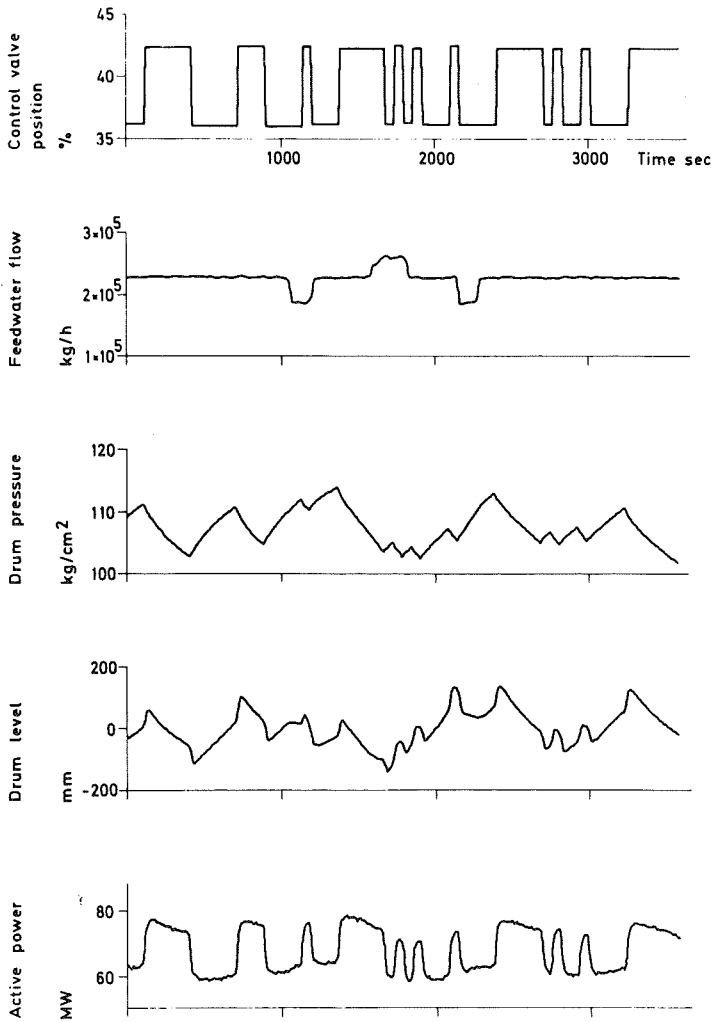


Fig 5.10 - Results of Exp. J.
Main input is control valve position.

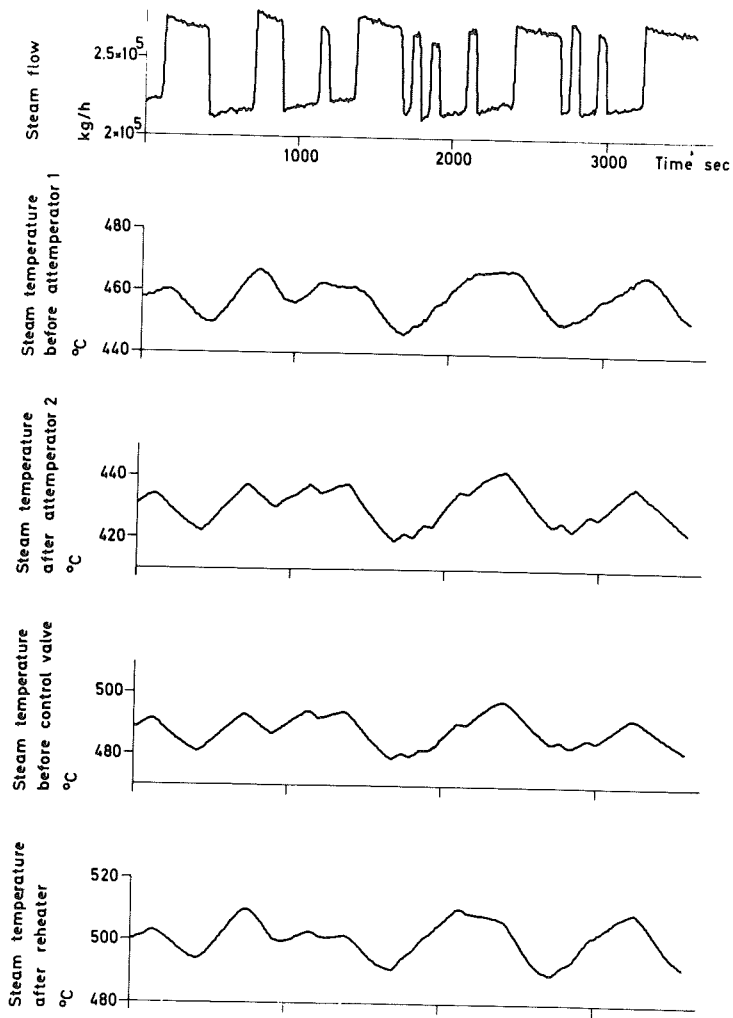


Fig 5.10 - Contd.

1. Introduction

The modelling of an industrial process from basic physical laws must start with a definition of the goal of the modelling. It is the goal which determines the degree and techniques of approximation. The size and complexity of the final model thus heavily depend on the goal.

In this study the model is primarily designed for steady state control of the boiler-turbine unit. As in every modelling process, however, the achieved knowledge of the process could be used for other purposes e.g. redesign of the process itself.

The steady state control of large boilers includes several control loops. The most essential are

- active power control,
- drum pressure control,
- temperature control,
- drum level control,
- combustion control (air/fuel) control.

The regulators act on

- control valve,
- fuel flow,
- attemperator flows,
- feedwater flow,
- air flow.

This means that not only the overall behaviour of the boiler is of interest but also intermediate process variables are important for the control. The model must properly describe the dynamic relations and cross-coupling between the inputs and outputs which are defined by the control task.

The multivariable process under consideration is quite complex. Heat exchangers such as superheaters and economiser are described by non-

linear partial differential equations, which probably also are time varying. The size of the boiler cause time delays. The two-phase flow, in the risers of the drum system, has very complicated characteristics. The presence of vapor in risers and drum gives non-minimum phase response to water level. Thus the need for approximations and simplifications is obvious.

The steady state control problem is usually solved using a set of linear time invariant ordinary differential equations (linear models). This is mainly for two reasons. Linear models are usually sufficient for stability considerations when the process is slightly perturbed around an equilibrium state. The theory for linear systems is almost complete and powerful. However, problems will still arise when high order and multivariable systems are to be treated.

For our purpose the goal must be to derive a linear model of as low order as possible. The model should include significant input and output variables to be able to solve the essential control problems of the boiler.

The access to a static model originating from e.g. the constructors design material is a good basis for the development of a dynamic model. The static model will contain a large amount of the construction data needed. The dynamic model could, to a certain extent, be regarded as a static model where certain equations have been extended with a derivative. The problem of choosing the derivatives of physical variables to be included is the main difficulty. It should be pointed out that this procedure is greatly simplified by rough estimates of the involved dynamics. Such an approach has been the approximation procedure used in this work.

When modelling a physical process the computational effort to derive constants of the model from construction data soon becomes a major task. Adopting the philosophy stated in Chapter 2 the final model will take the form of a computer programme. This will increase the generality as well as the analyzability of the model.

We will try to recognize characteristic physical components of the boiler and develop a model for each of these. The models have the form of computer subroutines. There will be conflicts between the demand for model generality and model simplicity. The size and construction of different boilers vary e.g. the circulation of the drum system can be forced or natural and the number of superheaters as well as their heat transfer characteristics are different. The approach taken is to develop a model for each one of the essential components of the boiler. In cases where several types of components are possible a typical situation is chosen and elaborated in more detail. In such cases it is commented upon possible extensions.

The components chosen for modelling are

- drum system,
- superheater,
- attemperator,
- control valve,
- turbine.

The list is lacking e.g. economiser, air and combustion fans, sensors and actuators. The reasons for this will be stated in more detail in Section 3. However, it is possible to build up a number of drum boilers from these components. They are also considered to be invariant to an extent qualifying them to be quite generally modelled.

A number of investigators have considered the modelling of drum-type boilers. The approaches taken in the papers differ quite considerably. The main reason for this is that the ultimate goal of the models are not the same. Also the investigators have treated drum boilers of different types. For example, the boilers are oil- or coalfired, the number of superheaters and turbines vary and the circulation in drum system is forced or natural. A detailed comparison of the models presented will not be given. However, some characteristics such as model order and comparison to field measurements are treated.

An early attempt to model a complete drum-type boiler was made by Chien et al.[10]. The dynamics of the drum system and one superheater is included which gives a ninth order model. Model responses are not compared to field measurements. In [35] the model used is essentially that of Chien et al. The approach taken in Section 3 to the modelling of the drum system is partly adopted from [10].

The boiler considered in [12] is a power station boiler of 200 MW equipped with a reheater, controlled circulation and coal-firing. Model order is very high. The validity of the model is evaluated using measurements in [11]. The duration of field experiments is 300 seconds. This appears to be a too short time interval for a valid comparison. The model of [12] was elaborated in [43] using higher order approximations of distributed parameter processes such as the superheaters. Model responses was evaluated using recordings of boiler responses during 300 seconds. An improvement was established but model order is increased.

Three models for different boilers have been developed by Anderson et al. [4], [32]. Model order range from twenty to thirty. In [4] the responses to a step change in control valve position are compared to model responses.

Recently a fourteenth order model was published in [33], [34]. These reports give both the responses of the linearized as well as the nonlinear models. Step responses of both models to main input variables such as fuel flow and control valve position are compared to field measurements. The agreement is in general good especially when comparing measurements and responses of the nonlinear model.

The model derived in [45] is designed especially for the control task under consideration. The validity is thus limited. A detailed treatment of different boiler subprocesses is found in [38].

The superheater is a significant component of the boiler-turbine unit. The dynamics of heat exchanges has been treated in e.g. [3], [19], [42], [29]. The first three papers discuss the influence and importance of different approximations.

The model presented in this chapter is based on two earlier published reports, [17] and [55]. The later one is a master thesis supervised by the author. In Section 2 the structure of the model computer programme is discussed. All equations which constitute the boiler model are given in Section 3. Different drum system models are derived in Section 4. A comparison of drum system responses shows that a fifth order model is suitable. Section 5 gives an application to the Öresundsverket power plant unit P16-G16. The final choice of model order is nine. This choice was based on a comparison to a fifteenth order model where superheaters were approximated by higher order dynamical systems.

2. Model Programme and Subroutines

The process is divided into a number of components and a model is derived for each of these. The components are linked up with a number of internal variables which are eliminated when the complete model is established. The final model is on state space form $S(A, B, C, D)$.

2.1 Model Main Programme

There are two different approaches to the model building. The computer subroutines of the models can generate either a state space model or a set of unreduced linearized equations. In the first case the reduction procedure is applied inside each subroutine and the main programme is

used to build the complete A, B, C and D matrices from the component matrices. In the second case the main programme connects the component parts to a linearized set of equations for the entire process. Finally, the reduction to state space form is made. It was decided to use the later approach mainly because the connecting procedure appeared simpler than in the first approach. A drawback is that the system to be reduced is quite large. This can give rise to numerical difficulties.

It was found that for all components of the boiler except the drum system the alternative and simpler reduction method could be used. The drum system required the general method. However, as will be shown later in this chapter, a reduced order drum system model was satisfactory and this model could be reduced using the simpler method. Thus all model subroutines shall generate two matrices \hat{A}_i and \hat{Q}_i defined by

$$\hat{A}_i z_1 = 0 \quad (2.1a)$$

$$\hat{Q}_i z_2 = 0 \quad (2.1b)$$

where

$$\hat{A}_i = \left(\begin{array}{c|cc|c} E_i & F_i & G_i & H_i \end{array} \right) \quad (2.2)$$

$$\hat{Q}_i = \left(\begin{array}{c|cc|c} P_i & Q_i & R_i & S_i \end{array} \right) \quad (2.3)$$

and

$$z_1 = \left(\begin{array}{c} \frac{\dot{x}}{x} \\ \frac{u}{v} \end{array} \right) \quad (2.4)$$

$$z_2 = \left(\begin{array}{c} \frac{y}{x} \\ \frac{u}{v} \end{array} \right) \quad (2.5)$$

Eqs. (2.1a) and (2.1b) are those discussed in Section 2 which apply to the i :th process component.

For each component we thus define input, output, internal and state variables. As stated before these variables do not need to be processes input and output variables but only input or output variables for another component and used to link components together.

It was further decided that all communication between and with model subroutines should be executed through the formal parameters of the computer subroutines.

The structure of the model main programme is now roughly given. All input statements are executed by the main programme. The body will consist of a string of calls to model subroutines and manipulations with the returned \hat{A}_i and \hat{Q}_i matrices in order to establish the \hat{A} and \hat{Q} matrices for the entire process. Finally, the reduction subroutine is called twice to give the final model $S(A, B, C, D)$.

2.2 Model Subroutines

The task for the model subroutines has been limited to produce the matrices \hat{A}_i and \hat{Q}_i . This means that the computations are restricted to the calculation of steady state values, values of introduced proportional constants such as heat transfer coefficients and finally the coefficients of the linearized set of equations. Only in the drum system subroutine there is a more complex calculation of steady state values. The linearization of equations is made analytically. No numerical differentiation has thus been used in model subroutines.

Input data are physical dimensions, steady state steam conditions and so forth. The data are arranged in vectors each containing similar information. As an example of the organization of a model subroutine the listing of the subroutine DR5M (Drum system 5:th order model) is given in Appendix A. The subroutine is quite self-explanatory but, of course, the understanding is simplified by also using the text presented under Drum System in Section 3.

3. Derivation of Equations

To meet the request for low order and wide applicability of the model the following initial assumptions are made

- (a) partial differential equations are approximated by ordinary differential equations,
- (b) the flow of combustion gases is not considered but the heat input to risers and superheaters is taken to be a constant times fuel flow,

- (c) steam flow is considered incompressible,
- (d) dynamics of actuators and sensors are not included.

An alternative to assumption (b) could be to neglect the dynamics of combustion gases but include a calculation of the temperature distribution along the boiler. The heat transfer to risers and superheaters would then depend on both gas and wall temperature. This is a more realistic assumption than the one made in (b) which implies the dependence on wall temperature only.

A static treatment of both the flows of combustion gases and steam is fully justified. The dominant time constants can be estimated to lie in the interval 1 - 10 seconds. Boiler dominant time constants is of the magnitude of several hundreds of seconds.

The last assumption or simplification is caused by the aim for generality. This part of the equipment differs greatly between boilers. In most cases the dynamic properties of actuators for small changes can be considered fast and treated as static. Sensors such as thermocouples could contribute to the dynamic behaviour of the entire plant.

The thermal state equations, which are used, are linearized equations, where the coefficients for certain steady state conditions may be found in e.g. steam tables. The heat transfer rates are empirical relations found in literature.

A list of symbols used in this chapter is found in Appendix D.

3.1 Drum System

The process configuration is shown in Fig 3.1. Into the drum enter the feedwater flow and the steam-water mixture from the risers. The flows which leave the drum are the output steam flow and the water flow into the downcomers. A heat flow is supplied to the risers. The process input variables are

- feedwater flow,
- feedwater enthalpy,
- heat flow to risers,
- steam outlet flow,

and the process output variables are

- drum pressure,
- drum liquid level.

Notice that the fuel flow is not the heat input variable. If the fuel is oil there is approximately a static relation between the fuel flow and the heat flow to the risers. The heat may be transferred by radiation or convection or both. The proportions in which the heat is transferred are different in different boilers. The fuel-heat flow relation is then also different.

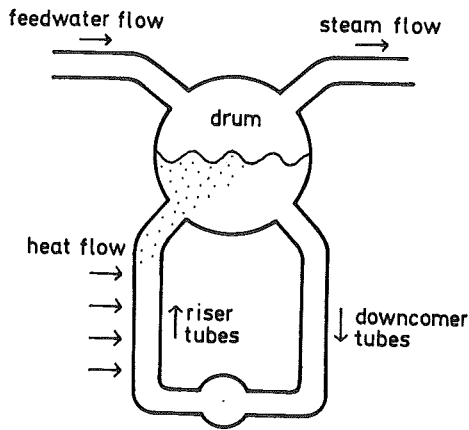


Fig 3.1 - The considered drum-downcomer-riser loop of a drum boiler.

We have taken the steam flow as an input to the drum system. When the drum system is connected with the other boiler components the control valve position will replace steam flow as an input variable. The control valve has the steam flow as an output variable.

The process includes some very intricate physical phenomena. The risers contain a boiling liquid and thus both a vapor phase and a liquid phase are present. The amount of each phase changes along the risers. The two phases have different densities and move with different velocities. There is a heat exchange between the vapor and the liquid. The temperature of the risers is not the same everywhere. The heat flow to the risers and the refrigeration supplied by the fluid are different in different parts of the riser banks.

The temperature of the feedwater is normally less than the saturation temperature. The temperature difference causes vapor to condense and effect the bubble formation in the drum. Thus both the pressure and the liquid level are influenced. The influence on these two variables will, however, depend on the way in which the feedwater is inserted into the drum.

An accurate description of the dynamic behaviour of such processes becomes very complex. The process is a distributed system. Some of the phenomena are difficult to express in mathematical terms. If the ambition is to derive a model of low order some simplifying assumptions must be applied.

Two possible approaches are recognized. The simplest way is to regard the drum system as an energy reservoir where the energy content is governed only by the drum pressure. The drum level is only influenced by feedwater and output steam flow. Applying these ideas two differential equations are sufficient. The drawback of this approach is that the non - minimum phase characteristics of drum level responses are not modelled. The second way then is to make an attempt to include this phenomenon. To do so, it is necessary to consider the behaviour of steam bubbles in risers and drum liquid. Since non-minimum phase behaviour is essential from a control point of view the later approach will be used here.

The drum system is divided into three components which are treated separately

- the downcomers,
- the drum,
- the risers.

In addition to the general assumptions stated previously we assume

- downcomers
 - (a) no boiling occur in the downcomers,
 - (b) liquid temperature is the same as drum liquid temperature,
- drum
 - (c) circulation is natural,
 - (d) there is no temperature gradient in the liquid and the vapor phase in the drum,

- (e) vapor phase is always of saturation state,
 - (f) feedwater is entered into the drum in such a way that the liquid phase becomes slightly undercooled,
 - (g) condensation or evaporation rate in the drum is proportional to the difference between liquid temperature and the saturation temperature,
 - (h) feedwater temperature does not vary,
- risers
- (i) there is no velocity difference between the vapor and the liquid phases in the risers,
 - (j) steam quality is linearly distributed along the risers,
 - (k) there is always saturation state in the risers and the same saturation state along the risers.

If the drum pressure is decreasing fast enough, boiling will occur in the downcomers. The circulation flow decreases and the refrigeration of the riser tubes may become insufficient. The result is a process failure. If we want to take this phenomenon into account we have to describe the behaviour of the downcomers quite accurately [31]. No attempt to model constraints on the time derivative of the drum pressure has been made.

The treatment of the circulation as natural is an example of a simplifying assumption. Forced circulation can easily be handled by an additional term in the equations. Both possibilities might be included in the model subroutine and the choice governed by input data. Assumptions (d) and (e) are physically well-grounded since the turbulence in the drum is considerable. Assumptions (f) and (g) allow us to describe the mass transportation phenomena caused by the subcooled feedwater. These assumptions are due to Chien and collaborators [10]. The liquid level variations due to the bubble formation is taken into account through the steam quality variable. This will introduce a non-minimum phase characteristic for the drum level dynamics. The feedwater temperature variations due to small load disturbances are assumed to be neglectable. This process input is thus set equal to a constant.

Assumptions (i) and (j) are coupled to each other. In the real process there is a velocity difference between the vapor and liquid phase. If we assume constant steam quality along the riser, it will be difficult to reach the true value of the steam quality at the outlet of the risers with a rea-

sonable circulation rate in the downcomer-riser loop. Assumption (j) will supply a solution to this problem and is physically motivated. If a mean value of the steam quality is used in the calculations, we will get two times this value at the outlet of the risers. If we want to take the velocity difference explicitly into account we have to introduce the so called slip factor. This is the standard technique in the theory of two-phase flow and is found in e.g. [6], [41].

Downcomers

The component is shown in Fig 3.2 and the variables used are indicated.

Since the fluid in the downcomers is water, it can be considered incompressible and since there is no heat exchange with the environment, we only have to apply a momentum equation. Notice, that the water in the downcomers instantaneously assume the temperature of the water in the drum. The downcomers terminate in a mud drum where a certain amount of the kinetic energy is dissipated due to turbulence. The downcomers are several parallel coupled tubes and may be treated as one tube. The Bernoulli equations for nonstationary flow without friction yields

$$\int_{p_d}^{p_{md}} \frac{dp}{\rho_w} + \int_{L_{d1}}^o g dz + \int_0^c c dc + \int_{L_{d1}}^o \frac{dc}{dt} dz = 0 \quad (3.1)$$

The integration shall be performed along a streamline A with the co-ordinate z . The integration is possible since the variables ρ_w , c and dc/dt can be considered as constant or zero throughout the streamline A. Integrating and adding correction terms of friction we get

$$(p_d - p_{md}) \frac{1}{g} = \left\{ f_d \frac{L_d}{D} + \zeta_{d1} + \zeta_{d2} + 1 \right\} \cdot \frac{m_w^2}{2g A_d^2 \rho_w} - \rho_w L_{d1} + \frac{L_{d1}}{g A_d} \frac{dm_w}{dt} \quad (3.2)$$

The velocity c_w is replaced with the mass flow m_w . The proportional constant f_d also takes energy losses in tube bends into account.

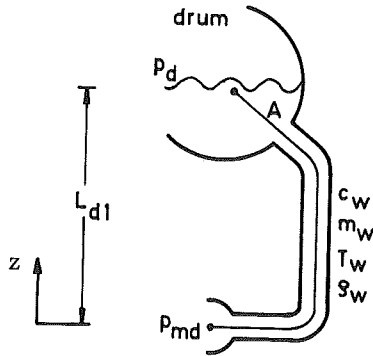


Fig 3.2 - Simplified diagram of the downcomer.

Risers

In Fig 3.3 the component under consideration is shown and variables used are indicated. Again the parallel coupled tubes are treated as one tube. We have assumed that the steam quality is distributed along the riser. Hence the velocity, the density and the enthalpy of the steam water mixture are dependent of the length co-ordinate z . In the equations, according to the assumptions, we must use some mean values of these variables.

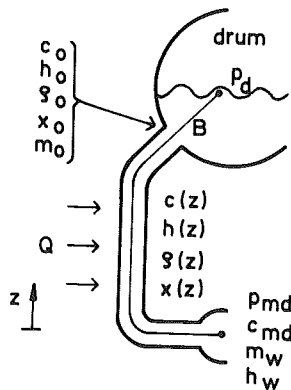


Fig 3.3 - Simplified diagram of the risers.

Fig 3.4 shows the simplified riser and the steam distribution. Let the steam distribution be

$$x = f(z) \tag{3.3}$$

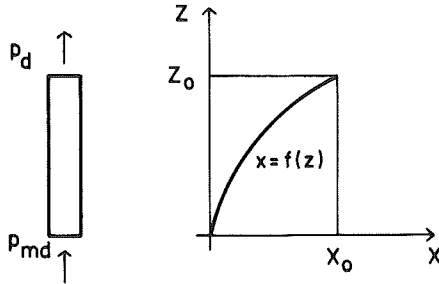


Fig 3.4 - The steam quality distribution along the riser.

Then the mean value x_m of the steam quality is defined as

$$x_m = \frac{1}{z_0} \int_0^{z_0} f(z) dz \tag{3.4}$$

In every section of the riser we have

$$\frac{1}{\rho} = \frac{x}{\rho_s} + \frac{1-x}{\rho_w} \tag{3.5}$$

If we define the mean value of the density of the steam-water mixture as the mean value of the steam quality above and use equations (3.3) and (3.5) we get

$$\rho_m = \frac{1}{z_0} \int_0^{z_0} \frac{\rho_s \rho_w}{\rho_s + f(z)(\rho_w - \rho_s)} dz \tag{3.6}$$

Since we assumed that there always is the same saturation state along the risers, the densities ρ_w and ρ_s are independent of the co-ordinate z .

Further we have in every section of the riser

$$h = h_{ws} + (h_{ss} - h_{ws})x \quad (3.7)$$

and thus the mean value is

$$h_m = h_{ws} + \frac{1}{z_o} \int_0^{z_o} (h_{ss} - h_{ws})f(z)dz \quad (3.8)$$

The enthalpies h_{ws} and h_{ss} are independent of the co-ordinate z according to the assumptions.

Assume a linear distribution. Hence

$$f(z) = Kz$$

and

$$x_m = \frac{Kz_o}{2}; \quad x_o = 2x_m \quad (3.9)$$

$$p_m = \frac{\rho_w \rho_s}{2x_m (\rho_w - \rho_s)} \ln \left(1 + 2 \frac{\rho_w - \rho_s}{\rho_s} x_m \right) \quad (3.10)$$

$$h_m = h_{ws} + (h_{ss} - h_{ws})x_m \quad (3.11)$$

The momentum equation yields

$$p_d \int_{p_{md}} \frac{dp}{\rho(z)} + \int_0^{L_{r1}} g dz + \int_{\sqrt{\xi} c_w}^{c_o} c dc + \int_0^{L_{r1}} \frac{dc(z)}{dt} dz = 0 \quad (3.12)$$

where the integration is taken along the streamline B in Fig 3.3. As indicated in the equation (3.12) the density ρ and the acceleration dc/dt are dependent of the variable z . This means that equation (3.12) cannot be directly integrated. However, using the mean value theorem for in-

tegrals we get

$$\int_{p_{md}}^{p_d} \frac{dp}{\rho(z)} = \frac{1}{\rho(z_1)} \int_{p_{md}}^{p_d} dp ; \quad 0 \leq z_1 \leq L_{r1} \quad (3.13)$$

$$\int_0^{L_{r1}} \frac{dc(z)}{dt} dz = \frac{dc(z_2)}{dt} \int_0^{L_{r1}} dz ; \quad 0 \leq z_2 \leq L_{r1} \quad (3.14)$$

The points z_1 and z_2 cannot be determined considering the assumptions made and will vary with changing operating conditions of the boiler. Then we have to guess the values of these variables. A simplifying assumption is

$$\frac{1}{\rho(z)} = \frac{1}{\rho_m} \quad (3.15)$$

and

$$\frac{dc(z_2)}{dt} = \frac{dc_o}{dt} \quad (3.16)$$

The preserved fraction of the kinetic energy in the mud drum is set equal to ξ . ξ is less than one and greater than zero. Integrating and adding correction terms for energy losses we get:

$$\begin{aligned} (p_{md} - p_d) \frac{1}{g} = & \left(f_r \frac{L_r}{D_r} + 1 \right) \frac{m_o^2 \rho_m}{2A_r^2 g \rho_o} + \zeta_3 \frac{m_w^2}{2A_r^2 g \rho_w} + \\ & + \zeta_4 \frac{m_o^2}{2A_r^2 g \rho_o} - \xi \frac{m_w^2 \rho_m}{2A_d^2 \rho_w} + \rho_m \frac{L_{r1}}{A_r g} + \frac{\rho_m L_{r1}}{A_r g} \frac{d}{dt} \left(\frac{m_o}{\rho_o} \right) \end{aligned} \quad (3.17)$$

The velocities c_{md} , c_w and c_o are replaced with the corresponding mass flows. The entrance and exit energy losses are set dependent of the entrance and exit velocities, respectively. The continuity equation becomes:

$$m_w - m_o = A_r L_{rl} \frac{d}{dt} \rho_m \quad (3.18)$$

and the energy equation

$$Q_r + m_w h_w - x_o m_o h_{ss} - (1-x_o) m_o h_{ws} = A_r L_{rl} \frac{d}{dt} (\rho h)_m \quad (3.19)$$

Terms due to the rate of change of the kinetic energy are neglected since they are small compared to the heat energy. It is very difficult to compute the exact mean value $d(\rho h)/dt$ along the riser, because ρ depends on pressure, flow etc. We use the approximation

$$\frac{d}{dt} (\rho h)_m = \frac{d}{dt} \rho_m h_m$$

where ρ_m and h_m are the mean values of the density and the enthalpy respectively. The linearized equation then contains the time derivative of ρ_m which is eliminated using the mass balance across the riser.

The heat flow to the risers Q_g is taken as a process input variable. The energy equation applied to the riser gives

$$Q_g - Q_r = M_r c_r \frac{d}{dt} T_r \quad (3.20)$$

where T_r is the mean temperature of the riser tubes. In literature e.g. [4] the following empirical formula is often used to describe the heat transportation from the riser tube walls to the steam water mixture

$$Q_r = k_r (T_r - T_s)^3 \quad (3.21)$$

The proportional constant k_r is calculated from steady state values.

Drum

Fig 3.5 gives the simplified diagram of the drum. The two phases, the vapor phase and the liquid phase, in the drum are treated separately. Energy and continuity equations are applied to the liquid phase and continuity equation to the vapor phase. The energy equation of the vapor phase is then automatically satisfied. Thus we get the following equations using variable notations indicated in Fig 3.5

$$(1-2x_m)h_{ws}m_o + h_{fw}m_{fw} - h_w m_w - h_{ss}m_e = \frac{d}{dt}(M_w h_w) \quad (3.22)$$

$$(1-2x_m)m_o + m_{fw} - m_w - m_e = \frac{d}{dt}M_w \quad (3.23)$$

and

$$2x_m m_o + m_e - m_s = \frac{d}{dt}(V_s \rho_s) \quad (3.24)$$

According to the assumptions the evaporation or condensation rate in the drum is

$$m_e = k_e(T_w - T_s) \quad (3.25)$$

In equations (3.22) and (3.24) two new variables, the mass of the liquid phase in the drum M_w and the volume of the vapor phase in the drum V_s , are introduced. Under small disturbances, these variables are approximately proportional to the drum system output variable, the drum level. The proportional constants are easily derived. This is used when the linearized set of equations are derived. However, in general we have

$$V_s = V_s(y) \quad (3.26)$$

$$M_w = M_w(y) \quad (3.27)$$

The functions are nonlinear due to the geometry of the drum.

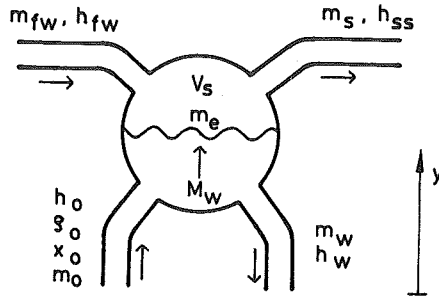


Fig 3.5 - The simplified drum diagram.

Thermal state equations

The thermal state of the steam-water mixture in the riser and of the vapor phase in the drum, is the saturation state. Then, there is only one independent thermal variable. Choose the drum pressure as the independent variable. Hence

$$T_s = T_s(p_d) \quad (3.28)$$

$$\rho_s = \rho_s(p_d) \quad (3.29)$$

$$h_{ss} = h_{ss}(p_d) \quad (3.30)$$

$$h_{ws} = h_{ws}(p_d) \quad (3.31)$$

The functions are nonlinear. The liquid phase in the drum is not in saturation state but is slightly undercooled. The dependence of the pressure of the enthalpy of the liquid phase is negligible and thus

$$h_w = h_w(T_w) \quad (3.32)$$

where $h_w(T_w)$ is a nonlinear function.

Steady state values

The set of equations which describes the drum system dynamic behaviour is given by the equations (3.2), (3.5), (3.9) through (3.11) and (3.17) through (3.32). If we include the process input variables in the m -vector u and the process output variables in the k -vector y and all other variables in the l -vector v , a compact notation is

$$f(\dot{v}, v, u) = 0 \quad (3.33a)$$

$$g(y, v, u) = 0 \quad (3.33b)$$

where f is an l -vector and g a k -vector whose components are nonlinear functions of the indicated variables. The set of equations is consistent if the dimensions of the vectors given above are the true dimensions. If all time derivatives are set equal to zero we get

$$f(0, v, u) = 0 \quad (3.34a)$$

$$g(y, v, u) = 0 \quad (3.34b)$$

If a solution to this set of nonlinear equations exists, this solution yields the steady state values of the variables v and y . Computer programmes which solve set of nonlinear equations are available. However, in this study, such a general approach to the problem has not been used since the structure of the equations is quite simple.

Except for construction parameters, such as the size of the drum, the length of tubes and the empirical correction constants, the steady state values of the following variables are known

- the heat input rate \overline{Q}_g
- the feedwater enthalpy \overline{h}_{fw}
- the drum pressure \overline{p}_d
- the temperature of the riser tubes \overline{T}_r
- the temperature of the liquid phase in the drum \overline{T}_w

The last two variables are not process input variables or otherwise given. Thus, they have to be guessed or measured on the actual physical process. However, usually it is possible to get a fairly good estimate of these variables.

The drum pressure determines all other variables associated with the fluid in saturation state. Hence we know the steady state values of

- the temperature \overline{T}_s
- the density of the vapor phase $\overline{\rho}_s$
- the density of the liquid phase $\overline{\rho}_w$
- the enthalpy of the vapor phase \overline{h}_{ss}
- the enthalpy of the liquid phase \overline{h}_{ws}

Equation (3.10) can be approximated with a straight line

$$o_m = c_1 x_m + c_2 \quad (3.35)$$

The line is adjusted to fit as good as possible in the interval, in which the mean value of the steam quality is supposed to vary. This approximation is used when the steady-state value of the mean value of the steam quality is computed. Manually the equations (3.2), (3.5), (3.17), (3.18), (3.19) and (3.35), with time derivatives set equal to zero, are reduced to a third order polynomial in the mean value of the steam quality. Using the real positive root of the polynomial, the original set of equations is solved for the other variables. Hence we know the steady state values of the variables

- the mean value of the steam quality \overline{x}_m
- the mean value of the density of the steam-water mixture $\overline{\rho}_m$
- the outlet density of the steam-water mixture $\overline{\rho}_o$
- the mean value of the enthalpy of the steam-water mixture \overline{h}_m
- the circulation mass flow \overline{m}_o

Equation (3.21) gives the heat transfer coefficient

$$k_r = \frac{\overline{Q}_r}{(\overline{T}_r - \overline{T}_s)^3} \quad (3.36)$$

The equations (3.22), (3.23), (3.24) and (3.25) with time derivatives set equal to zero give the evaporation constant

$$k_e = \frac{\overline{m}_o}{\overline{h}_{ss} - \overline{h}_{fw}} \left[2\overline{x}_m \frac{\overline{h}_{ws} - \overline{h}_{fw}}{\overline{T}_s - \overline{T}_w} - \frac{\overline{h}_{ws} - \overline{h}_w}{\overline{T}_s - \overline{T}_w} \right] \quad (3.37)$$

Now equations (3.25), (3.24) and (3.23) determines the steady state values of

- the evaporation mass flow \overline{m}_e
- the outlet steam flow \overline{m}_s
- the feedwater flow \overline{m}_{fw}

Linearized set of equations

The perturbed variables, that is, the difference between the actual value and the steady state value of the variables, are denoted as the variables themselves. The linearized set of thermal state equations become

$$T_s = k_T p_d \quad (3.38)$$

$$\rho_s = k_\rho p_d \quad (3.39)$$

$$h_{ss} = k_h p_d \quad (3.40)$$

$$h_{ws} = k_w p_d \quad (3.41)$$

where the proportional constants are obtained from a steam table. The linearized versions of equations (3.26) and (3.27) are

$$V_s = -Ay \quad (3.42)$$

$$M_w = A\rho_w y \quad (3.43)$$

Hence the geometry of the drum is neglected. Using the above equations the left-hand variables are eliminated from the other equations. It is further relatively simple to eliminate the outlet density ρ_o and one of the variables ρ_m and x_m using the linearized versions of the equations

(3.5) and (3.10). From a computational point of view the variables ρ_m and x_m are equivalent. However, the most informative variable is the mean value of the steam quality and we choose to keep this variable. The pressure difference in the two momentum equations (3.2) and (3.17) is also eliminated. The linearized system then is

$$a_1 \dot{p}_d + a_2 \dot{x}_m + a_3 m_o + a_4 m_w = 0 \quad (3.44)$$

$$a_5 \dot{m}_o + a_6 \dot{m}_w + a_7 p_d + a_8 x_m + a_9 m_o + a_{10} m_w = 0 \quad (3.45)$$

$$a_{11} \dot{p}_d + a_{12} \dot{x}_m + a_{13} p_d + a_{14} T_w + a_{15} x_m + a_{16} m_o + a_{17} m_w + a_{18} Q_r = 0 \quad (3.46)$$

$$a_{19} p_d + a_{20} T_r + a_{21} Q_r = 0 \quad (3.47)$$

$$a_{22} \dot{T}_r + a_{23} Q_g + a_{24} Q_r = 0 \quad (3.48)$$

$$a_{25} \dot{y} + a_{26} \dot{T}_w + a_{27} p_d + a_{28} T_w + a_{29} x_m + a_{30} m_{fw} + a_{31} m_o + a_{32} m_w + a_{33} m_e = 0 \quad (3.49)$$

$$a_{34} \dot{y} + a_{35} x_m + a_{36} m_{fw} + a_{37} m_o + a_{38} m_w + a_{39} m_e = 0 \quad (3.50)$$

$$a_{40} \dot{p}_d + a_{41} \dot{y} + a_{42} x_m + a_{43} m_s + a_{44} m_o + a_{45} m_e = 0 \quad (3.51)$$

$$a_{46} p_d + a_{47} T_w + a_{48} m_e = 0 \quad (3.52)$$

The first three equations are obtained by using the pairs (3.18), (3.10), and (3.2), (3.17), and (3.18), (3.19). The last six we get from eqs. (3.21), (3.20), (3.22), (3.23), (3.24) and (3.25) respectively. The coefficients are found in Appendix B expressed as functions of the steady state values of the variables and of the drum system construction parameters. Before the momentum equation for the riser is linearized, the acceleration term is simplified by setting $d/dt(m_o/\rho) = 1/\rho d/dt m_o$.

Rewriting this set of linear equations on the form of eq. (3.4a) in Chapter 2 we get

$$E \frac{dv}{dt} + Fv + Gu = 0 \quad (3.53)$$

where E, F and G are matrices of proper order and

$$v^T = (p \ y \ T_w \ T_r \ x_m \ m_o \ m_w \ m_e \ Q_r) \quad (3.54)$$

$$u^T = (Q_g \ m_{fw} \ m_s) \quad (3.55)$$

The set of equations for the drum contains seven derivatives of physical variables. It is, however, easy to see from the structure of the matrix E that the number of state variables for the drum system does not exceed six. It is then necessary to use the general approach to the model building problem presented in Chapter 2. In fact these equations were used as an example in Chapter 2.

The properties of this model will be discussed in Section 4.

3.2 Superheater

The number of papers treating different kinds of heat exchangers is indeed very large. Several investigators [3], [19], [42] have also compared different types of models which represent different degree of approximation. Generally, it can be said that the developed equations represent the dynamics of heat exchangers accurately. The model, however, becomes very complex and we end up with nonlinear partial differential equations. It is required e.g. that the dependence of heat transfer coefficients on physical variables such as flow and temperatures is known a priori.

The standard technique of approximation is to replace the partial differential equations with a number of ordinary differential equations. It can be shown that the approximation error is decreased with increased number of ordinary equations used.

Here this standard technique will be applied to a superheater. The original nonlinear equations will be linearized and the final model is a linear model.

To obtain a flexible model the number of ordinary differential equations used to approximate the superheater is free. That is, the model computer subroutine will have this number as an input variable. The physical motivation to this approach is that the size of different superheaters of the boiler vary considerably. It is also important to be able to investigate the influence of the choice of division number on the dynamics of the entire boiler.

Model equations

A schematic picture of the superheater is shown in Fig 3.6 where also the used notations are indicated.

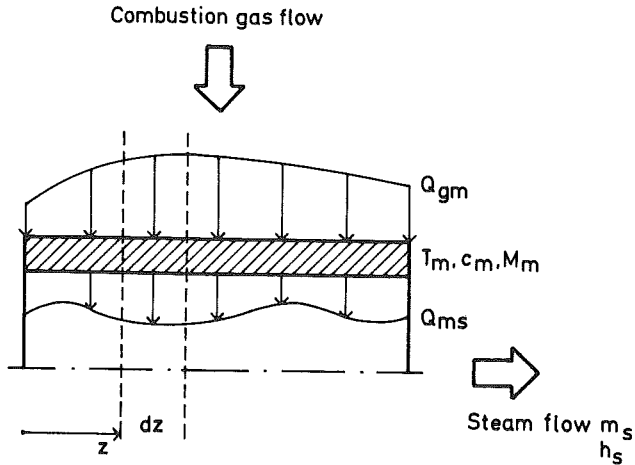


Fig 3.6 - A one tube representation of a superheater.

The superheater is assumed to be a heat exchanger of the cross flow type. The tubes are represented by one tube with constant dimensions throughout the whole length. The standard simplifying assumptions now are

- (a) there is no heat transportation in the axial direction neither in the tube nor in the steam,
- (b) radial distributions of variables are averaged and the only space variable is z measured in the flow direction,
- (c) heat conductivity of tube material is infinite,
- (d) flow is free from losses,
- (e) flow is incompressible.

A crude estimate of the time constant associated with the compressibility of the steam gives figures of the order of seconds. Hence assumption (e) is considered justified. Applying an energy balance to the element of length dz in Fig 3.6 we get for the tube

$$Q_{gm} dzdt = Q_{ms} dzdt + c_m M_m \frac{\partial T_m}{\partial t} dzdt$$

and for the steam

$$Q_{ms} dzdt = m_s \frac{\partial h_s}{\partial z} dzdt + M_s \frac{\partial h_s}{\partial t} dzdt$$

or

$$Q_{gm} = Q_{ms} + c_m M_m \frac{\partial T_m}{\partial t} \quad (3.56)$$

$$Q_{ms} = m_s \frac{\partial h_s}{\partial z} + M_s \frac{\partial h_s}{\partial t} \quad (3.57)$$

where

Q_{gm} heat transfer rate from gas to tube [kJ/s m]

Q_{ms} heat transfer rate from tube to steam [kJ/s m]

m_s steam flow [kg/s]

M_s, M_m mass of steam and tube respectively [kg/m]

c_m specific heat of tube material [kJ/kg °C]

h_s enthalpy of steam [kJ/kg]

T_m temperature of tube material

In order to simplify the superheater model further, a rough estimate of the dynamics of heat capacity of the steam is made. Again the time constant is about one second for typical cases. Consequently we put $\partial h_s / \partial t$ equal to zero.

The spatial derivative of eq. (3.57) can be eliminated using a difference approximation

$$\frac{\partial x}{\partial z} = \frac{x_2 - x_1}{\Delta z}$$

where x_2 and x_1 denote the value of the variable x at the end and beginning of a finite section of length Δz . The value of x can be chosen as any point in the interval Δz . The most obvious choices are

$$x = x_1(t)$$

$$x = x_2(t)$$

$$x = \frac{1}{2} \{x_1(t) + x_2(t)\}$$

referred to as forward, backward and central difference approximations respectively.

It is easily shown that the forward difference method gives an unstable system. The central difference method can, uncaredfully applied, give responses with no physical interpretation. The most satisfactory method is the backward difference method and is adopted here.

The superheater is divided into N sections as shown in Fig 3.7. Index n is used to refer variables to section n . As a consequence of this approximation, all variables are assumed to be constant within each section and equal to the output value. The equations governing heat dynamics for section n then are

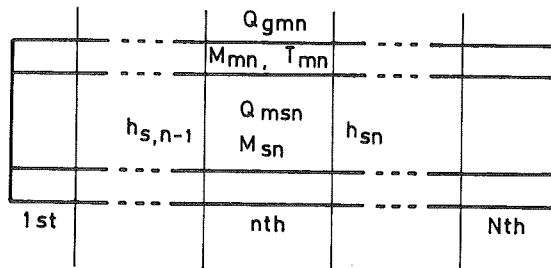


Fig 3.7 - The superheater divided into N sections.

$$Q_{gmn} = Q_{msn} + c_m M \frac{dT_{mn}}{dt} \quad (3.58)$$

$$Q_{msn} = m_s (h_{sn} - h_{s, n-1}) \quad (3.59)$$

The pressure drop over a superheater is essential and cannot be neglected. For each section of the superheater, the pressure drop is lumped to the end of the section. The assumptions reduce the momentum equation to

$$\Delta p = k_{p1} m_s^2 \quad (3.60)$$

The constant k_{p1} is first determined for the entire superheater. Assuming that the pressure drop is linearly distributed over the superheater, the proportional coefficient for each section is given as k_{p1} divided by the number of sections.

It was stated earlier in this chapter that heat transfer rates from combustion gases to risers and superheaters were taken to be proportional to the fuel flow. This certainly limits the validity range of the model. Depending on the type of heat transfer, the load dependent characteristics of the superheater will vary. This is schematically shown in Fig 3.8.

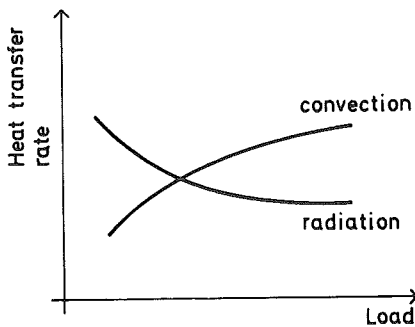


Fig 3.8 - Heat transfer characteristics of a superheater.

For small variations around the steady state value, the heat transfer rate Q_{gmn} approximately equals

$$Q_{gmn} = k_f m_f \quad (3.61)$$

The coefficient k_f is determined from steady state values.

The heat transfer rate Q_{msn} is supposed to follow the power law of Nussel

$$Q_{msn} = k_{sp} m_s^{0.8} (T_{mn} - T_{sn}) \quad (3.62)$$

This assumption is frequently [4], [38] used in literature. The constant k_{sp} is computed from steady state values.

Thermal state equations

In eq. (3.59) the enthalpy of steam at the inlet, $h_{s, n-1}$, and the outlet, h_{sn} , of the n :th section of the superheater is used. For superheated steam, the enthalpy depends both on pressure and temperature. The nonlinear functions are written as

$$h_{s, n-1} = h_{s, n-1}(p_{s, n-1}, T_{s, n-1}) \quad (3.63)$$

$$h_{sn} = h_{sn}(p_{sn}, T_{sn}) \quad (3.64)$$

Steady state values

The superheater is a typical process where a static model can be used to a large extent. The static model can supply the steady state values of the temperature distribution of steam and the temperature distribution of tube material along the superheater. Such a model can also give the value of the constant k_f since the heat transfer rates are known.

The value of the steam flow, which is required for the computations, is calculated in the drum system subroutine and transferred via input data.

The only derivative, which appears in eqs. (3.67) and (3.68), is that of the tube temperature in section n . The order of the complete linear model will then equal the division number N . If the state space form $S(A, B, C, D)$ of the superheater model is wanted only the simpler alternative model building approach has to be used.

The model properties can now be summarized as follows. The only dynamics considered is the heat capacity of tube walls. The stationary gain will show good agreement with the real one within the validity range of the linearized thermal state equations. The high frequency behaviour will improve with increased division number N . For details of model properties see e.g. [3].

3.3 Attemperator

A spray type attemperator is considered. The cooling of the steam is simply achieved by injecting water into the steam flow. The volume and material masses of such an attemperator are small. Therefore all dynamics of the attemperator is neglected. Using notations indicated in Fig 3.9 energy, mass and momentum equations give

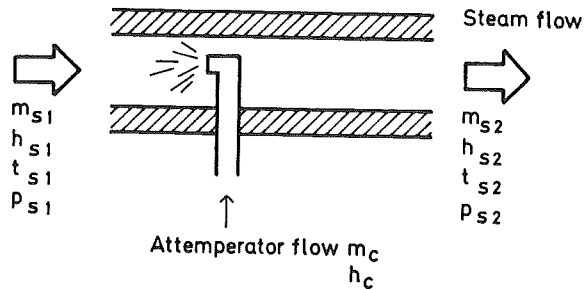


Fig 3.9 - A schematic diagram of a spray attemperator.

$$m_{s1} h_{s1} + m_c h_c = m_{s2} h_{s2} \quad (3.70)$$

$$m_{s1} + m_c = m_{s2} \quad (3.71)$$

$$p_{s1} - p_{s2} = k_{p2} m_{s2}^2 \quad (3.72)$$

The pressure drop is lumped to the end of the attemperator. The drop is small and if it is desirable to have it zero, the constant k_{p2} is set to zero.

The thermal equations required are

$$h_{s1} = h_{s1}(p_{s1}, T_{s1}) \quad (3.73)$$

$$h_{s2} = h_{s2}(p_{s2}, T_{s2}) \quad (3.74)$$

The enthalpy of the coolant is assumed to be constant. Often this is justified since the water supplied to the attemperators is feedwater taken at the outlet of the economiser.

Steady state values of flows and enthalpies are known. Steam flow is, as before, computed in the drum system subroutine. The constant k_{p2} can then be calculated.

Linearizing eqs. (3.70) through (3.74) and eliminating enthalpy variables we get

$$\begin{aligned} a_1 T_{s2} + a_2 p_{s2} + a_3 m_{s1} + a_4 T_{s1} + a_5 p_{s1} + \\ + a_6 m_{s2} + a_7 m_c = 0 \end{aligned} \quad (3.75)$$

$$a_8 m_{s1} + a_9 m_{s2} + a_{10} m_c = 0 \quad (3.76)$$

$$a_{11} p_{s2} + a_{12} p_{s1} + a_{13} m_{s2} = 0 \quad (3.77)$$

The coefficients are given in Appendix B. The introduced specific heat constants are defined as in eqs. (3.65) and (3.66).

The generated \hat{Q}_i matrix is defined by

$$\hat{Q}_i z = 0$$

where

$$z^T = (T_{s2} \ p_{s2} \ m_{s1} \ T_{s1} \ p_{s1} \ m_{s2} \ m_c) \quad (3.78)$$

3.4 Control Valve

Since the pressure ratio between inlet and outlet of the control valve may be above the critical ratio both the subcritical and overcritical cases are considered. In both cases, the control valve is assumed to be an ideal restriction which preserves the enthalpy of the steam. The approach taken is adopted from [38].

Subcritical case

The control valve area A_v is a function of the rod position u

$$A_v = f(u) \quad (3.79)$$

The function f has to be determined from construction data or measurements.

The flow through the valve is supposed to be governed by

$$m_s^2 = k_v (p_{s1} - p_{s2}) A_v^2 \quad (3.80)$$

where k_v is a constant and A_v is the control valve area. The indices 1 and 2 refer variables to the inlet and the outlet respectively.

Since enthalpy is preserved we have

$$h_{s1}(p_{s1}, T_{s1}) = h_{s2}(p_{s2}, T_{s2}) \quad (3.81)$$

The linearized set of equations for the control valve is, after the elimination of A_v

$$m_s + a_1 u + a_2 p_{s1} + a_3 p_{s2} = 0 \quad (3.82)$$

$$a_4 T_{s2} + a_5 p_{s1} + a_6 p_{s2} + a_7 T_{s1} = 0 \quad (3.83)$$

Again coefficients are found in Appendix B. The constant a_1 is computed from the calibration curve. Eq. (3.81) above is used to compute the steam temperature at the outlet of the valve.

The matrix \hat{Q}_i , valid for the control valve in the subcritical case, is defined by the relation

$$\tilde{Q}_i z = 0$$

where

$$z^T = (m_s^T \quad T_{s2}^u \quad p_{s1} \quad p_{s2}^T \quad T_{s1}^T) \quad (3.84)$$

Overcritical case

In the overcritical case, steam flow will only depend on inlet pressure, that is

$$m_s = k \frac{A}{v} \frac{p_{s1}}{v} \quad (3.85)$$

or linearized and using eq. (3.79) to eliminate A_v

$$m_s + a_8 u + a_9 p_{s1} = 0 \quad (3.86)$$

Together with eq. (3.83) the above equation completes the model. The matrix \tilde{Q}_i is defined using the same variable z as in the previous case eq. (3.84).

3.5 Turbine

Large power plants are usually equipped with a reheater thus requiring two turbine units. The expansion of the steam before the reheater takes place in the high pressure turbine (H. P. turbine) and after the reheater in the low pressure turbine (L. P. turbine). Two different models will be derived corresponding to two different approximations of the steam flow through the turbine.

The assumptions guiding the modelling process are

- (a) the prime output of the model is active power (as distinguished from the number of revolutions of the turbine),
- (b) turbine dynamics could be neglected,
- (c) efficiency of the turbine is constant,
- (d) condenser pressure is constant and an equivalent steam mass flow could be used to simulate the steam taken from turbine stages for preheating of feedwater.

To be able to model the number of revolutions of the turbine, a model of the alternator, the transmission lines and the load must be included. This is beyond the scope of this work. Assumption (b) is based on the general philosophy that minor dynamical effects are neglected in order to keep the model as simple as possible. This is also the motivation for assumptions (c) and (d) which are also believed to be satisfactory accurate.

Both models are based on the fact that active power equals the product of an equivalent steam flow and the enthalpy drop over the turbine reduced according to the efficiency of the turbine.

High pressure turbine

The state changes of the steam in the turbine can be visualized in an enthalpy-entropy diagram (h-s diagram) as in Fig 3.10. For the ideal

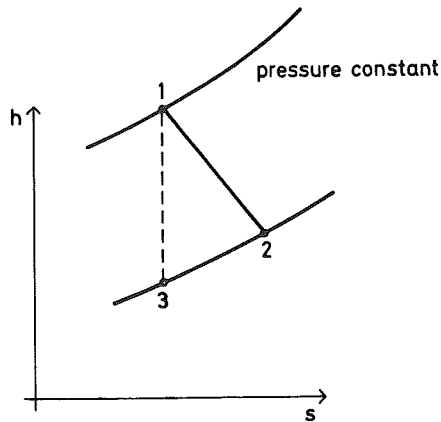


Fig 3.10 - An h-s diagram of steam expansion in H. P. turbine.

turbine, the change of the steam state takes place along the dashed line 1-3. Due to an efficiency less than one the state change will go from state 1 to state 2. Using indices 1, 2 and 3 to refer variables to state 1, state 2 and state 3 the following relation is used for active power P_{HT}

$$P_{HT} = m_s (h_{s1} - h_{s2}) \quad (3.87)$$

where

$$h_{s1} - h_{s2} = \eta_t (h_{s1} - h_{s3}) \quad (3.88)$$

The constant η_t is the turbine efficiency. If the pressure drop is assumed to be under the critical one along the steam path in the turbine a good approximation of the steam flow is given by [44].

$$m_s = C_t \sqrt{\frac{p_{s1}}{v_{s1}} \left[1 - \left(\frac{p_{s2}}{p_{s1}} \right)^2 \right]} \quad (3.89)$$

To eliminate the dependence of the specific volume v_{s1} a modification of the ideal gas law could be used [44]. Hence

$$\frac{p_{s1} v_{s1}}{T_{s1}} = C \quad (3.90)$$

where

$$C = \gamma R \quad (3.91)$$

The ideal gas law constant $R = 461.5 \text{ J/kg}^\circ\text{K}$ and a suitable value of γ is 0.933.

The thermal state equations necessary are

$$h_{s1} = h_{s1}(p_{s1}, T_{s1}) \quad (3.92)$$

$$s_{s1} = s_{s1}(p_{s1}, T_{s1}) \quad (3.93)$$

$$h_{s3} = h_{s3}(p_{s2}, s_{s3}) \quad (3.94)$$

$$h_{s2} = h_{s2}(p_{s2}, T_{s2}) \quad (3.95)$$

$$s_{s1} = s_{s3} \quad (3.96)$$

Since all steady state temperatures and pressures are known, all introduced proportional constants can be computed.

When linearizing the thermal state equations, the following constants are introduced in addition to those given by eq. (3.65) and (3.66)

$$c_s = \left(\frac{\partial h}{\partial p} \right)_{s = \text{constant}} \quad (3.97)$$

$$c_{sp} = \left(\frac{\partial h}{\partial s} \right)_{p = \text{constant}} \quad (3.98)$$

$$d_p = \left(\frac{\partial s}{\partial T} \right)_{p = \text{constant}} \quad (3.99)$$

$$d_T = \left(\frac{\partial s}{\partial p} \right)_{T = \text{constant}} \quad (3.100)$$

Eliminating all variables except for T_{s1} , p_{s1} , T_{s2} , P_{HT} and m_s the linearized set of equations is

$$a_1 p_{s1} + a_2 P_{HT} + a_3 T_{s1} + a_4 m_s = 0 \quad (3.101)$$

$$a_5 T_{s2} + a_6 p_{s1} + a_7 p_{s2} + a_8 T_{s1} + a_9 m_s = 0 \quad (3.102)$$

$$a_{10} p_{s1} + a_{11} p_{s2} + a_{12} T_{s1} + a_{13} m_s = 0 \quad (3.103)$$

Coefficients are given in Appendix B. Again we have a static model and the matrix \tilde{Q}_1 is determined by defining the z-vector as

$$z^T = (T_{s2} \ p_{s1} \ P_{HT} \ p_{s2} \ T_{s1} \ m_s) \quad (3.104)$$

Low pressure turbine

Assuming a pressure drop above the critical one along the steam path, the steam flow can be modelled as

$$m_s = \frac{1}{K} p_{s1} \quad (3.105)$$

which is also used in [38]. Except for the steam flow equation, all other equations are the same as in the previous case. Note, however, that the condenser pressure is assumed constant which means that in the linearized set of equations the variable p_{s2} vanishes.

Defining the z-vector as

$$z^T = (P_{LT} \ p_{s1} \ T_{s1} \ m_s) \quad (3.106)$$

the elements of the \hat{Q}_i matrix are given by the following set of linear equations where variables not contained in z are eliminated

$$a_1 P_{LT} + a_2 p_{s1} + a_3 T_{s1} + a_4 m_s = 0 \quad (3.107)$$

$$a_5 p_{s1} + a_6 m_s = 0. \quad (3.108)$$

The derived models are quite general. For the high pressure turbine the only model restriction is that the steam mass flow is governed by eq. (3.89). Obviously this model also can be used for a low pressure turbine if eq. (3.89) is true. In the low pressure turbine model the steam mass flow is proportional to the inlet pressure. In cases where this assumption is a relevant approximation and where the counter pressure is constant it can be applied regardless of the pressure range covered. The later model can be extended to include a variable counter pressure.

4. Comparison of Drum System Models

It is important that the derived model for the boiler is of as low order as possible. Inspecting the linearized set of equations given for the drum system we find seven derivatives of physical variables. In Chapter 2 an application of Theorem 1 showed that the order of the drum system model was at most six.

4.1 Model Order

Three drum system models of different order will be derived and compared. The sixth order model results from the equations derived in the previous section. The fastest modes of this model are those of the down-comer and riser. This implies the following assumptions to reduce model order.

- (a) neglect the acceleration terms in the Bernoulli equations for downcomer and riser,
- (b) neglect all dynamics of downcomer and riser.

The number of derivatives of physical variables in the models obtained are five and four respectively. An upper bound of the order is thus found immediately.

Using the general reduction technique for the sixth order model as described in Chapter 2 the state space model was obtained as

$$\frac{dx}{dt} = Ax + Bu \quad (4.1)$$

$$y = Cx \quad (4.2)$$

The state variables are

- x_1 drum pressure [bar]
- x_2 drum liquid level [m]
- x_3 drum liquid mean temperature [$^{\circ}$ C]
- x_4 mean temperature of riser [$^{\circ}$ C]
- x_5 mean value of steam quality
- x_6 a linear combination of mass flow at outlet of riser and mass flow of downcomer [kg/s]

and the input variables are

- u_1 heat input rate to riser [kJ/s]
- u_2 feedwater flow [kg/s]
- u_3 steam outlet flow [kg/s]

The output variables y_1 and y_2 equal the first two state variables.

Applying the alternative reduction method to the set of equations obtained, when assumptions (a) and (b) are imposed, the model order is found to equal five and four respectively. The inputs to these models are the same as for the sixth order model. The state variables for the fifth order model can be chosen as the first five components of the state

vector given above and for the fourth order model as the first four components.

To be able to compare the different models, it is necessary to introduce a numerical example. Such an example is given below. The eigenvalues as well as the model responses to step changes of input variables will be compared. The influence of input data on model properties is discussed.

4.2 Numerical Example

The boiler data used is taken from a thermal power plant boiler. The maximum steam flow is 350 t/h and the drum pressure is 140 bar. The energy loss coefficients of flow are calculated from empirical equations given in literature. The friction coefficients f_r and f_d can be used to adjust the steam quality at the outlet of the risers. The feedwater temperature is $\sim 230^\circ\text{C}$. The heat flow to the risers is calculated from a heat balance in steady state. Two temperatures have to be guessed, the drum liquid temperature and the temperature of riser tubes. The riser temperature is often approximately known. A straight line is manually fitted to eq. (3.10) in the interval $0.07 \leq x_m \leq 0.09$. The thermal state data and proportional constants are taken from steam tables. If the pressure is changed, we thus have to change thermal state data, proportional constants and the coefficients of the straight line fit.

In this case drum liquid temperature has been guessed to be 326°C which is about 10°C below the saturation temperature. The mean temperature of riser is set to 480°C . The factor ξ is 0.5 and friction coefficients f_r and f_d are 0.1 and 0.2 respectively. All other data are boiler construction data or thermal state data determined by the drum pressure.

Eigenvalues

In Table 4.1 below the eigenvalues of matrix A for the three models are given. Notable is the unstable mode of all models. The existence of such a mode is physically motivated.

Consider the drum system as an energy reservoir with stored energy H, input power P_i and output power P_o then an energy balance gives

$$\frac{dH}{dt} = P_i - P_o \quad (4.3)$$

| Eigen-
value
No. | 4:th order
model | 5:th order
model | 6:th order
model |
|------------------------|-----------------------|-----------------------|-----------------------|
| 1 | 0.000 | 0.000 | 0.000 |
| 2 | $3.95 \cdot 10^{-3}$ | $1.35 \cdot 10^{-3}$ | $1.42 \cdot 10^{-3}$ |
| 3 | $-8.89 \cdot 10^{-2}$ | $-9.19 \cdot 10^{-2}$ | $-9.19 \cdot 10^{-2}$ |
| 4 | $-3.26 \cdot 10^{-1}$ | $-1.23 \cdot 10^{-1}$ | $-1.22 \cdot 10^{-1}$ |
| 5 | | $-7.34 \cdot 10^{-2}$ | $-7.40 \cdot 10^{-2}$ |
| 6 | | | -1.58 |

Table 4.1 - Eigenvalues of the 4:th, 5:th and 6:th order drum system models.

Input power is a function of fuel flow and power contained in feedwater. Output power equal steam mass flow times steam enthalpy. Assume that all inputs that is, fuel flow, feedwater power and steam flow are kept constant. Linearizing eq. (4.3) we get

$$\frac{d}{dt} \Delta H = -m_s \Delta h_s \quad (4.4)$$

If we assume saturation state in the entire drum system we have

$$\Delta h_s = k_s \Delta p_d$$

$$\Delta \dot{H} = k_H \Delta p_d$$

where k_s is a negative constant. The sign of the constant k_H depends on the mass of steam and water in the drum system and on how the iron masses are taken into account. If the influence of iron masses is neglected, we get for $p_d = 140$ bar

$$\frac{V_w}{V_s} < 7.1 \Rightarrow k_H \text{ positive}$$

where V_s and V_w are the volumes of steam and water in the drum

system respectively. In this case the total volume of water in downcomer, riser and drum is 88 m^3 and that of steam is 14 m^3 . The ratio is less than 7.1 and the mode of eq. (4.4) is unstable. This simple analysis thus indicates that it is possible to get an unstable model of the drum system. However, moderate errors when estimating the steam and water volumes could change stable model dynamics into unstable and conversely.

When the complete model is built, steam mass flow is no longer an input variable. Other components are coupled to the drum system and the unstable mode is changed into a stable mode.

Starting with the fifth order model it is possible to give a physical interpretation to some of the eigenvalues. The zero eigenvalue is obviously associated with the drum liquid level. The unstable mode is the dominating eigenvalue and generated by the heat capacity of the water, iron and steam masses. The three remaining eigenvalues are of the same order of magnitude and it is difficult to separate them. Thus the order between the fourth and the fifth eigenvalue is arbitrary. The sixth eigenvalue, -1.58 , is associated with the mass flow derivatives of the momentum equations. Since the corresponding mode respond rapidly assumption (a) is a good approximation.

Between the fifth and sixth order models the first five eigenvalues of matrix A only differ slightly. Comparing the fourth order model with the other models there is a more marked difference.

Simulated stepresponses

The open loop responses of state variables of the three models to a step change in the heat input flow, the feedwater flow and the steam outlet flow are given in Figs 4.1, 4.2 and 4.3. Comparing the responses, we find an extremely good agreement between the fifth and sixth order models. We thus conclude that the dynamic behaviour of the model is not strongly affected by approximation (a). The essential difference between the fourth and fifth order models is that the non-minimum phase response of the drum liquid level does not appear in the fourth order model. This non-minimum phase behaviour is a significant property of the real process. Thus the steam quality variable, which is a state variable in the fifth order model, takes at least qualitatively the effects of bubble formation in the riser and the drum into account. If we want to include this effect in the model, the dynamic behaviour of the riser cannot be neglected. There seems also to be a considerable difference in gain between the fourth and sixth order models. The difference is, however, partly due to the difference between the unstable mode of the models.

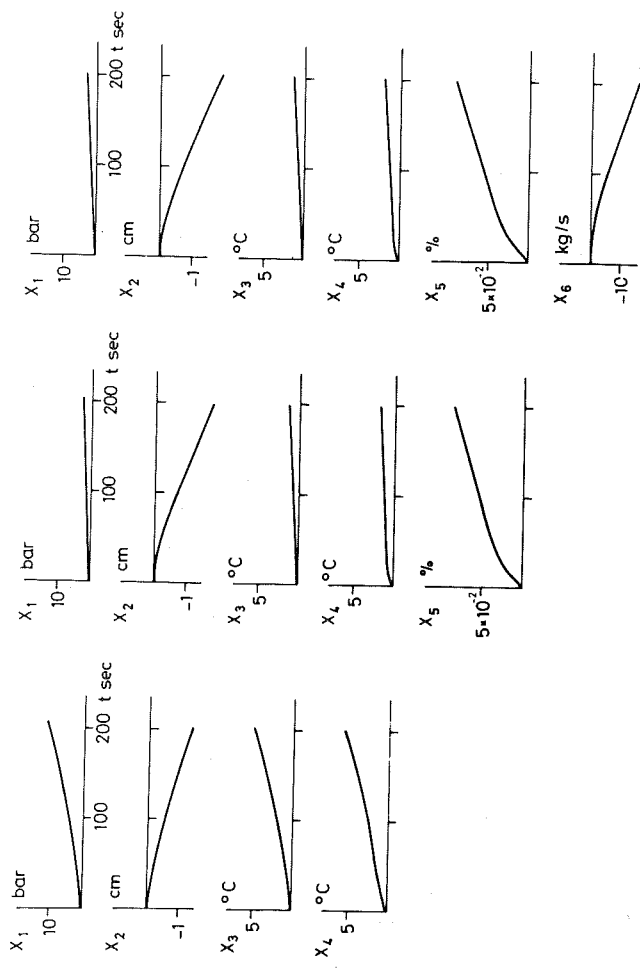


Fig 4.1 - Open loop responses of the state variables of the 4:th, 5:th and 6:th order models to a step change in the heat flow to the risers of 200 kJ/s ($\sim 1\%$).

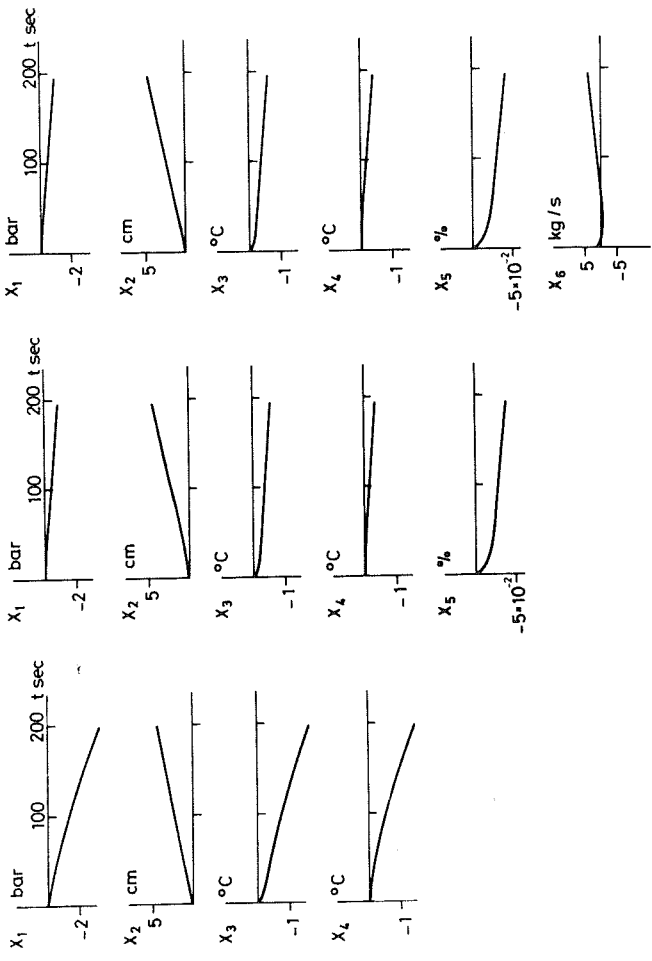


Fig 4.2 - Open loop responses of the state variables of the 4:th, 5:th and 6:th order models to a step change in the feedwater flow of 2 kg/s ($\sim 1\%$).

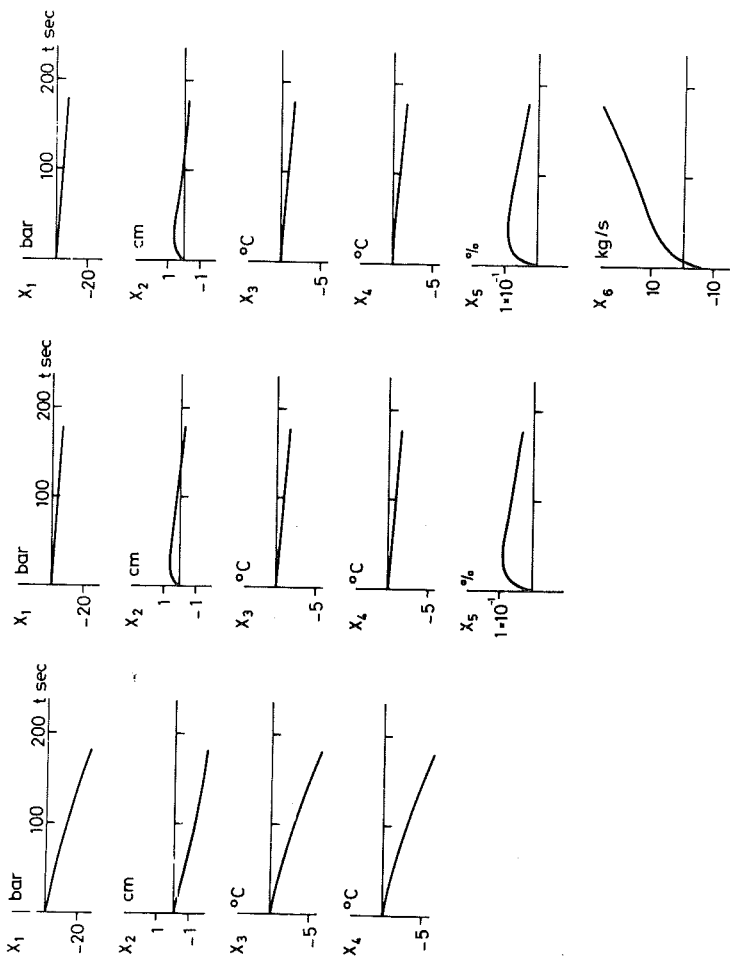


Fig 4.3 - Open loop responses of the state variables of the 4:th, 5:th and 6:th order models to a step change in the outlet steam flow of 2 kg/s ($\sim 1\%$).

Parameter variations

A number of drum system models were generated with different input data. It was found that the factor ξ did not influence the value of the eigenvalues. When the guessed mean temperature of riser tubes was changed 20°C only a very slight change of the system eigenvalues resulted. If the drum liquid temperature was raised to a value only 1°C from the saturation temperature a considerable change of one of the eigenvalues (No. 4 in the fourth order model) took place. For a difference between drum liquid temperature and saturation temperature larger than 5°C it is believed that the estimated liquid temperature is not critical.

4.3 Conclusions

The comparison of drum system models above clearly indicates that for our purposes the fifth order model is the most satisfactory. Thus this model will be used when modelling the entire process. The computer subroutine DR5M is given in Appendix A.

The acceleration terms of the momentum equations for the riser and downcomer can be neglected. If a non-minimum phase behaviour of drum liquid level is desirable the dynamics of the risers must be included. Finally, it was found that model properties did not critically depend on estimated physical variables.

5. Application to Öresundsverket Power Plant

A number of models for different boiler subprocesses have been derived. To be able to apply these models, the considered power plant first has to be divided into subprocesses which are recognized. This procedure requires that the assumptions stated in Section 3 are valid and may also require additional simplifications.

5.1 Simplified Configuration

In Fig 5.1 a simplified diagram of the Öresundsverket power plant unit P16-G16 is given. The development of this figure is based on the assumptions made in Section 3.

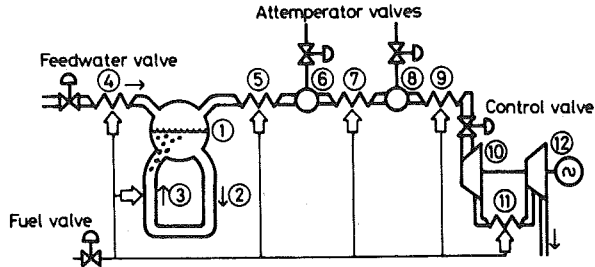


Fig 5.1 - A simplified plant configuration.

- | | |
|-------------------|---------------------------|
| 1. Drum | 8. Attemperator 2 |
| 2. Downcomer | 9. Superheater 3 |
| 3. Riser | 10. High pressure turbine |
| 4. Economiser | 11. Reheater |
| 5. Superheater 1 | 12. Low pressure turbine |
| 6. Attemperator 1 | |
| 7. Superheater 2 | |

The drum system model applies without any further simplification. The steam path of the boiler between drum and control valve is divided into two nominally equal paths. There are for example four attemperator valves instead of the two valves which are indicated. The two paths are lumped together in the model. Tubes for transporting steam to and from the turbines are neglected. The heat transferred to superheater 1 is not only due to convection but also to radiation. The heat flows, to the two different parts, have approximately the ratio 4:1. No model has been developed which can handle both types of heat transfer. Since the heat transfer by convection is the dominating part, it is assumed that all heat transfer takes place by convection in superheater 1. Superheaters 2, 3 and the reheater are of the standard type and the derived model can be used. The attemperator, the control valve and the two turbines create no problems. Of course, this is not a coincidence but the choice of model to be developed was naturally guided by the actual application.

The dynamics of actuators and transmitters were not included when modelling the boiler-turbine components. In Table 5.1 typical positioning times are given for the actuators. For small changes positioning times will be less than ten seconds in all cases. Compared to boiler dynamics,

| Actuator for: | Position | Time |
|--------------------|-----------|--------|
| control valve | 0 - 100 % | 5 sec. |
| | 100 - 0 % | 0.4 " |
| feedwater pumps | 0 - 100 % | 70 " |
| fuel valve | 0 - 100 % | 25 " |
| attemperator valve | 0 - 100 % | 75 " |

Table 5.1 - Typical positioning times for actuators.

the positioning times are considered small. Transmitter dynamics are fast, order of magnitude is seconds, except for the thermocouples.

As inputs to the boiler model the flows of fuel, feedwater, coolant water and the position of control valve will be used. Valves can easily be included using calibration curves relating rod position to flow.

5.2 Model Order

Accepting the simplified boiler configuration in Fig 5.1 as the basis for further development, the minimal order of the boiler-turbine unit is obtained as follows. The drum system requires five state variables and the four heat exchanger at least one state variable each. Hence the minimal order of the complete model is nine. Recalling the properties of the reduction technique, this figure is only an upper limit. However, in this case it is also the true order. By dividing the superheaters into sections, the model order can be increased arbitrarily.

The temperature raise of steam in superheater 1 is considerably larger than in superheaters 2 and 3. The reheater is also large compared to superheaters 2 and 3. Then it seems motivated that if a model of higher order than nine is derived, superheater 1 and the reheater are approximated more accurately.

It was decided to derive two models. One model of minimal order and one model of fifteenth order. The order is increased by dividing superheater 1 and the reheater into four sections each. The improvement of the complete model using more accurate approximations of the superheaters can be judged from a comparison.

5.3 Model Main Programme

The matrices \tilde{A} and \tilde{Q} of the equations

$$\tilde{A}z_1 = 0$$

$$\tilde{Q}z_2 = 0$$

have to be generated before the reduction programme is called. The elements of \tilde{A} and \tilde{Q} are determined by the z_1 and z_2 vectors and the component matrices \tilde{A}_i and \tilde{Q}_i . This defining and connecting procedure is made manually and the result is a table for the elements of \tilde{A} and \tilde{Q} assigning to these elements, an element of an \tilde{A}_i or a \tilde{Q}_i matrix.

The model subroutines are

| | |
|---------|----------------------|
| DR5M | drum system model |
| SHEAT | superheater model |
| ATTEMP | attperator model |
| VALVE | control valve model |
| TURBINE | turbine models |
| SPERED | reduction subroutine |

Moreover, some mathematical subroutines for determining roots of polynomials and for solving linear equations are needed.

The structure of the main program will be

- read input data
- call DR5M
- updata \tilde{A} and \tilde{Q} matrices
- call SHEAT the required number of times
- update \tilde{A} and \tilde{Q} matrices
- call ATTEMP, VALVE and TURBINE
- update \tilde{A} and \tilde{Q} matrices
- call REDUCE two times
- print S(A, B, C, D)

The steam mass flow is computed in subroutine DR5M which makes it necessary to call this routine first. To save core memory space, matrices \tilde{A} and \tilde{Q} are updated after each model subroutine call.

The computational effort required to model the process is small. Typical execution times for the UNIVAC 1108 computer are

| | |
|-------------------|--------------|
| 9:th order model | 9.5 seconds |
| 15:th order model | 12.0 seconds |

These figures do not include compilation time and time required for tape operations.

5.4 Input Data

No static model of the boiler-turbine unit was available. It was then decided only to produce data for one load point corresponding to the measurements made at roughly 90 % load.

Masses and lengths of tubes were calculated from data given in design drawings. Steam temperatures were found in boiler documentation and measurements made during the acceptance test. At this occasion, the boiler was equipped with a number of additional thermocouples thus making it possible to get a more detailed picture of the temperature distribution. In this way an approximate temperature distribution of superheater 1 was obtained and used in the fifteenth order model. For the reheater a linear temperature increase was assumed. Temperatures of tube material have been guessed on the basis of reasonable heat transfer coefficients. All proportional constants, in the linearized thermal state equations, are calculated from steam tables. Specific heat constant of tube matter is assumed to be the same for all materials. Proportional constants relating heat flow to fuel flow are obtained from steady state values of two load levels around the considered stationary load. Steady state values of attemperator flows are determined by the temperature drop across the attemperator since the spray water enthalpy is equal to feedwater enthalpy. Drum system input data was discussed in the previous section. The set of input data was checked by a heat balance calculation for the entire system. The computed value of the required fuel flow was very close to the measured value. The details of the input data development are accounted for in [55].

If the considered stationary point is changed, a new set of input data should be derived. In this work the same input data will be used to cover a load interval of about 5 - 10 %. This assumption means great time savings and only a minor error is introduced.

5.5 Complete Model

The state space model for Öresundsverket power station unit is given by

$$\begin{aligned} \frac{dx}{dt} &= Ax + Bu \\ y &= Cx + Du \end{aligned} \tag{5.1}$$

where the state vector for the ninth order model is

| | | | |
|-------|--|---|---------------|
| x_1 | drum pressure [bar] | } | drum system |
| x_2 | drum liquid level [m] | | |
| x_3 | drum liquid mean temperature [$^{\circ}$ C] | | |
| x_4 | mean temperature of riser [$^{\circ}$ C] | | |
| x_5 | mean value of steam quality | | |
| x_6 | mean tube temperature [$^{\circ}$ C] | | superheater 1 |
| x_7 | mean tube temperature [$^{\circ}$ C] | | superheater 2 |
| x_8 | mean tube temperature [$^{\circ}$ C] | | superheater 3 |
| x_9 | mean tube temperature [$^{\circ}$ C] | | reheater |

and for the fifteenth order model:

| | | | |
|----------|--|---|---------------|
| x_1 | drum pressure [bar] | } | drum system |
| x_2 | drum liquid level [m] | | |
| x_3 | drum liquid mean temperature [$^{\circ}$ C] | | |
| x_4 | mean temperature of riser [$^{\circ}$ C] | | |
| x_5 | mean value of steam quality | | |
| x_6 | mean tube temperature 1 [$^{\circ}$ C] | } | superheater 1 |
| x_7 | mean tube temperature 2 [$^{\circ}$ C] | | |
| x_8 | mean tube temperature 3 [$^{\circ}$ C] | | |
| x_9 | mean tube temperature 4 [$^{\circ}$ C] | | |
| x_{10} | mean tube temperature [$^{\circ}$ C] | | superheater 2 |
| x_{11} | mean tube temperature [$^{\circ}$ C] | | superheater 3 |

| | | | |
|----------|---|---|----------|
| x_{12} | mean tube temperature 1 [$^{\circ}$ C] | } | reheater |
| x_{13} | mean tube temperature 2 [$^{\circ}$ C] | | |
| x_{14} | mean tube temperature 3 [$^{\circ}$ C] | | |
| x_{15} | mean tube temperature 4 [$^{\circ}$ C] | | |

The input variables and output variables are the same in both models.
 The input variables are

u_1 fuel flow [kg/s]
 u_2 feedwater flow [kg/s]
 u_3 attemperator flow 1 [kg/s]
 u_4 attemperator flow 2 [kg/s]
 u_5 control valve position [%]

and the output variables:

y_1 steam temperature before attemperator 1 [$^{\circ}$ C]
 y_2 steam temperature after attemperator 1 [$^{\circ}$ C]
 y_3 steam flow before attemperator 1 [kg/s]
 y_4 steam temperature before attemperator 2 [$^{\circ}$ C]
 y_5 steam temperature after attemperator 2 [$^{\circ}$ C]
 y_6 steam flow, before attemperator 2 [kg/s]
 y_7 steam temperature before control valve [$^{\circ}$ C]
 y_8 steam flow before H. P. turbine [kg/s]
 y_9 steam temperature before reheater [$^{\circ}$ C]
 y_{10} steam pressure after control valve [bar]
 y_{11} active power of H. P. turbine [kW]
 y_{12} steam temperature after reheater [$^{\circ}$ C]
 y_{13} steam pressure before reheater [bar]
 y_{14} active power of L. P. turbine [kW]

The number of output variables is, in a sense, arbitrary. The output variables have not been defined as physical variables which are measured and used for control or display purposes. But significant variables bearing information of the model were chosen. No state variables were included since they are already available.

The matrices A, B, C and D for the ninth order model are given in Appendix C as an example.

Eigenvalues

An estimate of the model dynamics can be gained from the eigenvalues of the system matrix A. In Table 5.2 eigenvalues for the ninth and fifteenth order models are given. The eigenvalues are arranged in two groups containing the real eigenvalues and the complex conjugate pairs of eigenvalues respectively.

All eigenvalues in the ninth order model are not found in the fifteenth order model. Preserved are Nos. 1, 3, 8 and 9 which equal eigenvalues Nos. 1, 7, 14 and 15 in the fifteenth order model. Since the drum system

| Eigen-
value no. | 9:th order model | | Eigen-
value no. | 15:th order model | |
|---------------------|-----------------------|--------------------------|---------------------|-----------------------|--------------------------|
| | Real part | Imag. part | | Real part | Imag. part |
| 1 | 0.0000 | | 1 | 0.0000 | |
| 2 | $-2.29 \cdot 10^{-3}$ | | 2 | $-2.65 \cdot 10^{-3}$ | |
| 3 | $-3.44 \cdot 10^{-2}$ | | 3 | $-1.32 \cdot 10^{-2}$ | |
| 4,5 | $-4.82 \cdot 10^{-3}$ | $\pm 2.91 \cdot 10^{-3}$ | 4 | $-1.98 \cdot 10^{-2}$ | |
| 6,7 | $-1.56 \cdot 10^{-2}$ | $\pm 1.45 \cdot 10^{-3}$ | 5 | $-2.77 \cdot 10^{-2}$ | |
| 8,9 | $-8.21 \cdot 10^{-2}$ | $\pm 8.95 \cdot 10^{-3}$ | 6 | $-2.99 \cdot 10^{-2}$ | |
| | | | 7 | $-3.44 \cdot 10^{-2}$ | |
| | | | 8,9 | $-5.65 \cdot 10^{-3}$ | $\pm 3.08 \cdot 10^{-3}$ |
| | | | 10,11 | $-1.31 \cdot 10^{-2}$ | $\pm 7.75 \cdot 10^{-5}$ |
| | | | 12,13 | $-1.70 \cdot 10^{-2}$ | $\pm 5.09 \cdot 10^{-3}$ |
| | | | 14,15 | $-8.21 \cdot 10^{-2}$ | $\pm 8.95 \cdot 10^{-3}$ |

Table 5.2 - Eigenvalues of 9:th and 15:th order models for Öresunds-
verket power plant.

model is common for both models it seems reasonable to assume that these eigenvalues originate from the drum system. The zero eigenvalue is clearly associated with the drum liquid level. It is difficult to assign any particular subprocess to the other eigenvalues. However, perturbation of input data showed, that for the ninth order model, eigenvalue No. 2, No. 6 and No. 7, Nos. 8 and 9 are associated with the reheater, superheaters 2 and 3, superheater 1 and drum system respectively. This also verifies that the right eigenvalues were assigned to the drum system.

Superheater models with steam temperature and heat flows as inputs and steam temperature as output will have only real eigenvalues regardless of the number of sections. However, the entire model shows several complex conjugate pairs. The explanation is, the coupling between the subprocesses established by the steam flow and numerical inaccuracy.

Parameter variations

The influence of the guessed tube temperatures were investigated. In a first order superheater model of the type used here, the time constant is inversely proportional to the heat transfer coefficient. If the temperature difference between steam and tube matter was increased with a factor three, a proper number of eigenvalues moved to the right in the complex plane. As expected these eigenvalues were reduced roughly three times.

Only the steam volume in the drum has been included in the model. A possible way to take other steam volumes into consideration is to increase the drum volume. Only very slight changes resulted if the drum volume was increased four times.

Choice of model order

Both the 9:th and 15:th order models were simulated using input sequences from measurements. No significant difference between the two models could be established. Considering the advantages of low order models it was decided to prefer the ninth order model.

CHAPTER 5 - IDENTIFICATION OF DIFFERENCE EQUATION MODELS

1. Introduction

This chapter presents linear models with one input and one output. The purposes are

- to derive models for design of regulators of essentially single input-single output loops,
- to give insight into the dynamic properties of the boiler such as necessary model order, nonlinearities and noise intensity,
- to guide the evaluation of models from construction data.

Since no implementation of control strategies was possible in this case the interest has been concentrated on the last two items.

A number of identification methods are available for estimation of linear models. Frequently used are

- the maximum likelihood method,
- the least squares method,
- spectral analysis.

For the modelling of the Öresundsverket boiler-turbine unit it was decided to use the maximum likelihood method. This method gives a parametric model which also includes a model of the disturbances. An efficient numerical algorithm was available which also gave the least squares estimate as a byproduct.

The data used throughout this section was presented in Chapter 3. The numerical results obtained in Section 3 are thus restricted to the boiler on which the experiments were made. However, some of the results such as the effect of nonlinearities are valid for most drum-type boilers. Especially the results are valuable when used to evaluate models from construction data.

The maximum likelihood method is well documented in literature [51],

[52]. The numerical algorithms which have been used in this work are presented in [24], [25]. But for convenience and for the introduction of notations a short resumé is given in Section 2. Most problems arising when modelling from industrial data have been extensively discussed in [26]. This paper is a valuable guide for the choice of model order and other practical matters. Section 3 of this chapter gives a selection of results and models obtained. The considered outputs are drum pressure and active power and the inputs are fuel flow and control valve position. In the last section we discuss the results on boiler nonlinearities and noise. Also the choice of experiment characteristics is discussed.

2. Resumé of the maximum likelihood Method

The identification problem is to estimate a number of unknown parameters in a model of known structure. The available information is a sequence of measured values of the input variable $\{u(t), t = 1, 2, \dots, N\}$ and the output variable $\{y(t), t = 1, \dots, N\}$ of the process under consideration. The sampling interval is fixed and normalized to 1.

Using the maximum likelihood method it is assumed that the process can be described by a linear model of n :th order and that the disturbance is a stationary gaussian process with rational power spectra. A general model under these assumptions is

$$A^* (q^{-1})y(t) = B_1^* (q^{-1})u(t) + \lambda C^* (q^{-1})e(t) \quad (2.1)$$

In eq. (2.1), $\{e(t)\}$ is a sequence of independent normal $(0, 1)$ random variables and q denotes the shift operator

$$qx(t) = x(t+1)$$

The polynomials A^* , B_1^* and C^* are defined as

$$\begin{aligned} A^* (z) &= 1 + a_1 z + \dots + a_n z^n \\ B_1^* (z) &= b_1 z + b_2 z^2 + \dots + b_n z^n \\ C^* (z) &= 1 + c_1 z + \dots + c_n z^n \end{aligned} \quad (2.2)$$

It is assumed that the polynomials $A(z) = z^n A^* (z^{-1})$ and $C(z) = z^n C^* (z^{-1})$ have all zeros inside the unit circle and that there are no factors in com-

mon to all polynomials $A(z)$, $B_1(z)$, $C(z)$.

The parameter λ in the model (2.1) controls the variance of the noise since $\text{var}[e(t)]$ is normalized to 1.

The problem is solved by establishing the maximum likelihood function for the estimation of the parameters

$$\theta^T = (a_1 \ a_2 \ \dots \ a_n \ b_1 \ \dots \ b_n \ c_1 \ \dots \ c_n)$$

and the parameter λ . The maximizing of the logarithm of the likelihood function

$$\log L(\theta, \lambda) = -\frac{1}{2} \sum_{t=1}^N \frac{\epsilon^2(t)}{\lambda} - \frac{N}{2} \log \lambda - \frac{N}{2} \log 2\pi \quad (2.3)$$

is equivalent to minimizing the loss function

$$V(\theta) = \frac{1}{2} \sum_{t=1}^N \epsilon^2(t) \quad (2.4)$$

where the residuals $\epsilon(t)$ are obtained from

$$\hat{C}^*(q^{-1})\epsilon(t) = \hat{A}^*(q^{-1})y(t) - \hat{B}_1^*(q^{-1})u(t) \quad (2.5)$$

and \hat{A} , \hat{B}_1 and \hat{C} denotes the estimates of the polynomials A , B_1 and C . The estimation problem is thus equivalent to minimizing a function of several variables.

Knowing the estimate $\hat{\theta}$ and the minimal value $V(\hat{\theta})$ of the loss function the parameter λ is estimated as

$$\hat{\lambda}^2 = \frac{2}{N} V(\hat{\theta}) \quad (2.6)$$

It has been shown [52] that the maximum likelihood estimates are consistent, asymptotically normal and efficient under mild conditions.

The residuals $\epsilon(t)$ have a nice interpretation. It can be shown that the residuals equal the one-step ahead prediction error. Thus the maximum likelihood method tries to estimate the parameters of the model (2.1) in such a way that the sum of squared prediction errors is minimized.

An iterative technique is used to find the minimum of $V(\theta)$ and both the gradient V_{θ} and the matrix of second derivatives $V_{\theta\theta}$ are utilized in the recursive formula for improving the estimate $\hat{\theta}$. Apart from improving the rate of convergence the matrix $V_{\theta\theta}$ also gives the accuracy of the parameters since an estimate of the covariance matrix $\lambda^2 V_{\theta\theta}^{-1}$ then is available.

The order of the model is usually not known a priori. This problem is solved by repeated identification of the parameters in models of increasing order. A statistical test may then be applied to judge, if the loss function has decreased significantly, when model order is increased from n to $n+1$. Let V_i be the minimal value of the loss function for the i :th order model. The null hypothesis is that the model is of order n . Then the test variable

$$F_{n+1, n} = \frac{V_n - V_{n+1}}{V_{n+1}} \frac{N - 3(n+1)}{3} \quad (2.7)$$

has an $F[3, N - 3(n+1)]$ distribution under null hypothesis. When N is large $3F_{n+1, n}$ tends towards a χ^2 distribution with 3 degrees of freedom. Usually the risk level 5 % is used that is, if the test quantity is greater than 2.6 ($N > 100$) then the loss function has been decreased significantly and model order is at least $n+1$.

The material given above is somewhat simplified. The model (2.1) is easily extended to have more than one input. By shifting the time series $\{u(t), t = 1, \dots, N\}$ or $\{y(t), t = 1, \dots, N\}$ the model (2.1) can also be applied to processes where the $B_1^*(z)$ polynomial contains a constant term b_0 . In the same way processes described by the model

$$A^*(q^{-1})y(t) = B^*(q^{-1})u(t-k) + \lambda C^*(q^{-1})e(t) \quad (2.8)$$

where

$$B^*(z) = b_0 + b_1 z + \dots + b_n z^n = b_0 + B_1^*(z)$$

can be handled. The model can thus be extended to contain k time delays.

3. Results of Identification

As stated in Chapter 3, the variables were not sampled simultaneously. The maximum time delay between the measurements was 4.8 seconds. Before identifying all data of each experiment were adjusted to a reference sampling point using linear interpolation.

The full material motivating the final choice of a model will only be given for the first derived model. For the other models only samples of the calculations are given.

Experiments were made at two different load levels corresponding to 90 % and 50 % of full load. The models for both load levels will be given and treated together. Load dependent boiler dynamics are thus clearly seen.

3.1 Drum Pressure

The output drum pressure is strongly influenced by the inputs fuel flow and control valve position. When controlling the boiler, drum pressure is usually kept constant or manipulated to follow a prescribed curve depending on the load. The control action is essentially performed using the fuel flow, and the control valve position can be regarded as a disturbance.

Exps. A, F, E and J are used. In the first two experiments the fuel flow is perturbed and in the last two the control valve setting is perturbed.

Fuel flow

To establish the number of time delays in the model (2.8), models of different order and different number of time delays were computed and the minimal values of the loss function (2.4) compared. The resulting values of V are shown in Table 3.1. From the table it is clear

| | | Exp. A | | Exp. F | |
|---|---|--------|-------|--------|-------|
| | | 0 | 1 | 0 | 1 |
| 1 | k | 0.559 | 1.080 | 2.537 | 4.323 |
| 2 | n | 0.259 | 0.817 | 1.322 | 2.219 |
| 3 | | 0.198 | 0.648 | 1.170 | 1.987 |

Table 3.1 - The values of the loss function V for models from Exps. A and F.

that a model with $k = 0$ should be chosen, since the values of the loss function is reduced by roughly a factor 2. The reduction is not only due to the change of k but also to the shifting of data for $k = 0$ which affects the initialization of the identification algorithm.

From a physical point of view one would expect $k \geq 1$. The presence of a direct coupling between $u(t)$ and $y(t)$ is due to the sequential scanning of data, the interpolation of data and to the fact that $u(t)$ is not changed instantaneously. The last statement follows from the fact that the algorithm used assumes the input signal constant over the sampling interval. Using a more sophisticated preprocessing of data it might be possible to reduce the magnitude of the direct connection.

Table 3.2 shows the estimated coefficients of the model (2.8) for increasing model order and both experiments. The coefficients are given with their estimated standard deviation σ . The value of λ , the loss function, the test quantity $F_{n, n-1}$ and the stationary gain K_{st}

are also given. Notice that the gain depend on the units of the input and output variables. In this subsection fuel flow and drum pressure are measured in ton/hour and kg/cm^2 respectively.

From this table the model orders can be determined. First, consider the high load level experiment. The test quantity $F_{n, n-1}$ indicates that the order of the model is greater than 3. Inspecting the accuracy of coefficients of the fourth order model it is found that a_4 , b_4 and c_4 do not differ significantly from zero.

If model order is chosen properly the residuals $\{\epsilon(t)\}$ defined by eq. (2.5) are a sequence of independent normal random variables. Model order can thus be checked by computing the covariance function $r(\tau)$ of the residuals. The covariance function for the third order model of Exp. A is given in Fig. 3.1. According to the theory [52] the covariance function should be equal to zero for $\tau \neq 0$. The dashed line of Fig 3.1 gives the one σ limit for $r(\tau)$, $\tau \neq 0$. The sample covariance function indicates that the residuals $\epsilon(t)$ are uncorrelated and we conclude that the model order is three.

The coefficient b_1 of the third order model of Exp. A in Table 3.2 is significantly equal to zero. Putting this parameter equal to zero and estimating all other parameters we get

| Load | High load level Exp. A | | | | Low load level Exp. F | | |
|---------------------|------------------------|--------------|--------------|--------------|-----------------------|--------------|--------------|
| | 1 | 2 | 3 | 4 | 1 | 2 | 3 |
| n | | | | | | | |
| a ₁ | -0.971±0.002 | -1.472±0.038 | -2.462±0.028 | -2.248±0.190 | -0.979±0.002 | -1.499±0.035 | -2.481±0.037 |
| a ₂ | | 0.480±0.037 | 1.962±0.055 | 1.523±0.470 | | 0.505±0.034 | 1.993±0.068 |
| a ₃ | | | -0.498±0.027 | -0.258±0.381 | | | -0.511±0.032 |
| a ₄ | | | | -0.016±0.102 | | | |
| b ₀ | 0.071±0.004 | 0.088±0.003 | 0.085±0.003 | 0.084±0.003 | 0.111±0.007 | 0.083±0.005 | 0.080±0.005 |
| b ₁ | 0.099±0.004 | 0.085±0.005 | 0.001±0.006 | 0.022±0.017 | 0.086±0.007 | 0.134±0.011 | 0.058±0.015 |
| b ₂ | | -0.097±0.004 | -0.182±0.006 | -0.171±0.006 | | -0.132±0.005 | -0.264±0.015 |
| b ₃ | | | 0.101±0.003 | 0.049±0.035 | | | 0.131±0.006 |
| b ₄ | | | | 0.021±0.020 | | | |
| c ₁ | 0.796±0.028 | 0.395±0.059 | -0.861±0.057 | -0.632±0.196 | 0.309±0.048 | -0.690±0.068 | -1.742±0.066 |
| c ₂ | | -0.032±0.049 | -0.313±0.066 | -0.408±0.178 | | 0.355±0.050 | 1.058±0.103 |
| c ₃ | | | 0.333±0.053 | 0.208±0.088 | | | -0.240±0.061 |
| c ₄ | | | | 0.028±0.092 | | | |
| λ | 0.056 | 0.0380 | 0.0333 | 0.0327 | 0.119 | 0.086 | 0.081 |
| V | 0.559 | 0.259 | 0.198 | 0.192 | 2.537 | 1.322 | 1.170 |
| F _{n, n-1} | - | 134 | 35 | 4 | - | 106 | 14.8 |
| K _{st} | 5.90 | 8.65 | 4.28 | 4.01 | 9.24 | 14.6 | 9.26 |

Table 3.2 - Models of increasing order relating drum pressure (kg/cm²) to fuel flow (ton/h) at high and low load levels.

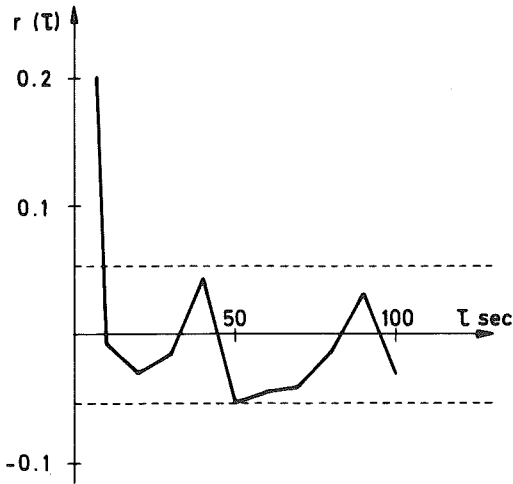


Fig 3.1 - The sample correlation function for the residuals $\{\epsilon(t)\}$ of the third order model of Exp. A. The dashed line gives the one σ limit for $r(\tau)$, $\tau \neq 0$.

| | | | | |
|-------|--------------------|-----------|--------------------|-------|
| a_1 | -2.465 ± 0.026 | c_1 | -0.860 ± 0.057 | |
| a_2 | 1.966 ± 0.051 | c_2 | -0.316 ± 0.064 | |
| a_3 | -0.500 ± 0.026 | c_3 | 0.335 ± 0.051 | |
| b_0 | 0.085 ± 0.002 | λ | 0.0333 | (3.1) |
| b_1 | $0.$ | V | 0.198 | |
| b_2 | -0.181 ± 0.003 | K_{st} | 4.27 | |
| b_3 | 0.101 ± 0.003 | | | |

The statistical F-test does not indicate a significant decrease of the loss function, if the b_1 parameter is included in the third order model.

In Fig 3.2 a simulation of the third order model (3.1) is shown. The curves are

1. input $u(t)$
2. output $y(t)$

3. residuals or one step ahead prediction error $\epsilon(t)$
4. output of deterministic model

$$y_d(t) = \frac{B^* (q^{-1})}{A^* (q^{-1})} u(t)$$

5. error of deterministic model

$$e_d(t) = y(t) - y_d(t)$$

Notice that different scales are used. The maximum error of the deterministic model is -1.6 kg/cm^2 .

The raise of the error e_d in the interval 1200-1800 seconds and the drop in the interval 2200-2600 is probably due to changes of feedwater flow, compare Fig 5.1 in Chapter 3. An increased feedwater flow results in a decreased feedwater temperature. Heat available for evaporation thus decreases and the drum pressure will drop.

If the model is used for control purposes the goodness of the model should be judged from the prediction error. In this case, the standard deviation of the prediction of the drum pressure 10 seconds ahead based on old measurements of $u(t)$ and $y(t)$ is 0.033 kg/cm^2 . The residuals are shown in Fig 3.2. According to the sample covariance function Fig 3.1 the time series can be regarded as uncorrelated. The diagram shows that the amplitude is systematically larger at time points of large changes of the input. This is due to the properties of data and identification scheme as mentioned previously.

Now consider the low load level models. The F-test of Table 3.2 indicates at least a third order model. The computer algorithm failed to converge to a fourth order model despite several restarts using different initial parameter guesses. A test of the covariance function of residuals does not reject this proposal and we accept model order as three.

The standard simulation is shown in Fig 3.3. The sudden raise of the error curve at time 1600 seconds can be explained by changes of feedwater flow, compare Fig 5.6 in Chapter 3. The maximum error e_d is 2.5 kg/cm^2 . In both models the relative deterministic error is of the same magnitude, if computed in relation to the peak-to-peak values of the outputs.

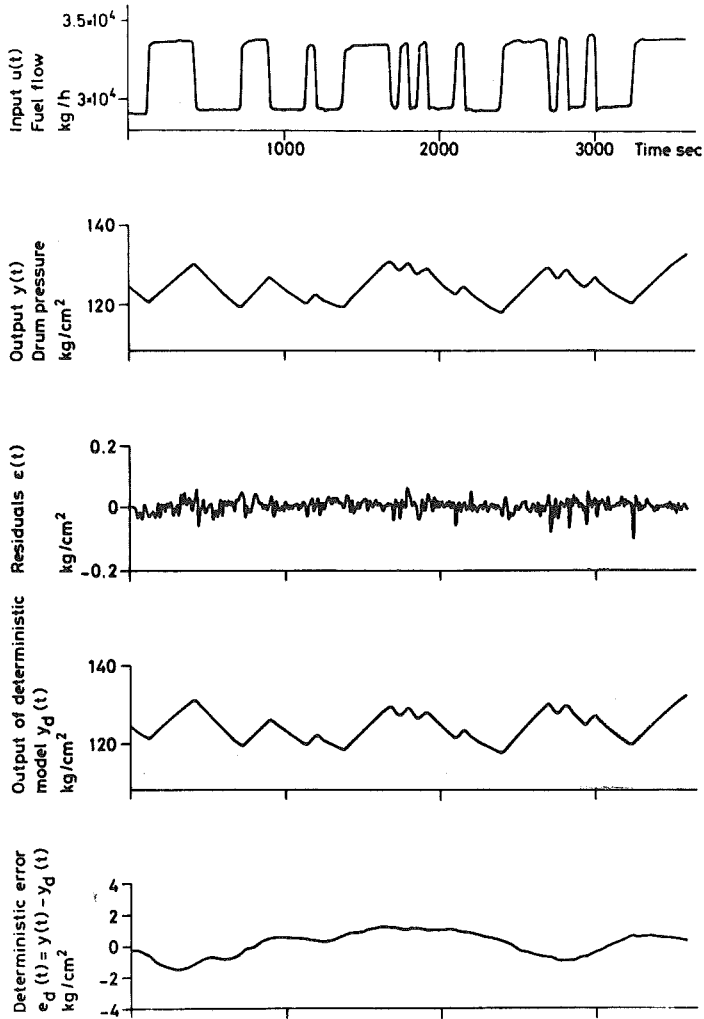


Fig 3.2 - Results of the identification of a third order model relating drum pressure to fuel flow. Input and output time series from Exp. A.

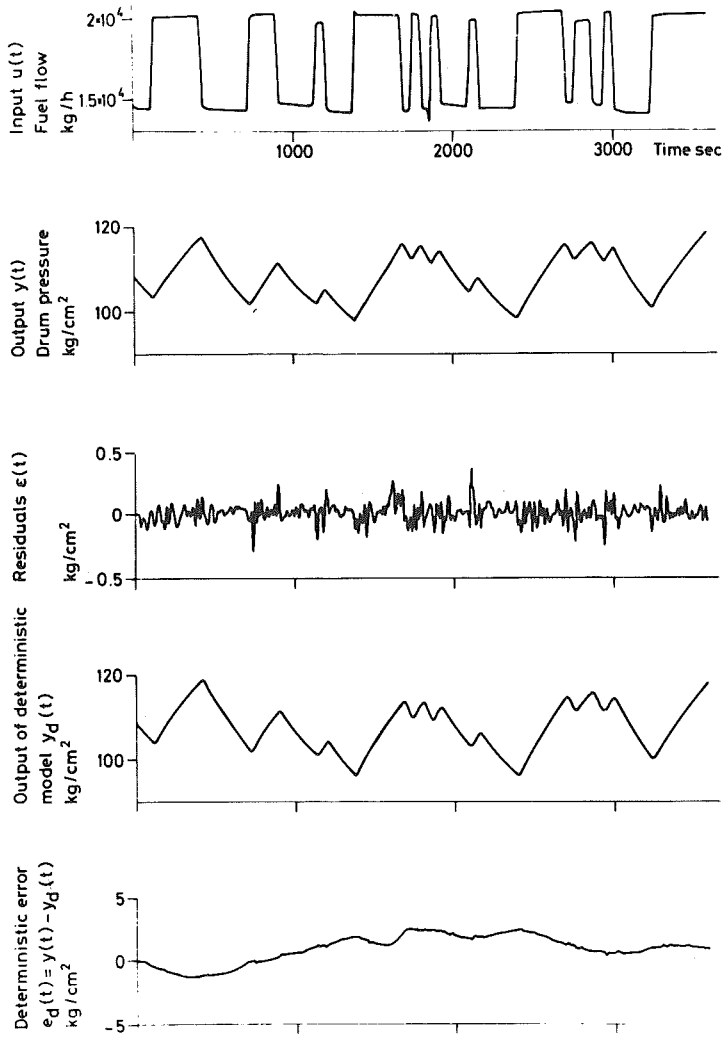


Fig 3.3 - Results of the identification of a third order model relating drum pressure to fuel flow. Input and output time series from Exp. F.

The least squares estimate of the parameters of the model

$$A^* (q^{-1})u(t) = B^* (q^{-1})u(t) + \lambda e(t) \quad (3.2)$$

is obtained in the first iteration of the used maximum likelihood algorithm. For the third order models discussed we get

$$\begin{aligned} \lambda_H &= 0.042 & \lambda_L &= 0.088 \\ V_H &= 0.316 & V_L &= 1.394 \end{aligned} \quad (3.3)$$

where indices H and L stand for high and low load level respectively.

None of the $A(q)$ polynomials of the maximum likelihood models have any zeros on the negative real axis. The transformation to continuous time thus behaves well. The transfer functions have both the form

$$G(s) = K_1 + K_2 \frac{1}{1 + T_1 s} + K_3 \frac{(1 + T_2 s)}{1 + 2\zeta T_3 s + T_3^2 s^2} \quad (3.4)$$

where the coefficients are given in Table 3.3.

| Parameter | High load level | Low load level |
|------------|-----------------|----------------|
| K_1 | 0.085 | 0.080 |
| K_2 | 0.199 | 0.211 |
| K_3 | 3.92 | 8.93 |
| T_1 | 16.2 | 16.5 |
| T_2 | 109 | 156 |
| T_3 | 190 | 294 |
| ζ | 0.714 | 0.955 |
| ω_n | 0.0052 | 0.0034 |

Table 3.3 - Coefficients of the transfer function

$$G(s) = K_1 + K_2 \frac{1}{1 + T_1 s} + K_3 \frac{1 + T_2 s}{1 + 2\zeta T_3 s + T_3^2 s^2}$$

relating drum pressure (kg/cm^2) to fuel flow (ton/h) at high and low load levels.

The table also includes $\omega_n = 1/T_3$. The constant term K_1 is practically the same in both cases and compared to the gain of the third term of $G(s)$ it is very small.

It seems possible to give a physical interpretation of the first and second order dynamics of (3.4) The first order dynamics represent the storage of energy in the risers. The second order dynamics represent the energy storage in the drum, superheaters and reheater. This is further discussed in Chapter 7 when comparing models from measurement and from construction data.

A straightforward comparison of the model dynamics, for the two load levels, is possible since both models are of the same order. The first order mode is the same in both cases which verify the physical interpretation. In the second order transfer function gain, damping factor and natural resonant frequency are altered indicating load depending dynamics.

In [53] a simple nonlinear first order model is derived for a drum boiler-turbine unit. The model is based on physical arguments and has the form

$$\frac{dp}{dt} = f(p, u_1, u_2, u_3) \quad (3.5)$$

$$P = g(p, u_2)$$

where

- p drum pressure
- P active power
- u_1 fuel flow
- u_2 control valve position (normalized units)
- u_3 feedwater flow.

Linearizing eq. (3.5) the time constant T and gain K of the first order dynamics relating any of the inputs u_1 , u_2 and u_3 to the drum pressure is

$$T = \frac{8\bar{p}^{5/8}}{5\alpha_1 \bar{u}_2} \quad (3.6)$$

$$K = k_{u_1} T \quad (3.7)$$

where α_1 and k_{u_i} , $i = 1, 2, 3$, are constants and \bar{v} is the steady

state value of the variable v . If the drum pressure is constant and if the control valve setting is reduced to half its previous value then the model (3.5) predicts an increase of the time constant and the gain with a factor 2. Recalling that the difference in experimental conditions between Exps. A and F were that the control valve was partly closed and the drum pressure 15 kg/cm² lower in Exp. F we find that the results of the maximum likelihood identification well agree with physical properties.

Control valve position

The results of the identification is shown in Table 3.4. The position of control valve is measured in % of the full stroke. Also for this input the lowest value of the loss function was achieved for $k = 0$. Considering the test quantity F and accuracies of parameters model orders are found to be 3 and 2 for the high and low level experiments respectively. Putting the parameters b_2 and c_3 of the third order model equal to zero we get

| | | | | |
|-------|--------------|-----------|--------------|-------|
| a_1 | -2.271±0.098 | c_1 | -1.003±0.103 | |
| a_2 | 1.645±0.166 | c_2 | 0.271±0.074 | |
| a_3 | -0.370±0.071 | c_3 | 0. | |
| b_0 | -0.069±0.002 | λ | 0.0546 | (3.8) |
| b_1 | 0.075±0.004 | V | 0.533 | |
| b_2 | 0. | K_{st} | -1.87 | |
| b_3 | -0.013±0.003 | | | |

The standard plots of the two models are given in Fig 3.4 and Fig 3.5. The deterministic error e_d is roughly two times greater in the low load experiment. The influence of feedwater changes could also be recognized and an improvement could be achieved by including feedwater flow as a second input signal. The residuals of Exp. J in Fig 3.5 appears to contain a low frequency component but according to Table 3.4 no significant improvement is obtained by increasing model order.

The continuous time equivalents of the discrete time models are

| Load | High load level Exp. E | | | Low load level Exp. J | | |
|---------------------|------------------------|--------------|--------------|-----------------------|--------------|--------------|
| | 1 | 2 | 3 | 1 | 2 | 3 |
| n | | | | | | |
| a ₁ | -0.964±0.002 | -1.751±0.070 | -2.440±0.159 | -0.985±0.002 | -1.856±0.049 | -2.239±0.380 |
| a ₂ | | 0.759±0.068 | 1.942±0.299 | | 0.857±0.049 | 1.537±0.717 |
| a ₃ | | | -0.500±0.141 | | | -0.297±0.337 |
| b ₀ | -0.068±0.002 | -0.070±0.002 | -0.069±0.002 | -0.116±0.004 | -0.118±0.004 | -0.116±0.004 |
| b ₁ | -0.014±0.002 | 0.044±0.007 | 0.089±0.012 | 0.026±0.004 | 0.124±0.010 | 0.161±0.045 |
| b ₂ | | 0.010±0.002 | -0.010±0.011 | | -0.016±0.005 | -0.043±0.052 |
| b ₃ | | | -0.013±0.002 | | | -0.005±0.009 |
| c ₁ | 0.327±0.043 | -0.474±0.089 | -1.185±0.169 | 0.181±0.047 | -0.781±0.076 | -1.167±0.383 |
| c ₂ | | 0.097±0.061 | 0.391±0.131 | | 0.082±0.054 | 0.302±0.321 |
| c ₃ | | | -0.052±0.060 | | | 0.026±0.065 |
| λ | 0.0613 | 0.0557 | 0.0545 | 0.104 | 0.096 | 0.094 |
| V | 0.670 | 0.554 | 0.531 | 1.93 | 1.64 | 1.59 |
| F _{n, n-1} | - | 24.2 | 4.9 | - | 20.6 | 3.1 |
| K _{st} | -2.30 | -2.21 | -1.74 | -6.13 | -8.47 | -4.93 |

Table 3.4 - Models of increasing order relating drum pressure (kg/cm²) to control valve position (%) at high and low load levels.

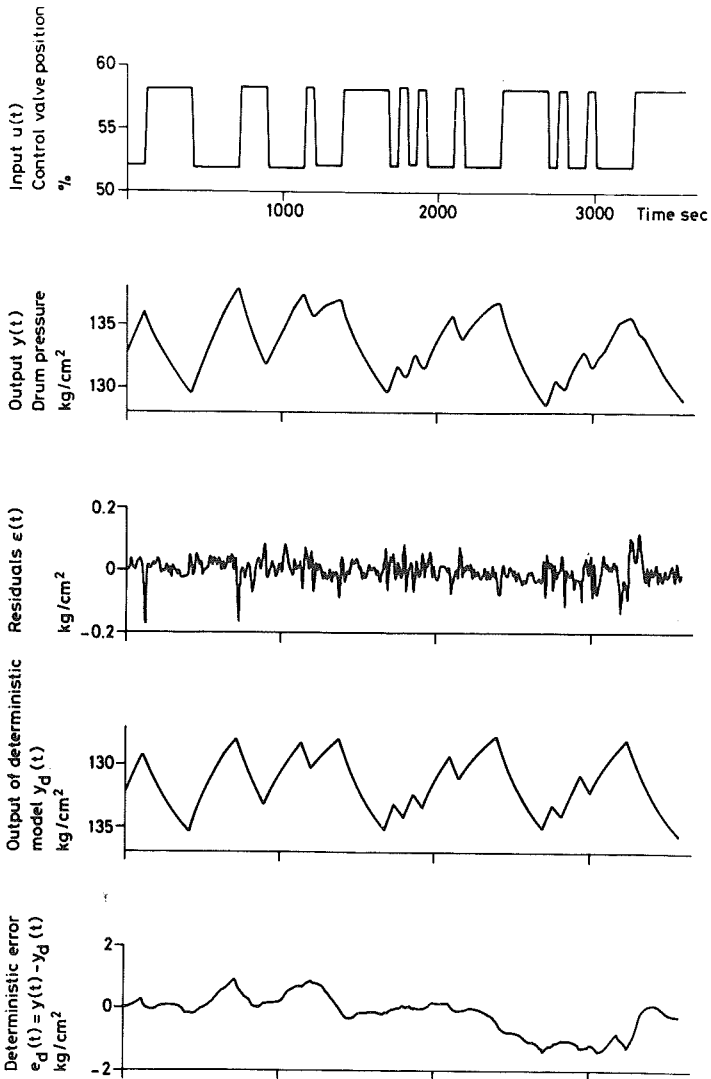


Fig 3.4 - Results of the identification of a third order model relating drum pressure to control valve setting. Input and output time series from Exp. E.

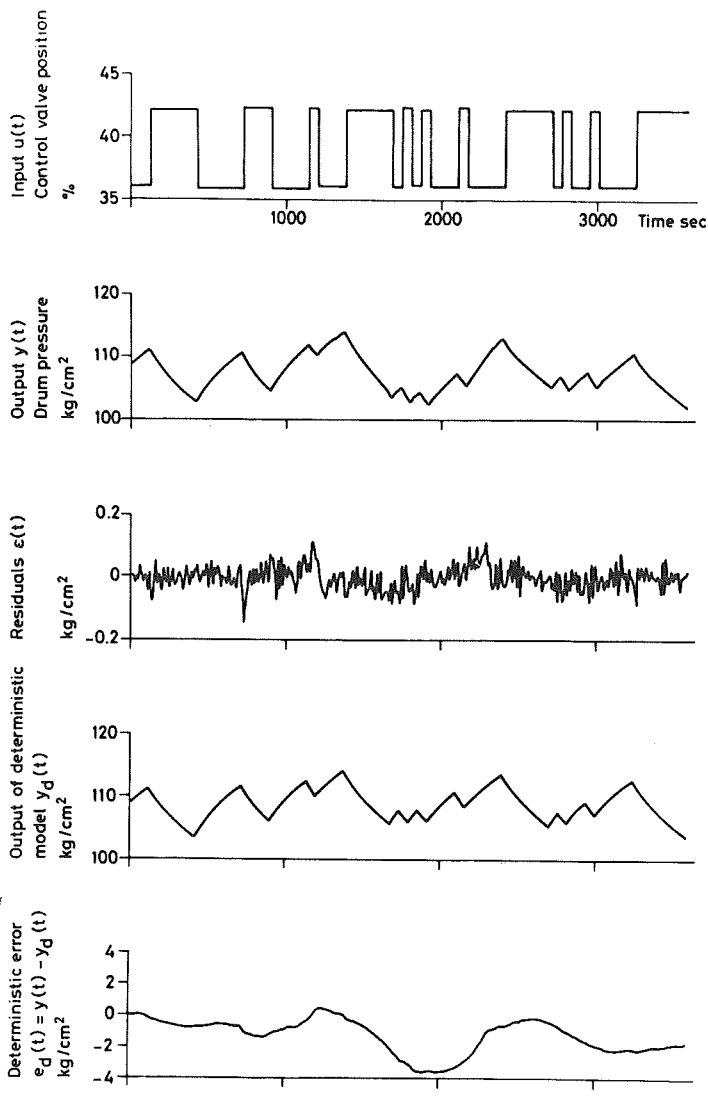


Fig 3.5 - Results of the identification of a second order model relating drum pressure to control valve setting. Input and output time series from Exp. J.

$$G(s) = K_1 + K_2 \frac{1}{1 + T_1 s} + K_3 \frac{1}{1 + T_2 s} + K_4 \frac{1}{1 + T_3 s} \quad (3.9)$$

where the coefficients are given in Table 3.5.

The direct coupling between input and output is small for both models. It is not clear how to give physical interpretations to the different terms of the transfer function. However, the dominant time constant T_1 is associated with energy storage in drum and superheaters. The remarkable difference of the value of T_1 could only partly be explained by the increase of the time constant as given by eq. (3.6) used previously.

| Parameter | High load level | Low load level |
|-----------|-----------------|----------------|
| K_1 | -0.0693 | -0.1167 |
| K_2 | -2.219 | -8.418 |
| K_3 | -0.0312 | -0.2186 |
| K_4 | 0.4464 | - |
| T_1 | 183 | 1252 |
| T_2 | 12.2 | 75.4 |
| T_3 | 79.2 | - |

Table 3.5 - Coefficients of the transfer functions

$$G(s) = K_1 + K_2 \frac{1}{1 + T_1 s} + K_3 \frac{1}{1 + T_2 s} + K_4 \frac{1}{1 + T_3 s}$$

relating drum pressure (kg/cm^2) to control valve setting (%) at high and low load levels.

The roots of the $A(z)$ polynomial of the second order model are

$$z_1 = 0.9916$$

$$z_2 = 0.8642$$

The root z_1 is very close to the unit circle, and this mode behaves practically as an integrator over the sampling interval. The accuracy of the obtained value of T_1 can thus be quite poor.

The difference in model gain is not only due to the change of operating conditions of the boiler. The nonlinear characteristic of the control valve has contributed considerably.

3.2 Active Power

The main input variables which affect the active power are fuel flow and control valve position. The presented models are derived from the same experiments as in the previous subsection. The power unit is MW.

Fuel flow

The models which will be discussed are shown in Table 3.6. In all models the number of delays k equals one.

| Exp. | High load level.
Exp. A | | Low load level.
Exp. F |
|--------------|----------------------------|---------------|---------------------------|
| | 1 | 2 | 1 |
| n | | | |
| a_1 | -0.9816±0.003 | -1.9786±0.003 | -0.9849±0.002 |
| a_2 | | 0.9795±0.003 | |
| b_1 | 0.1964±0.006 | 0.1837±0.006 | 0.1149±0.003 |
| b_2 | | -0.1826±0.006 | |
| c_1 | -0.4363±0.047 | -1.5183±0.054 | -0.6453±0.045 |
| c_2 | | 0.5183±0.055 | |
| λ | 0.373 | 0.356 | 0.378 |
| V | 25.03 | 22.73 | 25.59 |
| $F_{n, n-1}$ | - | 11.9 | - |
| K_{st} | 10.7 | 1.22 | 7.6 |

Table 3.6 - Parameters of models relating active power (MW) to fuel flow (ton/h) at high and low load levels.

For the low load level the F-test works well and $F_{2,1} = 2.5$. In the Exp. A, we should choose a second order model according to the test quantity. The roots of the $A(z)$, $B(z)$ and $C(z)$ polynomials are given in Table 3.7. For the second order model there is nearly one root in common which indicates that model order is too high. Comparing the sample correlation functions of the models shown in Fig 3.6 no improvement is achieved by increasing model order from 1 to 2. A first order model is thus preferred for both load levels.

| n | 1 | 2 |
|------|-------|------------------------------|
| A(z) | 0.982 | 0.989+0.028i
0.989-0.028i |
| B(z) | | 0.994 |
| C(z) | 0.436 | 0.518
1.000 |

Table 3.7 - Roots of A, B and C polynomials of first and second order models of Exp. A.

The standard plots are given in Figs. 3.7 and 3.8. Note the different scales. The deterministic error is quite large in Fig 3.7 which partly may be due to an error in the initial conditions.

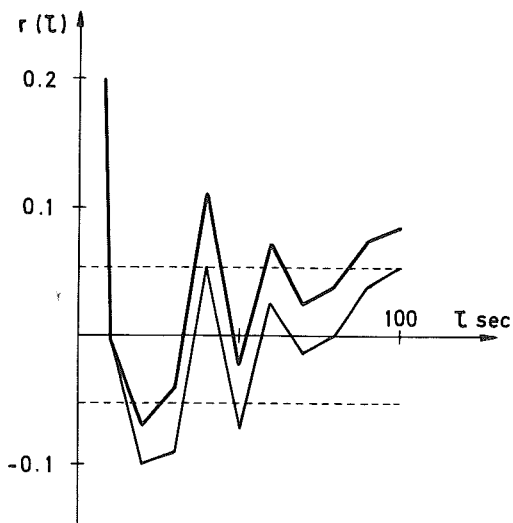


Fig 3.6 - Sample correlation functions for the residuals $\{\varepsilon(t)\}$ of the first order model (heavy line) and second order model of Exp. A given in Table 3.6. The dashed line gives the one σ limit for $r(\tau)$, $\tau \neq 0$.

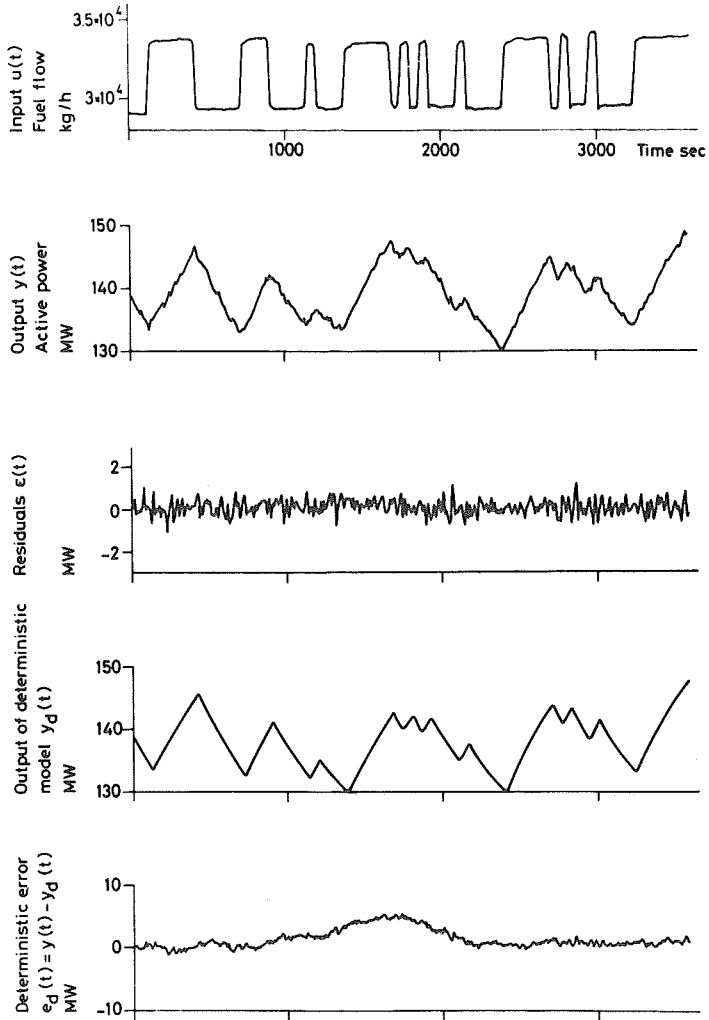


Fig 3.7 - Results of the identification of a first order model relating active power to fuel flow. Input and output time series from Exp. A.

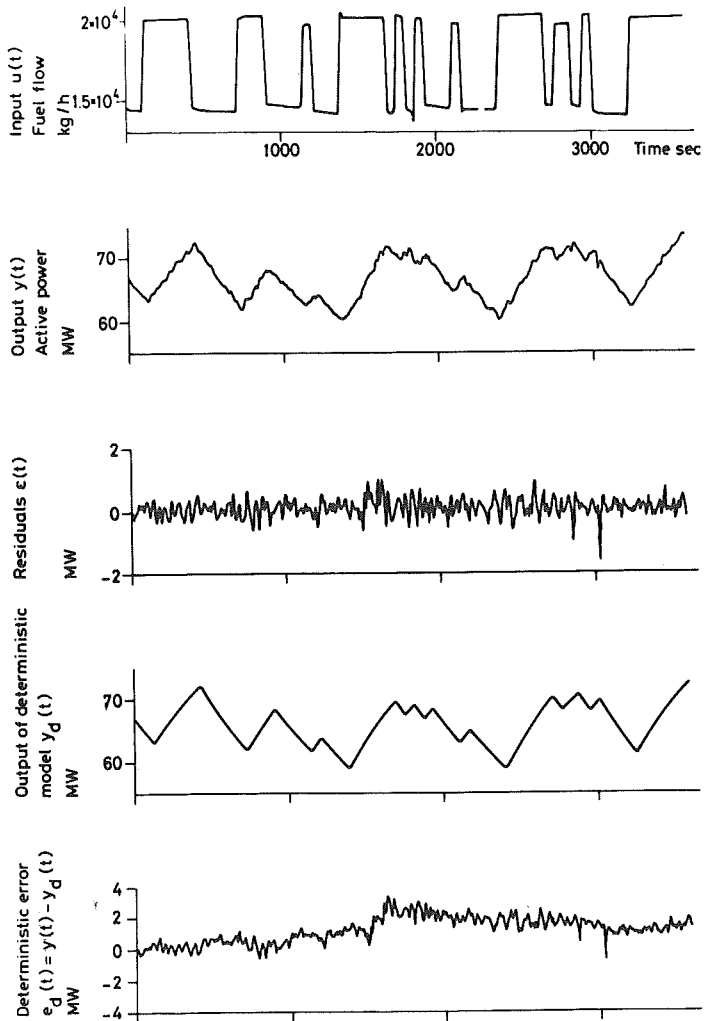


Fig 3.8 - Results of the identification of a first order model relating active power to fuel flow. Input and output time series from Exp. F.

The continuous time model is

$$G(s) = \frac{K}{1 + Ts} \quad (3.10)$$

where the gain and time constant for both models are given in Table 3.8.

| Para-
meter | High load level | Low load level |
|----------------|-----------------|----------------|
| K | 10.7 | 7.6 |
| T | 538 | 659 |

Table 3.8 - Coefficients of the transfer function

$$G(s) = \frac{K}{1 + Ts}$$

relating active power (MW) to fuel flow (ton/h) at high and low load levels.

According to eq. (3.6) the increase of the time constant is physically motivated. The steady state gain of the dynamical system relating fuel flow to active power can easily be computed theoretically. The gain is approximately 5 for both models. The gain estimates are thus quite poor in this case.

Control valve position

The best choice of k was found to be zero. A second order model is for both load levels believed to be satisfactory. In the low load level case, the statistical F-test indicated a third order model, $F = 5.5$. However, the third order model polynomials have nearly one root in common. The final model parameters are given in Table 3.9.

The model of Exp. J is unstable. This is not in accordance with the physical properties of the boiler. However, the obtained model is the one of order two which minimizes the sum of the one-step-ahead prediction errors.

| Exp. | High Load level
Exp E | Low Load level
Exp J |
|-----------|--------------------------|-------------------------|
| n | 2 | 2 |
| a_1 | -1.521 ± 0.047 | -1.539 ± 0.034 |
| a_2 | 0.535 ± 0.046 | 0.534 ± 0.035 |
| b_0 | 1.101 ± 0.023 | 1.470 ± 0.025 |
| b_1 | -1.464 ± 0.080 | -1.954 ± 0.084 |
| b_2 | 0.343 ± 0.071 | 0.442 ± 0.072 |
| c_1 | -0.788 ± 0.074 | -0.887 ± 0.072 |
| c_2 | 0.096 ± 0.060 | 0.153 ± 0.059 |
| λ | 0.580 | 0.569 |
| K_{st} | -1.544 | - |

Table 3.9 - Parameters of models relating active power (MW) to control valve setting (%) at high and low load levels.

Since input power is constant, a change of control valve position cannot affect the steady state output power, providing that boiler efficiency does not vary. The gain K_{st} should then be near zero, but is estimated to -1.54 MW/% in the high load level case.

The standard plots are given in Figs. 3.9 and 3.10. Both curves for the error e_d show some step-like changes. This is probably due to errors in the recording of the input sequence which was registered manually. This is certainly true at time 3200 of Exp. E where a change of the control valve position was made and not recorded. The effect on both residuals and error e_d is clearly visible.

Comparing to the least squares estimate the value of the loss function has decreased from 72 to 60 and the value of λ from 0.637 to 0.580. The given figures are valid for Exp. E. In this experiment a first degree C polynomial is probably sufficient considering the uncertainty of the estimate of the parameter c_2 .

Parameters of the continuous models represented as a transfer function

$$G(s) = K_1 + \frac{K_2}{1 + T_1 s} + \frac{K_3}{1 + T_2 s} \quad (3.11)$$

are given in Table 3.10.

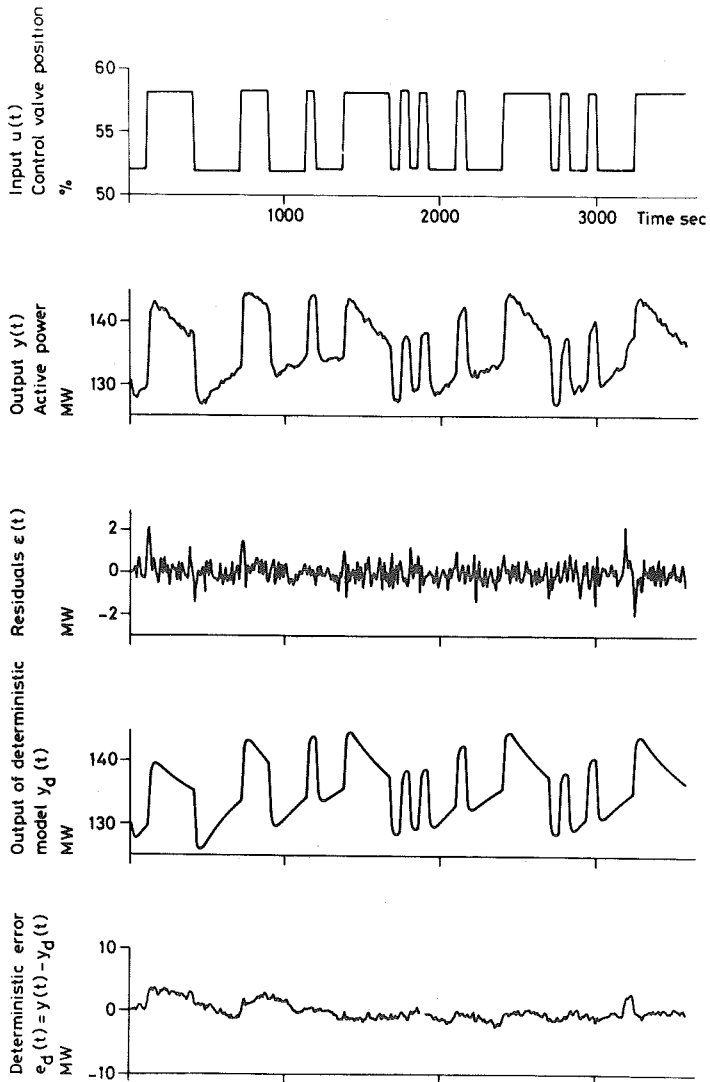


Fig 3.9 - Results of the identification of a second order model relating active power to control valve setting. Input and output time series from Exp. E.

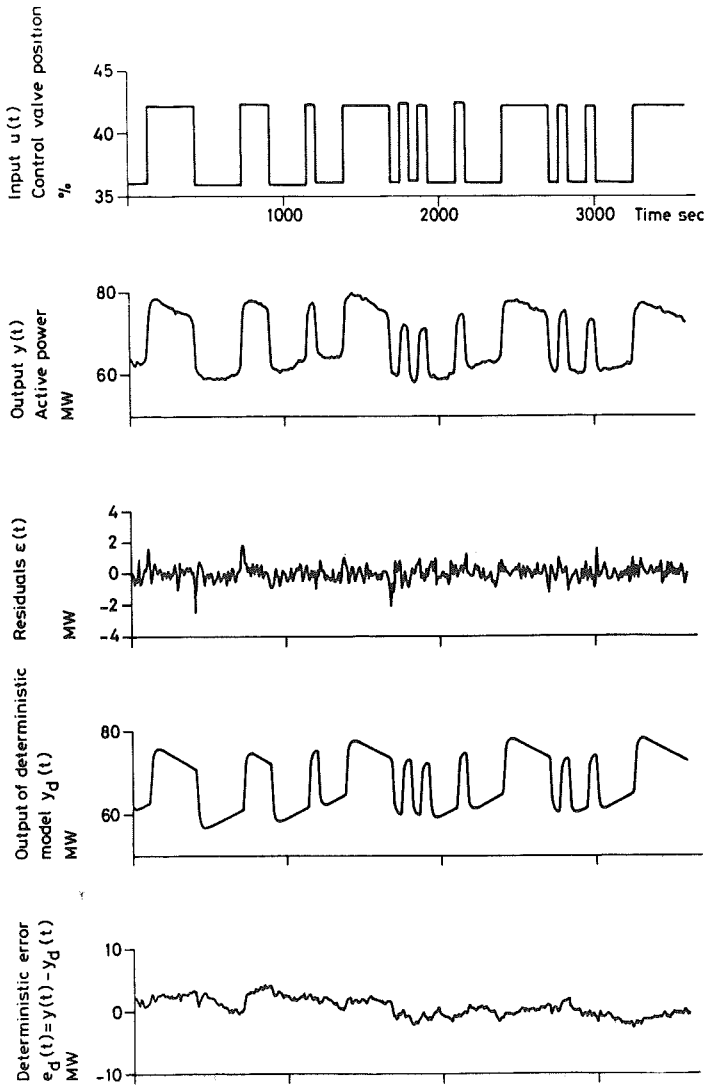


Fig 3.10 - Results of the identification of a second order model relating active power to control valve setting. Input and output time series from Exp. J.

| Parameter | High load level | Low load level |
|-----------|-----------------|----------------|
| K_1 | 1.101 | 1.470 |
| K_2 | -3.37 | 5.9 |
| K_3 | 0.693 | 0.790 |
| T_1 | 333 | -908 |
| T_2 | 16.8 | 15.7 |

Table 3.10 - Coefficients of the transfer function

$$G(s) = K_1 + \frac{K_2}{1 + T_1 s} + \frac{K_3}{1 + T_2 s}$$

relating active power (MW) to control valve setting (%) at high and low load levels.

The direct coupling K_1 is quite large and reflects the fast response of active power to a change of control valve setting. The nonlinear valve characteristic gives rise to the higher gains in the low level model.

The physical reason for the mode associated with the time constant T_2 may be the large steam volume contained in the reheater of the boiler.

4. Conclusions

In all cases presented in this chapter we have been able to establish a model. In most cases it was also possible to assign a physical interpretation to model dynamics. Two important properties of the boiler dynamics have been illustrated namely the noise characteristics and the nonlinearities. Since a linear model is assumed a priori, the nonlinear effects recognized, when perturbing the boiler in steady state, could also influence the noise characteristics.

The results of the identification have shown that an improvement is achieved if the C^* -polynomial is included. However, neither the maximum likelihood model nor the least squares model implies that there is only output noise in a state space representation. This is true only if the A^* - and C^* -polynomials are identical. A continuous state space model

should thus be

$$\dot{\mathbf{x}}(t) = \mathbf{A} \mathbf{x}(t) + \mathbf{B} u(t) + \mathbf{v}(t)$$

$$y(t) = \mathbf{C} \mathbf{x}(t) + \mathbf{D} u(t) + e(t)$$

where $\mathbf{v}(t)$ and $e(t)$ are white noise with the covariance matrices \mathbf{R}_1 and \mathbf{R}_2 . The modelling of noise characteristics from physical arguments is not easy. Possibly, the covariance matrix \mathbf{R}_2 could be estimated from sensor and transmitter properties.

The gain and time constants of the derived models change significantly when load is changed from 90 % to 50 %. It has been shown in [53] that the dominant time constant and the gains depend on stored energy and control valve position. For the design of regulators for the boiler, the nonlinearities are not of the worst kind since the dominant time constant will not decrease when gain increases. However, the magnitude of changes of the boiler dynamics, when load is varied, is such that it cannot be neglected when designing control systems.

The design of the experiment included the choice of

- multiple input or single input experiments,
- measurement time,
- input sequences,
- sampling interval.

For reasons stated previously there was in this case only a rather unrestricted choice regarding the input sequence. The results of the identification have shown that especially the steady state gain of the models relating active power to fuel flow and control valve setting is inaccurate. This could be due to the choice of input sequence and sampling rate but also to nonlinearities of boiler dynamics. A possible way to improve the estimates is to choose an input sequence as in Fig 3.11. Two "step inputs" of opposite sign are thus included. The length of each step is chosen so that the steady state is nearly approached. The demand on the time required for the measurement will, however, increase.

The signal to noise ratio is rather high in the experiments. To reduce the effects of nonlinearities of boiler dynamics it seems possible to use a smaller input amplitude.

The order of the maximum likelihood models range from 1 to 4. The fourth order models were needed when modelling drum level using two

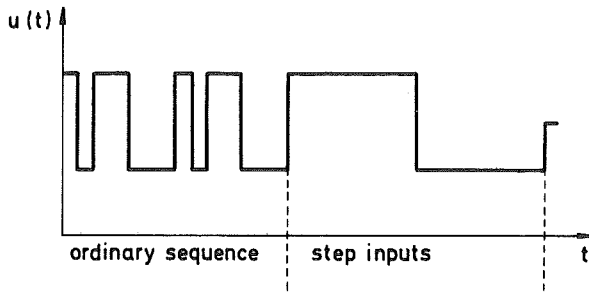


Fig 3.11 - An input sequence including two "step inputs" of opposite sign.

inputs. Low order linear models is thus obtained in spite of the very complex phenomena of the real process.

Accuracy of parameters of model polynomials is in general good. Only the attempted identification of drum level using two inputs gave bad results. This should be expected since feedwater, which was one of the inputs, was only intentionally changed a small number of times. A successful modelling with several inputs at least requires experiments especially designed for this purpose.

The peak to peak value of the deterministic error represents in all cases 20-30 % of the peak to peak value of the measured output. A large portion of the output is thus modelled as caused by the input.

1. Introduction

The methods for modelling multivariable processes from measurements are not as well established as for single input-single output processes. The choice of model structure becomes more involved and the number of unknown parameters grows very rapidly with increasing model order and increasing number of inputs and outputs. In this situation, it becomes more worthwhile to look for solutions where all available a priori knowledge can be used.

In many cases, a state space model derived from basic physical equations is available. The model might be derived using rough approximations and might also include physical quantities, such as heat transfer rates which are difficult to compute in advance. On the other hand, the model might include the basic physical phenomena which constitute the essential dynamic behaviour of the process. Such a model might possess a correct structure and it can possibly be improved by adjusting the parameters to measurements.

The state space representation of the process thus has several attractive features. It allows the process to be multivariable and full advantage can be taken of a construction data model. Also when designing a control system, based on a construction data model, this system can be regarded as preliminary. The final design is made, when measurements are available and model parameters have been identified.

In the boiler application we will use a drum system model to illustrate the feasibility of this identification approach. The drum system is the most essential process component since drum pressure strongly influences other important boiler variables. The complete boiler-turbine model is not considered since the data available are only from single input experiments. When identifying a multivariable process it is most advantageous to use multivariable experiments. In this case, this is achieved by shifting two experiments in time and then adding the inputs and outputs of the experiments, thus assuming that the principle of superposition is valid. The shifting of inputs is necessary since the inputs are identical. Also the number of unknown parameters, in the complete boiler-turbine

model, becomes very large and it is convenient to investigate the possibilities of the method on a system less complex.

The purpose of the material presented in this section is thus two-fold. The possibilities of improving state space models from construction data are investigated. Further additional information can be obtained about the dynamics of the boiler and the validity of the construction data model.

In Section 2 the identification method is outlined. Two different state space models, called open and closed loop models, are also discussed. The results of the identification are given in Section 3. The identified models are evaluated by comparing simulated responses and measurements, by the properties of residuals and by comparing the eigenvalues to those of the construction data model. Finally, the gained information is summarized in Section 4.

2. Resumé of the identification method

The problem is to estimate an unknown parameter vector θ in a model of the process. In this case, the model chosen to represent the boiler is a state space model, which is allowed to be multivariable. Since a construction data model will be used as an initial guess, model order is assumed to be known. The available information is sequences of measured values of input variables

$$\{u_i(t), t = 1, \dots, N\} \quad i = 1, \dots, m$$

and output variables

$$\{y_i(t), t = 1, \dots, N\} \quad i = 1, \dots, k$$

The input variables $\{u_i(t), i = 1, \dots, m\}$, are assumed to be constant over the sampling interval.

A stochastic discrete time model of a multivariable linear system is

$$\begin{aligned}
 \mathbf{x}(t+1) &= \phi(\theta)\mathbf{x}(t) + \Gamma(\theta)\mathbf{u}(t) + \mathbf{K}(\theta)\boldsymbol{\epsilon}(t) \\
 \mathbf{y}(t) &= \mathbf{C}(\theta)\mathbf{x}(t) + \mathbf{D}(\theta)\mathbf{u}(t) + \boldsymbol{\epsilon}(t)
 \end{aligned}
 \tag{2.1}$$

where the sampling rate is taken to unity and where $\{\boldsymbol{\epsilon}(t)\}$ is a sequence of independent equally distributed gaussian variables with zero mean and covariance matrix \mathbf{R} . The state vector \mathbf{x} , the input \mathbf{u} and the output \mathbf{y} have dimensions n , m and k . The matrices ϕ , Γ , \mathbf{K} , \mathbf{C} and \mathbf{D} may all depend on the unknown parameter vector θ . The model (2.1) will in the sequel be referred to as a closed loop model. The continuous time model is obtained by transforming the deterministic part of (2.1).

If the process under consideration is identical to the model with the same initial conditions, the model state vector $\mathbf{x}(t)$ has physical interpretation as the conditional mean of the state of the process and the matrix \mathbf{K} is the Kalman filter gains [48], [54]. This is a nice property since the implementation of a Kalman filter for reconstruction then requires no additional computation.

The likelihood function for estimating the parameter vector θ and the covariance matrix \mathbf{R} is given by

$$-2 \log L(\theta, \mathbf{R}) = N \log \det \mathbf{R} + \sum_{t=1}^N \boldsymbol{\epsilon}^T(t) \mathbf{R}^{-1} \boldsymbol{\epsilon}(t) + nN \log 2\pi \tag{2.2}$$

The maximization of $L(\theta, \mathbf{R})$ can be performed separately with respect to θ and \mathbf{R} and it has been shown [14] that the maximum of $L(\theta, \mathbf{R})$ is obtained by finding the minimum of

$$V(\theta) = \det \left\{ \sum_{t=1}^N \boldsymbol{\epsilon}(t) \boldsymbol{\epsilon}^T(t) \right\} \tag{2.3}$$

with respect to θ . Using the residuals $\boldsymbol{\epsilon}(t)$ computed at the minimum point, the covariance matrix \mathbf{R} is estimated by

$$\hat{\mathbf{R}} = \frac{1}{N} \sum_{t=1}^N \boldsymbol{\epsilon}(t) \boldsymbol{\epsilon}^T(t) \tag{2.4}$$

The residuals $\boldsymbol{\epsilon}(t)$ are defined by

$$\epsilon(t) = y(t) - \hat{y}(t) \quad (2.5)$$

where $\hat{y}(t)$ is the output of the model using the current value of $\hat{\theta}$.

Under mild conditions the maximum likelihood estimates are consistent, efficient and asymptotically normal [9], [47]. If the numerical algorithm also calculates the matrix of second derivatives, an estimate of the accuracy of the parameter vector θ is also obtained.

The state space model (2.1) is not a unique representation of the input-output relations. If no a priori information of the system matrices ϕ , Γ , K , C and D is available the number of parameters must be reduced. In general the number of parameters equals

$$N_1 = n(n + m + 2k) + k \left(m + \frac{k}{2} + \frac{1}{2} \right) \quad (2.6)$$

where the fact that R is symmetric has been used. A canonical representation has

$$N_2 = n(m + 2k) + k \left(m + \frac{k}{2} + \frac{1}{2} \right) \quad (2.7)$$

parameters. This number is less than N_1 and constitutes an upper bound of the number of parameters which can be identified. Choosing ϕ diagonal and by imposing a condition such as

$$\max_j \gamma_{ij} = 1, \quad i = 1, \dots, n$$

on Γ a canonical representation is obtained. However, a construction data model, which is a type of a priori knowledge, is unlikely to be a canonical representation.

Identifiability is thus a severe problem in this case. The concept of identifiability has been treated in several papers [7], [50], [54]. In this report we use

- the model (2.1) is identifiable if there is a one-to-one correspondence between the parameter space and the input-output relations,
- the model (2.1) is locally identifiable at $\theta = \theta_0$ if there is a one-to-one correspondence between the parameter space and the input-output relations in a neighbourhood of θ_0 .

Unfortunately there exists no general criterion which makes it possible to determine, if a given parametric model with unknown parameters is identifiable. Local identifiability can in this case be established if the minimum of (2.3) is unique. However, this requires that the minimum is known and that the matrix of second order derivatives can be computed.

From (2.3) it follows that the identification is equivalent to the minimization of a function of several variables. Since the computation of an analytical gradient and matrix of second derivatives is quite complex, the identification programme utilizes a minimization algorithm which numerically estimates these quantities. The minimization algorithm is [18] which was constructed on the basis of [1], [21], [40]. The number of unknown parameters, in a multivariable model, will become quite large since there is usually no a priori knowledge of the K matrix. This may create numerical difficulties. In particular the matrix of second order derivatives has been found to be poor.

The model (2.1) is called the closed loop model because the model receives process outputs as well as inputs. Besides this model we will also use

$$\begin{aligned} x(t+1) &= \phi x(t) + \Gamma u(t) \\ y(t) &= Cx(t) + Du(t) + \epsilon(t) \end{aligned} \tag{2.8}$$

where $\{\epsilon(t)\}$ is measurement noise with the same properties as in model (2.1). The parameters are also in this case adjusted to minimize (2.3). The model (2.8) is referred to as an open loop model since only process inputs are used. The model (2.8) correspond to the case when the only disturbances are white measurement noise.

In the identification programme, the parameters are introduced as elements of the matrices A, B, C and D of the continuous time model. Thus

$$\begin{aligned} \phi &= e^{A(\theta)} \\ \Gamma &= \begin{pmatrix} 1 \\ \int_0^1 e^{A(\theta)s} ds \\ 0 \end{pmatrix} B(\theta) \end{aligned} \tag{2.9}$$

It is then easier to have physical interpretation of the parameters.

3. Results of Identification

A fifth order model for the drum system was chosen in Section 4 of Chapter 4. The model is

$$\begin{aligned}\frac{dx(t)}{dt} &= Ax(t) + Bu(t) \\ y(t) &= Cx(t) + Du(t)\end{aligned}\tag{3.1}$$

where the state vector x is

- x_1 drum pressure
- x_2 drum level
- x_3 drum liquid mean temperature
- x_4 riser tube mean temperature
- x_5 steam quality mean value

the input vector u is

- u_1 fuel flow
- u_2 feedwater flow
- u_3 steam flow

and the output vector y equals the first two state variables. Numerical values of matrices A , B , C and D were obtained using subroutine DR5M, see Appendix A, and construction data from Öresundsverket power plant.

Data for a multivariable experiment was created by adding the inputs and outputs of Exp. A and Exp. E. Since the main input sequence in both experiments are identical, the data sequences of Exp. E were delayed 30 sampling intervals viz. if T is the sampling rate and if $v^X(nT)$ is the value of variable v of Exp. X at time nT , then $v^A\{(n+30)T\}$ was added to $v^E(nT)$. The last thirty data points of Exp. E were not used and all variables of this experiment were taken to be equal to their mean value in the interval $t = T - 30T$. In this way, all data of Exp. A could be used. The input variable in Exp. E is control valve position, but steam flow changes accordingly as seen from Fig 5.5 in Chapter 3. Exp. B was not included since the feedwater flow was

changed in both Exps. A and E. Further it is essential to be able to test the resulting model against data not used in the identification.

3.1 Closed Loop Models

The model is defined by eq. (2.1). The initial estimates of matrices A, B, C and D are obtained from the construction data model (3.1). Matrices ϕ and Γ are obtained using eq. (2.9). No information of the elements of matrix K is available. Since the construction data model has been the starting point for the identification, the outputs drum pressure and drum level are measured in bar and mm respectively.

Choice and estimates of parameters

A canonical representation of model (2.1) will contain, in this case, 44 unknown parameters which gives an upper bound on parameters in an identifiable model. Since nothing is known about the matrix K, there are at least 10 parameters to be identified. The problem then is to find a set of parameters which gives an identifiable model and where the fixed elements of A, B, C and D do not essentially restrict the input-output relations defined by the model. It is also important, that the number of unknown parameters is as small as possible, to avoid numerical difficulties.

The structures of the continuous time matrices A and B are

$$A = \begin{pmatrix} a_{11} & 0 & a_{13} & a_{14} & a_{15} \\ a_{21} & 0 & a_{23} & a_{24} & a_{25} \\ a_{31} & 0 & a_{33} & a_{34} & a_{35} \\ a_{41} & 0 & 0 & a_{44} & 0 \\ a_{51} & 0 & a_{53} & a_{54} & a_{55} \end{pmatrix}$$

$$B = \begin{pmatrix} 0 & b_{12} & b_{13} \\ 0 & b_{22} & b_{23} \\ 0 & b_{32} & b_{33} \\ b_{41} & 0 & 0 \\ 0 & b_{52} & b_{53} \end{pmatrix}$$

The elements in A and B which equal zero are given as zero. The outputs simply equal the first two state variables which means that both the C and D matrices are entirely known. Certainly not all of the parameters of A and B can be identified since the total number of parameters in A, B and C is 37. The canonical representation has only 35 parameters (D is zero and R is not included). In general, it is very difficult to choose the elements of A and B which are most essential for the dynamics and crosscoupling. The choice of parameters was based on physical arguments such as

- drum pressure strongly influences other state variables,
- steam quality gives non-minimum phase characteristics to responses of drum level,
- the influence of inputs is essential and especially the influence of steam flow is not known accurately,
- fuel flow does not affect drum pressure directly but only riser tube temperature.

Several sets of parameters were tried. The number of parameters in A and B ranged from 2 to 10. The final choice, which gave reasonable good results, is shown in Table 3.1. This set of parameters may for physical reasons well establish an identifiable model. Other sets, which included the eighteen parameters in Table 3.1, gave only a small improvement of the loss function V. The computational aspects are discussed later in this section.

The value of the loss function has been decreased drastically by the identification. All parameters of the A and B matrices have changed significantly. Parameters a_{14} , a_{44} and b_{13} have been subjected to the largest changes, roughly a factor 4, 10 and 3 respectively. The first two parameters, a_{14} and a_{44} , strongly influence the coupling between mean temperature of risers and drum pressure, and the dynamics of heat storage in riser tube masses. The change of b_{13} represents a decrease of the influence of steam flow on drum pressure derivative.

The estimated covariance matrix R equals

$$R = \begin{pmatrix} 0.0240 & 0.016 \\ 0.016 & 12.43 \end{pmatrix} \quad (3.2)$$

| | Initial | Identified |
|-----------------|-------------------------|-------------------------|
| V | $0.2567 \cdot 10^{17}$ | $0.3850 \cdot 10^5$ |
| a ₁₁ | -0.02835 | -0.02052 |
| a ₁₄ | 0.0406 | 0.1678 |
| a ₂₅ | -0.2266 | -0.3622 |
| a ₃₁ | 0.01382 | 0.00896 |
| a ₄₄ | -0.0454 | -0.3295 |
| a ₅₁ | $-0.1341 \cdot 10^{-3}$ | $-0.0738 \cdot 10^{-3}$ |
| b ₁₃ | -0.01575 | -0.00496 |
| b ₄₁ | $0.1162 \cdot 10^{-4}$ | $0.1446 \cdot 10^{-4}$ |
| k ₁₁ | 0. | 1.271 |
| k ₁₂ | 0. | $-0.1041 \cdot 10^{-2}$ |
| k ₂₁ | 0. | 0.01027 |
| k ₂₂ | 0. | $0.1279 \cdot 10^{-2}$ |
| k ₃₁ | 0. | -0.1214 |
| k ₃₂ | 0. | -0.06576 |
| k ₄₁ | 0. | 0.5432 |
| k ₄₂ | 0. | 0.01398 |
| k ₅₁ | 0. | $-0.7702 \cdot 10^{-3}$ |
| k ₅₂ | 0. | $0.3585 \cdot 10^{-4}$ |

Table 3.1 - Initial and identified parameters of the closed loop model. Elements of matrix K are valid for the discrete time model.

The standard deviations of the one-step ahead prediction error then are

$$\sigma_{\epsilon_1} = 0.155 \text{ bar}$$

$$\sigma_{\epsilon_2} = 3.53 \text{ mm}$$

Compare the results in the previous chapter.

The residuals $\{\epsilon(t)\}$ should equal a realization of discrete time white gaussian noise if the conditions of the identification method are fulfilled and if the minimum is achieved. Fig 3.1 shows the residuals $\{\epsilon(t)\}$ and Fig 3.2 shows the sample correlation function of $\{\epsilon_1(t)\}$. It is clear

from Fig 3.1, that large values of residuals are obtained at time of changes of the inputs. Compare Fig 3.6 and the discussions in Chapter 5. At time $t = 300$ seconds, the residuals of drum level take extreme large values. The reason for this is, that we start to add the actual values of Exp. E to those of Exp. A at this point.

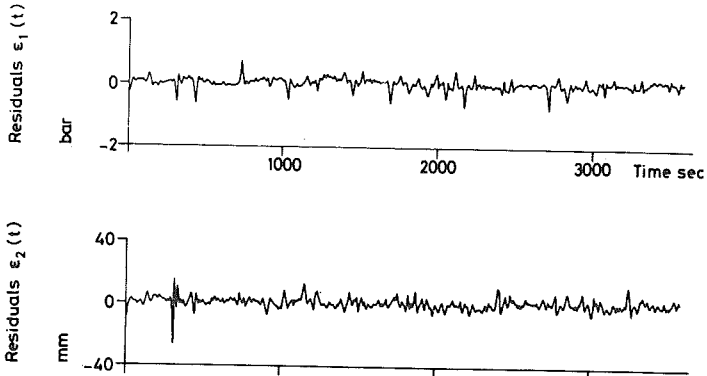


Fig 3.1 - Residuals $\epsilon_1(t)$ of drum pressure and $\epsilon_2(t)$ of drum level of the closed loop model.

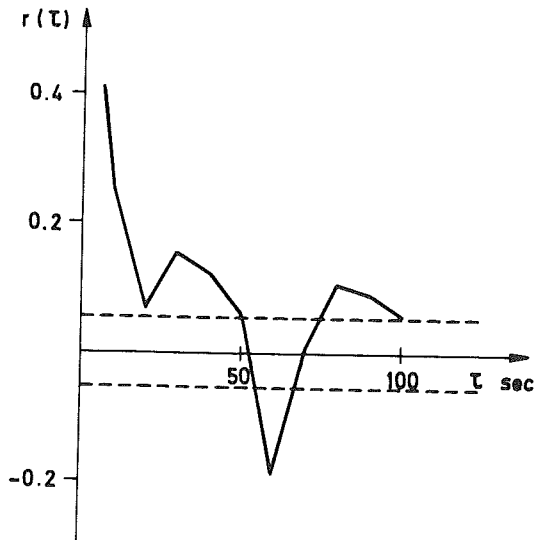


Fig 3.2 - Sample correlation function of residuals $\{\epsilon_1(t)\}$ of the closed loop model. The dashed line gives the one σ limit for $r(\tau)$, $\tau \neq 0$. Note that the basic interval of the input sequences is 60 seconds.

Since such errors now dominate the residuals, it means that further refinements of the model based on these particular measurements are not worthwhile. Should more accurate models be desired new experiments must be performed.

The sample correlation function of $\epsilon_1(t)$ shows that the sequence $\epsilon_1(t)$ differs significantly from a realization of discrete time white noise. The sample correlation function of $\epsilon_2(t)$ has the same characteristics.

Eigenvalues

The eigenvalues of the matrix A, corresponding to the initial guess and to the final model, are given in Table 3.2. The eigenvalues can be sensitive to parameter changes when transforming from discrete time models to continuous time models [27]. Especially eigenvalues corresponding to timeconstants smaller than the sampling interval.

| Eigen-
value
No. | Initial | Identified |
|------------------------|-----------------|------------|
| 1 | 0. | 0. |
| 2 | 0.00192 | -0.00166 |
| 3 | -0.0367 | -0.0449 |
| 4 | -0.0796+0.0177i | -0.0811 |
| 5 | -0.0796-0.0177i | -0.343 |

Table 3.2 - Eigenvalues of matrix A for the construction data model and for the identified model.

Since the column of zeros in A does not include any parameter, the zero eigenvalue is preserved exactly. The unstable mode of the construction data model is not found in the identified model and is thus not verified by measurements. This is not surprising since the eigenvalue of the identified model correspond to a timeconstant of 600 second and the model has been adjusted to predict the value of the outputs only 10 seconds ahead. During this time there is only a slight difference between the modes. The fast mode No. 5 of the identified model is due to the strongly changed parameter a_{44} which means that the dynamics associated with the riser masses appears very fast in the measurements. This fact can be used for further simplification of the construction data model.

Simulations

The simulated responses of the identified stochastic model, using the same data as used for the identification, agree extremely well with measurements. Any difference would not appear in a diagram and is therefore not shown. This situation is quite typical when simulation is done on the same dataset which was used in the identification. It is therefore of interest to make other comparisons. In this section we will investigate the deterministic part of the final model, that is

$$\begin{aligned}\frac{dx(t)}{dt} &= Ax(t) + Bu(t) \\ y(t) &= Cx(t) + Du(t)\end{aligned}\tag{3.3}$$

where A, B, C and D are the identified matrices.

The deterministic model will be investigated for the datasets A, E and B, Figs 3.3, 3.4 and 3.5 respectively. Notice that the identification was based on the superposition of Exps. A and E.

Only responses of the two output variables are given. The magnitudes of the responses of the other three state variables are, however, within reasonable limits.

In Figs 3.3 and 3.4 the differences of responses are largest when the feedwater flow is changed. A reason for this can be that the feedwater temperature, which varies due to the changing fuel, feedwater and steam flows, has been neglected in the model. Especially the difference in trend of drum level responses, in the time interval $t = 1000 - 1500$ of Exp. E in Fig 3.4, verifies this assumption. This is discussed in detail in the next chapter.

The drum pressure response of Exp. E in Fig 3.4 appears to be too sluggish or the gain is too small. The last alternative is most probable since the parameter b_{13} was decreased by a factor 3 in the identified model. The non-minimum phase characteristics of the drum level responses have been well adjusted to measurements.

The responses of Exp. B are shown in Fig 3.5. The discrepancies of drum level responses imply that feedwater flow affects the derivative of drum level too strongly. However, when element b_{22} of matrix B was included in the identification the sign of b_{22} was changed, which cannot be accepted for physical reasons. The drum pressure response of the identified model is not in accordance with measurements.

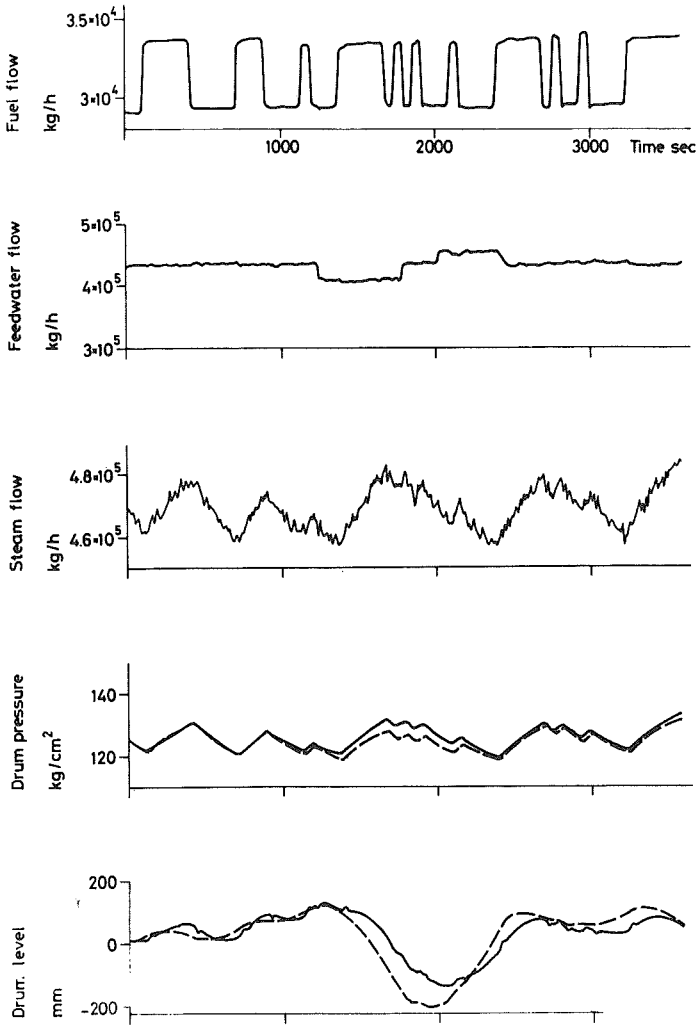


Fig 3.3 - Comparison of measured boiler (solid) and identified closed loop model (dashed) responses of Exp. A.

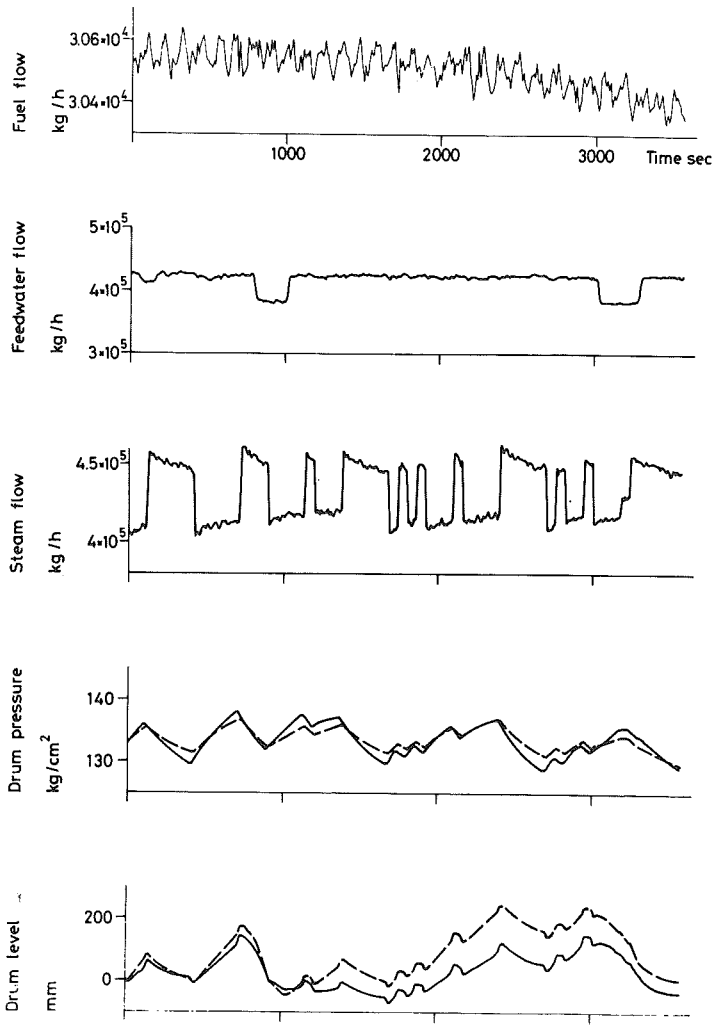


Fig 3.4 - Comparison of measured boiler (solid) and identified closed loop model (dashed) responses of Exp. E.

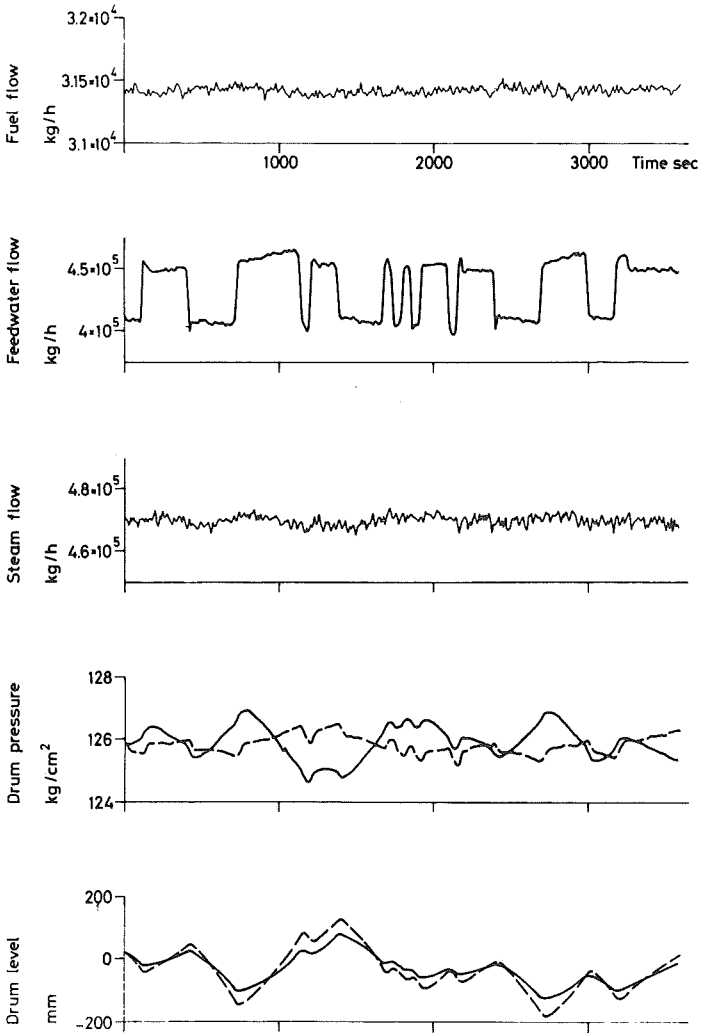


Fig 3.5 - Comparison of measured boiler (solid) and identified closed loop model (dashed) responses of Exp. B.

3.2 Open Loop Models

As seen in the previous subsection the number of unknown parameters soon becomes large. If we assume that no a priori information is available about the matrix K, which usually is true, the minimum number of parameters in the closed loop model (2.1) is nk which rapidly increases with the number of outputs k . For this reason an open loop model (2.8) is attractive. Notice that the statistical assumptions that lead to the open loop model correspond to the case when there are no process disturbances and white measurement noise only.

Choice and estimates of parameters

The same set of parameters of matrices A and B was used. The resulting values are given in Table 3.3.

| | Initial | Identified |
|----------|-------------------------|-------------------------|
| V | $0.2567 \cdot 10^{17}$ | $0.3591 \cdot 10^9$ |
| a_{11} | -0.02835 | -0.01731 |
| a_{14} | 0.0406 | 0.1255 |
| a_{25} | -0.2266 | -0.3572 |
| a_{31} | 0.01382 | 0.00513 |
| a_{44} | -0.0454 | -0.2401 |
| a_{51} | $-0.1341 \cdot 10^{-3}$ | $-0.0903 \cdot 10^{-3}$ |
| b_{13} | -0.01575 | -0.00462 |
| b_{14} | $0.1162 \cdot 10^{-4}$ | $0.1135 \cdot 10^{-4}$ |

Table 3.3 - Initial and identified parameters of the open loop model.

As an initial guess of parameters the values provided by the construction data model were used. Compare with the results for the closed loop model in Table 3.1.

The sample covariances decay very slowly thus indicating that the residuals are not realizations of white noise. The standard deviations of residuals are

$$\sigma_{\epsilon_1} = 1.70 \text{ bar}$$

$$\sigma_{\epsilon_2} = 50.1 \text{ mm}$$

Compare with $\sigma_{\epsilon_1} = 0.155 \text{ bar}$ and $\sigma_{\epsilon_2} = 3.53 \text{ mm}$ obtained for the closed loop model.

Eigenvalues

The eigenvalues of matrix A using the adjusted parameters are given in Table 3.4.

| Eigen-
value
No. | Initial | Identified |
|------------------------|-----------------|------------|
| 1 | 0. | 0. |
| 2 | 0.00192 | -0.000797 |
| 3 | -0.0367 | -0.0420 |
| 4 | -0.0796+0.0177i | -0.0815 |
| 5 | -0.0796-0.0177i | -0.253 |

Table 3.4 - Eigenvalues of matrix A for the construction data model and for the identified open loop model.

Eigenvalue No. 2 has changed to a stable mode but the change is smaller than in the closed loop model. The identified eigenvalue is now very close to zero and corresponds to a time constant of 1250 seconds which is a considerable amount of the measurement time. Eigenvalues 3, 4 and 5 of the identified model are similar to those given in Table 3.2. This verifies the conclusion that the dynamics of the riser tube masses can be considered fast.

Simulations

For this model we choose to show a comparison of responses for Exp. A + E, used in the identification, and for Exp. A. The steady state values

of inputs and outputs of Exps. A and E, at the beginning of the experiments, were not the same. Therefore in Fig 3.6, showing the results of Exp. A + E, only the deviations from the steady state values are given.

Drum pressure responses of both Figs 3.6 and 3.7 do not agree well in the middle part of experiments. This has been a characteristic property of all deterministic drum pressure loops considered both in this and the previous chapter. The drum level response in Fig 3.6 is, in general, not well adjusted to the measured curve but the non-minimum phase characteristics of both responses agree. Using data from Exp. A, as in Fig 3.7, the simulated drum level response differs completely from the measured one. This is a severe disagreement since the gross characteristics of the two curves are not the same. The results obtained using an open loop model is thus significantly worse than those of a closed loop model in this application. The reason may be that physical variables, such as feedwater temperature, are not included in the initial model structure. If we interpret the result of such model imperfections as noise, it is probable, that this noise can more easily be handled by the stochastic structure of the closed loop model.

3.3 Computational Aspects

The minimization algorithm uses a numerical estimate of both the gradient and the matrix of second order derivatives. A local minimum of V , with respect to the parameters θ , is achieved if the gradient equals zero at this point and if the matrix of second derivatives $V_{\theta\theta}$ is positive definite. The inverse of $V_{\theta\theta}$ contains information of the accuracy of estimated parameters.

The minimization could rarely be done in one run. It was frequently necessary to interfere manually, by choosing different starting values and to change various parameters of the algorithm, like test quantities for terminating conditions. It was sometimes difficult to know that a local minimum was obtained since the numerical gradients were not always small. By restarting the algorithm from different starting points, the algorithm would usually converge to the same parameter values, even if the numerical gradient had relatively large values. In this respect the open loop models were more difficult to handle than the closed loop models.

The estimates obtained of the matrix of second order derivatives were usually very poor. The identifiability of the models could not be verified. The assumption of identifiable models is then only based on physical arguments.

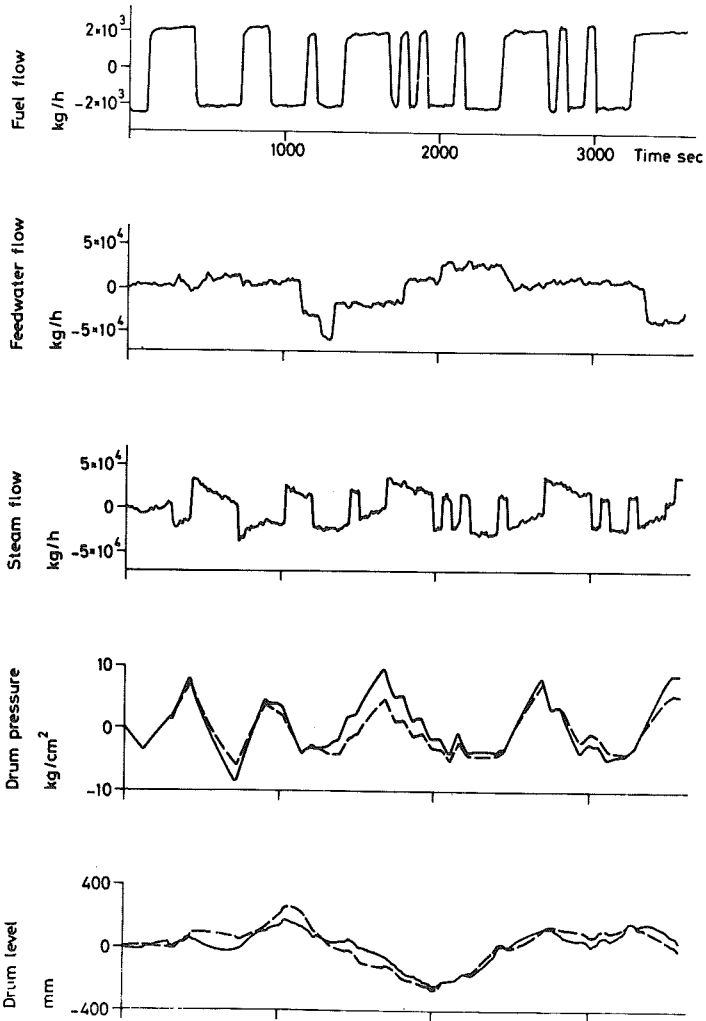


Fig 3.6 - Comparison of measured boiler (solid) and identified open loop model (dashed) responses of Exp. A + E.

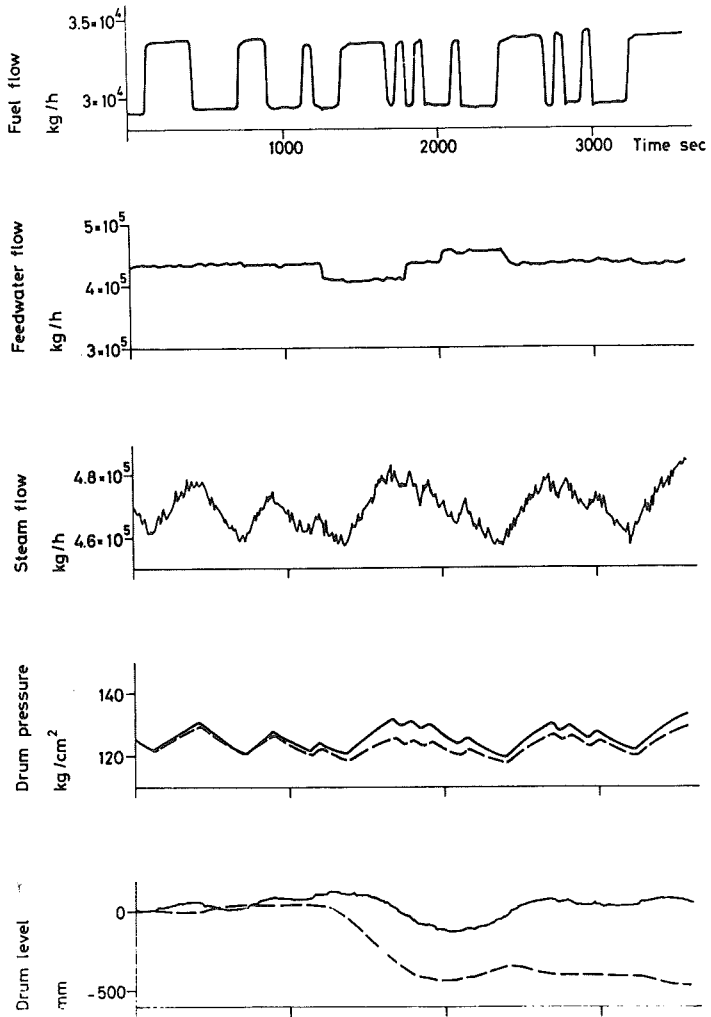


Fig 3.7 - Comparison of measured boiler (solid) and identified open loop model (dashed) responses of Exp. A.

It is not easy to give a meaningful figure of computing times. The final choice of parameters and parameter values was not obtained in one run of the programme. As initial values of one set of parameters, earlier computed estimates of partly another set were used. However, taking the construction data model as an initial guess the computing time ranged between 10 and 40 minutes for estimating between 8 and 20 parameters. The programmes were run on a UNIVAC 1108. The time depended on the number of parameters, the initial value of θ and the required accuracy.

4. Conclusions

In spite of the difficulties encountered with the minimization algorithm it is not believed possible to obtain significantly better models without using new experiments. This is indicated by the nature of the residuals of the closed loop model. The residuals obtained are actually dominated by factors which can be referred to experiment limitations, like finite raise time of the input signal and the nonsimultaneous sampling of the inputs.

The closed loop model has appeared to be superior to the open loop model in this application. The agreement between measurements and model responses were much better for the closed loop model. The residuals, for the closed loop model, were also significant smaller than those of the open loop model. The number of parameters in a closed loop model is, however, increasing rapidly with the number of outputs. If the identification method is applied to the complete boiler model, five significant outputs is easily found. Then the minimum number of parameters, that is the number of parameters in the matrix K , is 45. This will probably yield very long computing times if the minimization routine can be made to behave well.

Computing times have turned out to be long even for a moderate number of parameters. Since this number easily grows, the identification method heavily depends on the minimization algorithm which is used. Difficulties were encountered with the numerical differentiation in this particular algorithm. It would probably be a significant improvement to evaluate the gradient explicitly, even if this means a significant increase of the programming work. Further, to be able to benefit from the nice properties of the maximum likelihood scheme, which gives a complicated loss function requiring numerical differentiation, the minimization algorithm must produce reliable estimates of the matrix of second order derivatives.

The large discrepancies, between identified model responses and measurements of Exp. B in Fig 3.5, strongly point out the need of multivariable experiments for multivariable identification.

It is important that the structure of the initial model is correct. That is, physical phenomena which are important for the dynamical behaviour must be present in the model. This is clearly illustrated by the good model adjustment to non-minimum phase characteristics of drum level responses and the failure of adjustment to the assumed influence of feedwater temperature.

CHAPTER 7 - EVALUATION OF MODEL FROM CONSTRUCTION DATA

1. Introduction

A proper evaluation of model properties requires, that the purpose of the model is specified. The ultimate goal of all models derived has been to develop models suitable for steady state control. Since models from first principles and measurements have been developed it is possible to establish whether the assumptions made are compatible with the data. This is an essential result since, if a construction data model is available, the control system can be designed and tested beforehand. Also the influence of different physical parameters on model dynamics can be investigated and the process designed, if possible, to ease the control task. This chapter will thus be devoted to the comparison of models from construction data to measurements and results of identification.

The open loop properties of the construction data model can thus be evaluated using

- field measurements,
- deterministic responses of models from measurements,
- transfer functions from the deterministic part of the maximum likelihood models,
- parameter changes in state space models adjusted to measurements.

The first item for comparison is treated in Section 2 and the last three in Section 3.

For control purposes obviously, the prediction error of the model is a significant quantity. The variance and sample correlation functions of the prediction error were computed for the maximum likelihood models as well as for the state space model from measurements. Comparing these quantities to those calculated from the construction data model will indicate the improvement which is possible to achieve by adjusting the models to a set of measurements.

In Section 2 model responses are compared to field measurements. The comparison covers Exps. A, B, C, D and E. Responses to all main input variables, viz. fuel flow, feedwater flow, attemperator flows and control valve position are thus given. Outputs included in the comparison amounts to seven in Exps. A and E and to three and four in Exps. B and C, D respectively. In the simulations of Exp. E the computed control valve characteristic was erroneous and had to be adjusted to measurements. Notice, however, no other adjustments of the construction data model were made. The third section deals with the comparison of transfer functions and prediction errors. Since the number of input-output relations of the multi-variable boiler process is large (~ 70), only a limited number of important loops are considered. To the knowledge of the author an extensive comparison of model responses to field measurements such as that of Section 2 has only been published in [33], [34] and [43]. The first two reports are concerned with the same model. However, in these reports only step responses of a duration of 20 minutes are presented. The last report also presents a comparison of step responses but the duration is only 5 minutes which is a very short experiment time. None of these reports is concerned with identifications. In the last section the valid and invalid model simplifications and approximations are stated. Possible simplifications are also indicated.

2. Comparison to field measurements

In Chapter 3 the results of experiments were presented and some peculiarities were pointed out. In the comparison given here only the high load level experiments are used. In Figs 2.1 - 2.5 responses of both the real process and the model from construction data for Exps. A - E are presented. In the simulation the measured sequences of fuel flow, feedwater flow etc. are used as model inputs. The control valve position was not automatically recorded. Therefore an idealized sequence reconstructed from the manual recordings is used. The sampling rate is as in the measurements 10 seconds.

2.1 Fuel Flow Perturbations

Except for the main input, the feedwater flow was intentionally altered to keep drum level within acceptable limits. As a consequence of drum pressure fluctuations also the attemperator flows varied. In Fig 2.1 the flow of coolant water in attemperator 1 in the right steam path is given as an example.

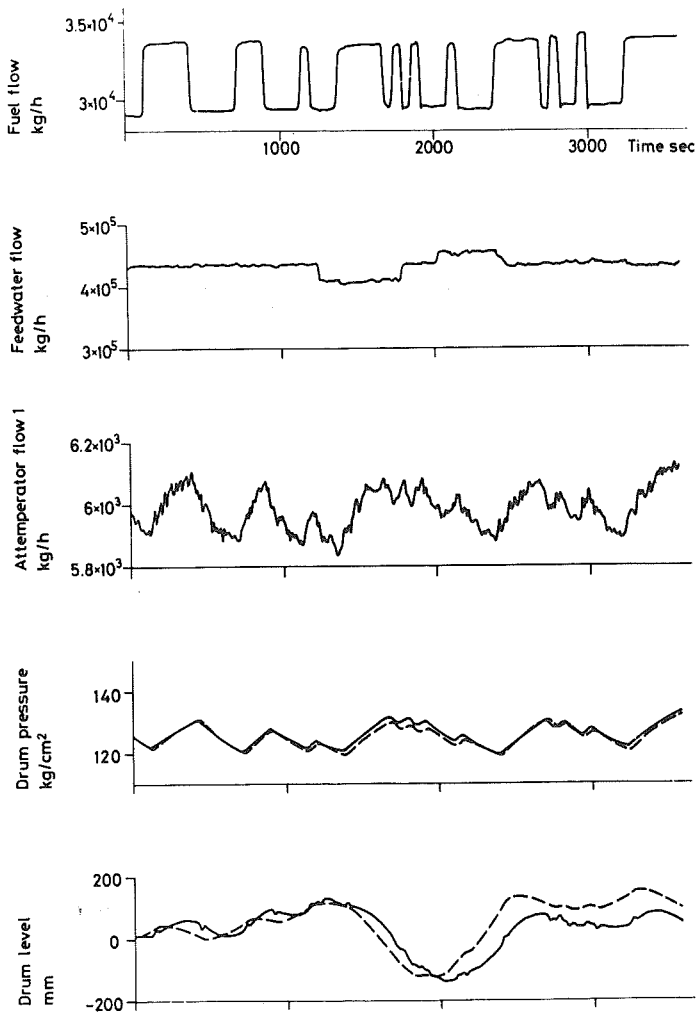


Fig 2.1 - Comparison of measured boiler-turbine (solid) and construction data model (dashed) responses of Exp. A.

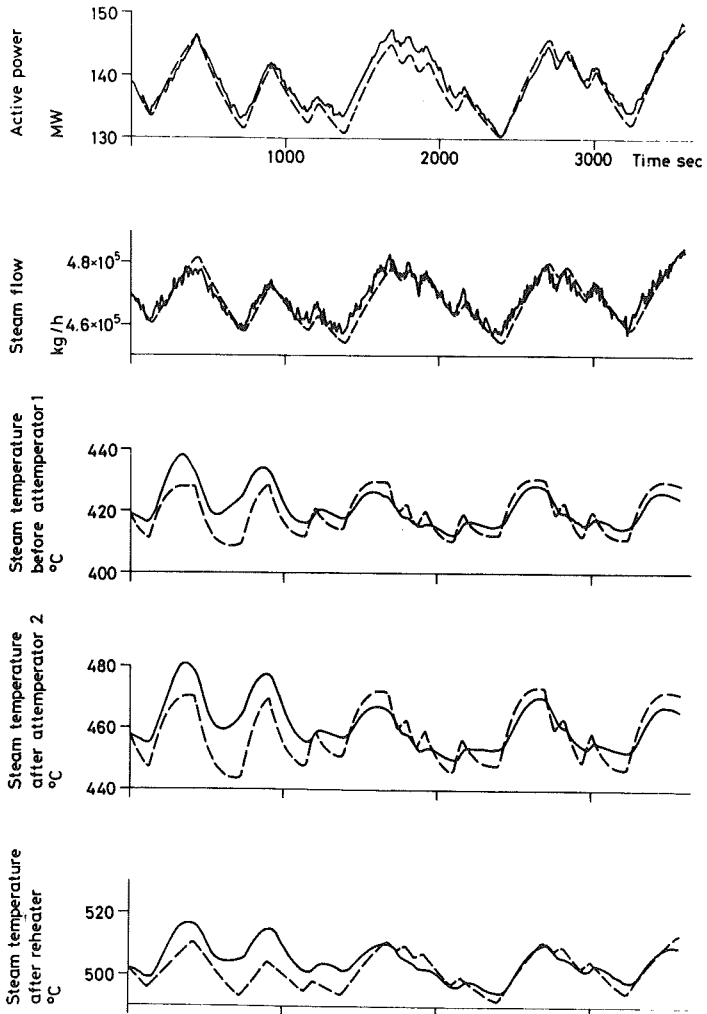


Fig 2.1 Contd.

The agreement of drum pressure, steam flow and active power responses is good. In the time interval 1500 - 2000 seconds there is a marked difference. The difference in drum pressure causes the differences in the other two responses. The reason for the high measured drum pressure is that feedwater flow was decreased at $t \approx 1200$ seconds and kept low until $t \approx 1800$ seconds. The influence of the changed flow is accounted for in the model but the assumption of constant enthalpy is violated. The decreased flow will raise the feedwater temperature. For constant input power to the risers, the amount of power available for evaporation then increases and pressure will raise.

Drum level responses differ considerably. There are two time points where the deviations seem to be initiated. The first point is at $t \approx 1200$ seconds and the second at $t \approx 1800$ seconds. Again this is where feedwater flow is changed. This indicates that the measured level response is due to changes of the volume of steam in drum water and risers. The increased evaporation due to higher feedwater temperature in the interval 1200 - 1800 seconds increase the steam volume in water, and drum level is raised in this interval. On the other hand the low feedwater temperature for $t \approx 2000 - 2400$ seconds gives the opposite effect and model drum level becomes higher than the measured one.

The last three curves of Fig 2.1 show the responses of temperature before attemperator 1, after attemperator 2 and after reheater. The large difference between responses in the first half of the experiment is due to an asymmetric heat distribution between the left and right steam paths of the boiler. This was commented upon when presenting the results of experiments in Chapter 3. Responses of temperatures measured before the H. P. turbine agree fairly well with model responses. However, model responses appear to be too fast. This is expected since the distributed parameter systems such as the superheaters have been approximated by one ordinary differential equation only. An improvement is achieved if a higher order approximation is used but to the prize of an increased model complexity. A fifth order model was also derived, but as stated in Chapter 4, the improvement was not significant enough to motivate an increased model order. More sluggish measured responses are also expected since the dynamics of temperature measuring devices are not included in the model and since heat flow to superheaters is modelled as a constant times fuel flow. Dynamics of temperature measuring devices is, however, fast and is further discussed in Exps. C and D. A more realistic model of heat flow to superheaters is obtained if the dependence on combustion gas temperature is included. This would probably improve model responses and does not increase model order.

2.2 Feedwater Flow Perturbations

In Exp. B shown in Fig 2.2 both feedwater flow and temperature are shown as input variables. Model responses are calculated using a constant feedwater temperature. The influence of feedwater changes on steam temperatures, active power and steam flow are small and due to drum pressure fluctuations. Therefore, only the steam temperature before the turbine is given to illustrate the magnitude of temperature variations.

In this experiment the influence of feedwater temperature on drum pressure and level responses is clearly shown and the arguments used in the previous subsection verified. Consider for example the increased feedwater flow in the interval $t \approx 800 - 1100$ seconds. Feedwater temperature drops and causes the drum pressure to drop since evaporation decreases. The volume of steam in water kept in drum and risers decreases. Model drum level response thus raises faster than the measured response.

From this discussion we conclude that the economiser should be included in the model and that a significant improvement of model responses can be expected. Most likely a first order model is sufficient and the complete model complexity is only slightly increased.

2.3 Attemperator Flow Perturbations

The attemperator flows 1 and 2 were perturbed in Exps. C and D and are shown in Figs 2.3 and 2.4 respectively. Only the flow in the right steam path was changed. The two steam paths were modelled as one path. In the simulations the measured attemperator flows thus were multiplied by two and the responses of drum pressure, active power and steam flow divided by two.

The magnitude of drum pressure variations in both experiments is small and responses agree well with model responses. Saturation temperature in drum will vary according to drum pressure and causes small temperature variations along the steam path. This is shown in Fig 2.4 where the temperature of steam is given before attemperator 2. The model predicts well the actual behaviour.

In both experiments steam temperature is measured directly after the attemperator. The model will give an instantaneous change of temperature followed by a response due to mass flow and drum pressure responses. The dynamics involved in the boiler responses are those of the attemperator

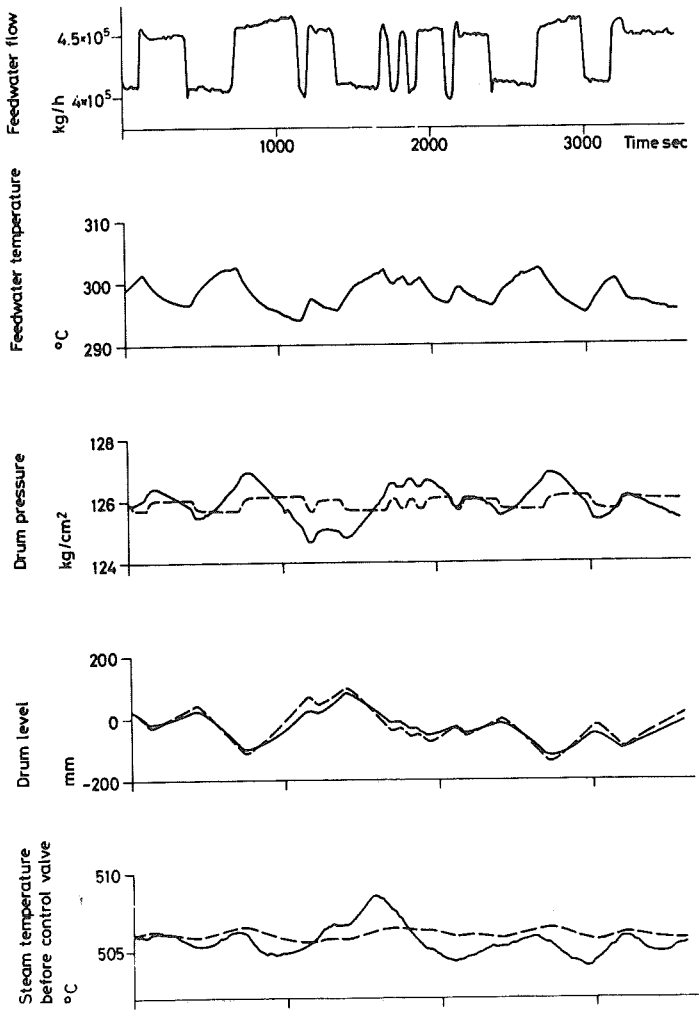


Fig 2.2 - Comparison of measured boiler-turbine (solid) and construction data model (dashed) responses of Exp. B.

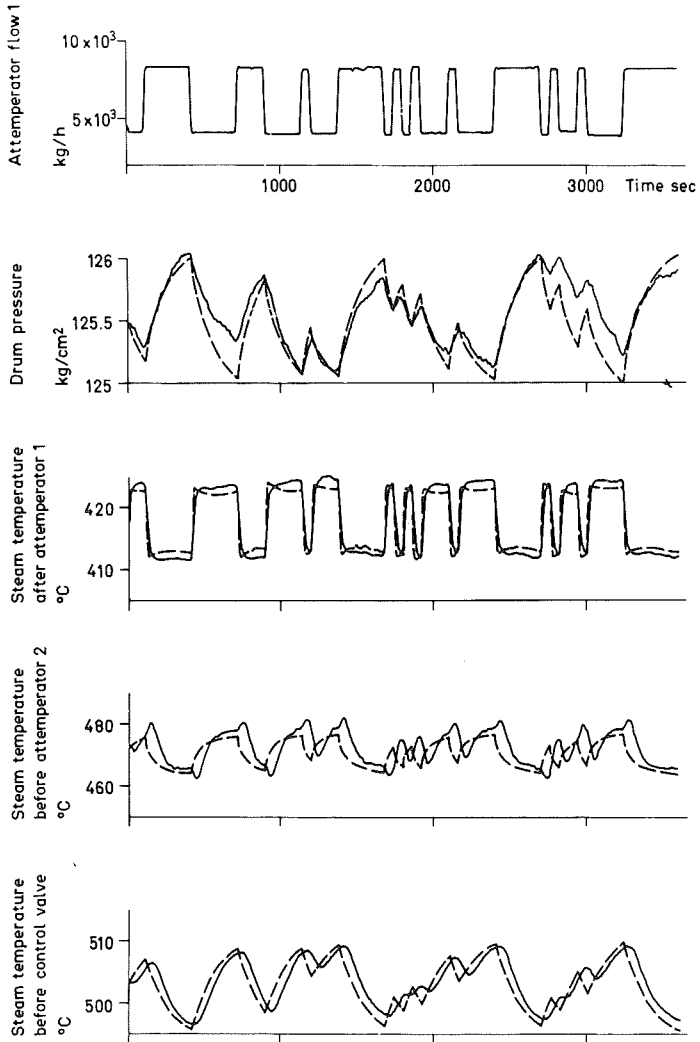


Fig 2.3 - Comparison of measured boiler-turbine (solid) and construction data model (dashed) responses of Exp. C.

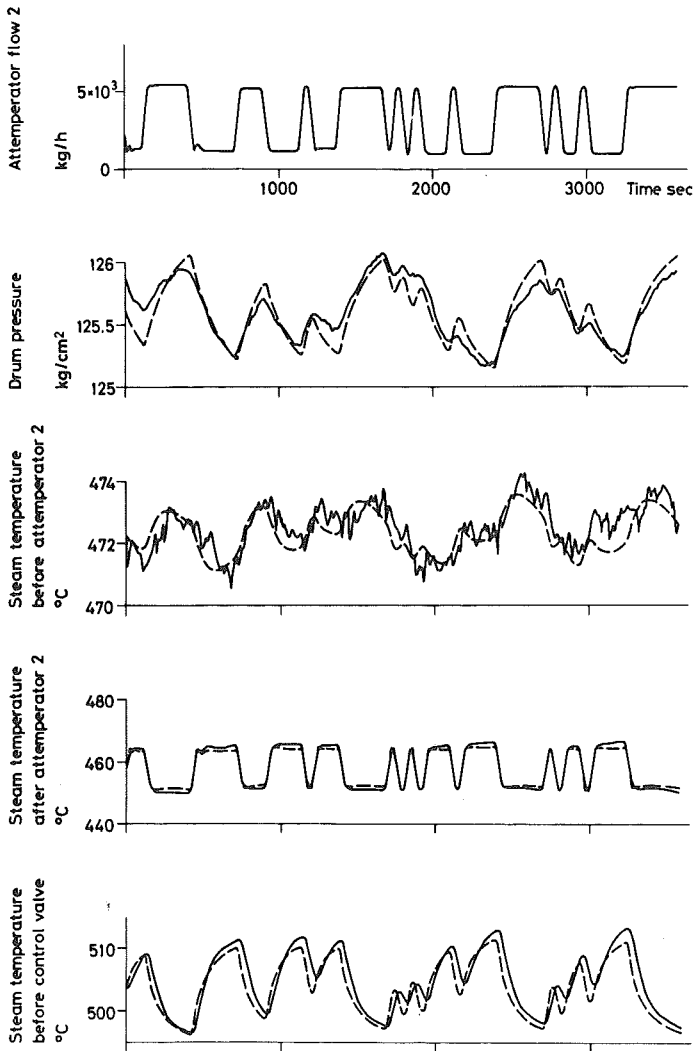


Fig 2. 4 - Comparison of measured boiler-turbine (solid) and construction data model (dashed) responses of Exp. D.

and the measuring device. Temperatures are measured by thermo-couples contained in a steel pipe mounted on the steam tube. The pipe is inserted to slightly more than half the tube diameter and the thermo-couple pressed to the bottom of the steel pipe by a spring. Maximum likelihood identification of a model relating steam temperature after attemperator to attemperator flow gave in both cases, for a first order model, a time constant roughly equal to 12 seconds. This figure can be taken as an estimate of the dynamics of the measuring device. However, the figure was not in accordance with established a priori knowledge. The estimates given by the working staff and companies delivering such equipment ranged from 80 to 120 seconds. It has not been verified that the results of measurements can be explained by physical arguments such as instantaneous heat transfer coefficients or that wet steam is hitting the inserted pipe. Heat transfer rates must then be high enough to yield the measured fast responses. This illustrates a typical situation where experiments of this kind contribute to the general knowledge of the plant dynamics.

The non-minimum phase characteristics of the measured temperature responses in Fig 2.3 is not a property of the model. The presence of such characteristics was not recognized when modelling the superheater. The responses of temperatures measured later in the steam path do not show non-minimum phase characteristics. Also steam temperature responses to changes of the flow in attemperator 2 show very little of this behaviour. A possible physical cause could then be that a fast change of the flow in attemperator 1 gives a rapid change of pressure in superheater 2. Numerical estimates of the temperature transient created gives, however, to small valves.

2.4 Control Valve Position Perturbations

Responses of model and boiler in Exp. E is shown in Fig 2.5. Due to drum pressure changes, also in this experiment, the attemperator flows varied significantly. The magnitude of variations is roughly 75 % of the magnitude in Exp. A.

A satisfactory model response of drum pressure is obtained. The discrepancies in drum level curves are, however, considerable. At least partly, the difference is explained by changes in feedwater temperature. However, most of the difference is explained by the difference in steam flow. Consider for example the interval $t \approx 500 - 750$ seconds. Obviously the lower steam flow of the boiler will give a faster raise of drum level than the model response. Notable is also the non-minimum phase characteristics of drum level dynamics. Physically this is caused by the steam bubbles

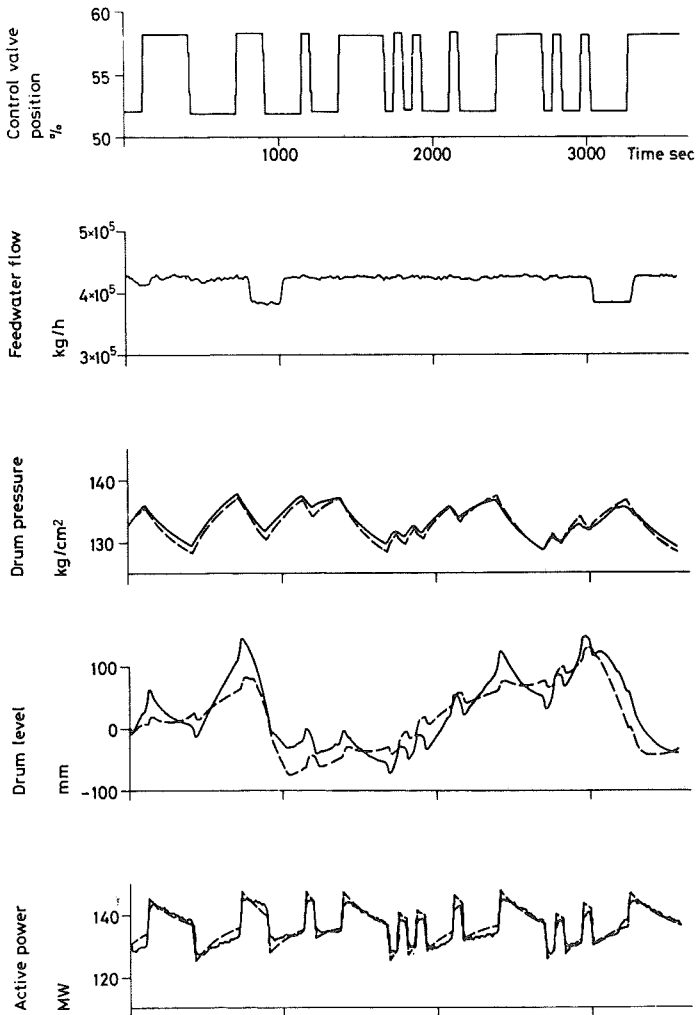


Fig 2.5 - Comparison of measured boiler-turbine (solid) and construction data model (dashed) responses of Exp. E.

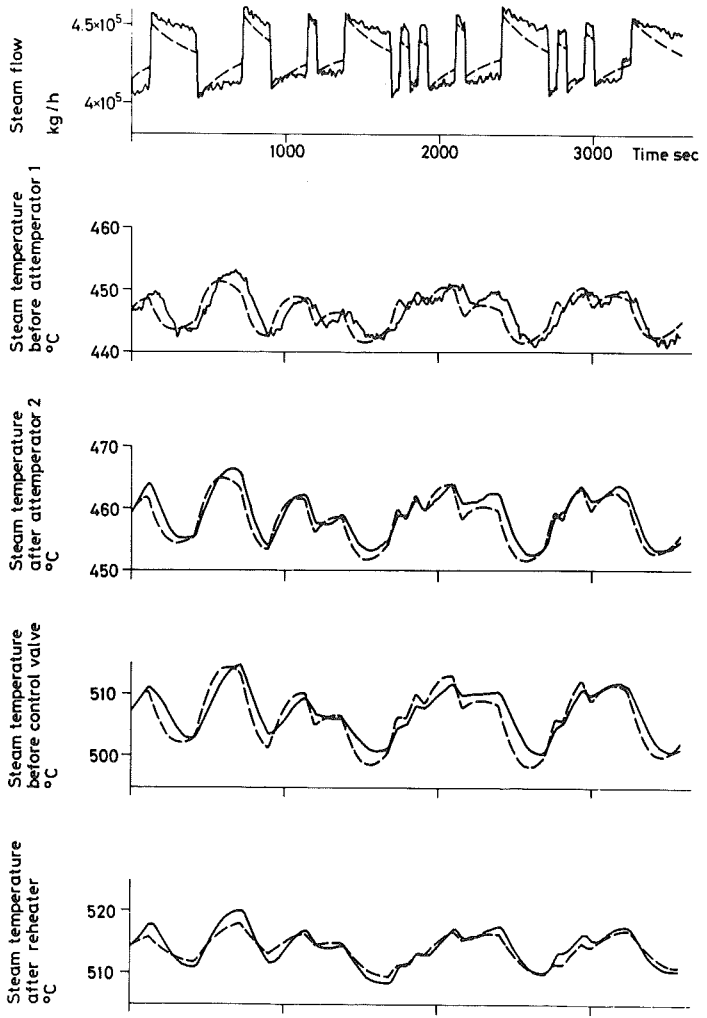


Fig 2.5 Contd.

contained in the water of the drum system which are affected by the initial fast drum pressure response to the control valve change. The phenomenon is predicted by the model but the amplitudes of peaks are too small. Since the steam content of water is only modelled for the water contained in risers this is an expected result. The model could be improved by treating a fraction of drum water as contained in the risers.

The active power diagram and especially the steam flow diagram show model responses which after the initial rapid change decline too fast. The model for steam flow used throughout was to take the squared steam mass flow proportional to the pressure difference. Since drum pressure responses agree well, we must conclude that the model does not predict changes of pressure after the control valve in a proper way.

Three steam temperatures measured before H. P. turbine and one measured after reheater are also shown in Fig 2.5. Considering the difference in steam flow between the actual plant and the model the result is satisfactory.

3. Comparison to results of identification

To resolve the steady state control problem of the boiler-turbine unit, it is essential to know the dynamics relating the outputs drum pressure, active power, drum level and steam temperature before control valve to the main inputs fuel flow and control valve position. Also the dynamics relating drum level to feedwater flow and steam temperatures to atomizer flows are important. Some of this dynamics as given by the boiler model will be compared to the results of identification. Both open loop models represented by transfer functions and closed loop models in the sense of one-step ahead prediction errors are discussed.

Some model transfer functions will be of ninth order. Most transfer functions will be of lower order, because some modes are either non-observable from a particular output or non-controllable from a particular input. The order of the M. L. models are frequently of significantly lower order. This can be explained by making a modal analysis and consider the orders of magnitude of mode gains. It will be shown in examples that some modes give a very small contribution to the transfer function.

The modal analysis is also used to obtain a reduced order construction

data (C.D.) model for comparison to the continuous equivalent of the M.L. model.

The one-step ahead prediction errors of the C.D. model are computed from

$$\epsilon(t) = A^* (q^{-1}) y_m(t) - B^* (q^{-1}) u_m(t)$$

where $y_m(t)$ and $u_m(t)$ are the measured output and input sequences. The polynomials A^* and B^* are obtained from the discrete time C.D. model. The order is again reduced using modal analysis. This is favourable from a computational point of view since it is well known that the simulation of high order dynamical systems represented by the pulse transfer functions can be extremely sensitive to disturbances in model parameters.

3.1 Transfer Functions

In Table 3.1 the model order and steady state gain of maximum likelihood models (M.L.) and the approximate models obtained from the construction data model (C.D.) are given. The model order, given for the construction data models, indicates the modes with large steady state gain.

Drum pressure

A modal expansion of the transfer function relating drum pressure to fuel flow gives the steady state gains shown in Table 3.2. The gain given for mode no 1 is the integrator gain.

| Mode No. | Eigenvalue | Gain |
|----------|--|-------|
| 1 | 0.000 | 0 |
| 2 | $-2.29 \cdot 10^{-3}$ | 0 |
| 3 | $-3.44 \cdot 10^{-2}$ | 0.49 |
| 4, 5 | $-4.82 \cdot 10^{-3} \pm 2.91 \cdot 10^{-3} i$ | 14.6 |
| 6, 7 | $-1.56 \cdot 10^{-2} \pm 1.45 \cdot 10^{-3} i$ | 0.73 |
| 8, 9 | $-8.21 \cdot 10^{-2} \pm 8.95 \cdot 10^{-3} i$ | -0.89 |

Table 3.2 - Steady state gains of the modes of the transfer function relating drum pressure to fuel flow.

| Input / Output | Fuel flow
[kg/s] | | Control
valve pos.
[%] | | Feedwater
flow
[kg/s] | | Attenuator
flow 2
[kg/s] | |
|--|---------------------|-------|------------------------------|-------|-----------------------------|-------|--------------------------------|-------|
| | M. L. | C. D. | M. L. | C. D. | M. L. | C. D. | M. L. | C. D. |
| Drum pressure
[bar] | n | 2 | 3 | 2 | | | | |
| | K | 15 | -1.7 | -2.1 | | | | |
| Active power
[MW] | n | 3 | 2 | 3 | | | | |
| | K | 39 | -1.5 | -0.2 | | | | |
| Steam tempera-
ture before
control valve
[°C] | n | 4 | 2 | 4 | | | 2 | 4 |
| | K | 12 | -3.3 | -2.5 | | | -14 | -8.0 |

Table 3.1 - Comparison of model order (n) and steady state gain (K) of maximum likelihood models (M. L.) and reduced order models from construction data (C. D.).

The dynamics of this loop is dominated by the modes 4 and 5. The gains of other modes are less than 6 % of the gain of modes 4 and 5. Thus it is not surprising that the M. L. method estimates the order as being 3. Physically the modes 4 and 5 can be interpreted as part of the dynamics generated by the drum and superheater 1. The transfer function of the reduced order model is

$$G_{CD}(s) = 4.6 \cdot 10^{-4} \frac{1 + 112s}{s^2 + 2\zeta\omega_0 s + \omega_0^2} \quad (3.1)$$

where

$$\omega_0 = 5.6 \cdot 10^{-3}$$

$$\zeta = 0.856$$

which should be compared to the transformation of the maximum likelihood model to continuous time.

$$G_{ML}(s) = 0.3 + 0.7 \frac{1}{1 + 16s} + 3.8 \cdot 10^{-4} \frac{1 + 109s}{s^2 + 2\zeta\omega_0 s + \omega_0^2} \quad (3.2)$$

where

$$\omega_0 = 5.2 \cdot 10^{-3}$$

$$\zeta = 0.71$$

The second order term of both models agree well, especially the natural resonant frequency. The first order term of (3.2) has a low gain and such modes were neglected in (3.1). The first order term of (3.2) did not change between the high and low load maximum likelihood models and was therefore interpreted as the dynamics of the risers. In Chapter 4 we assigned the modes 1, 3, 8 and 9 to the drum system. Only 3, 8 and 9 can possibly be associated with the dynamics of the risers. Neglecting the imaginary parts of eigenvalues 3, 8 and 9 the corresponding time constants are 29, 12 and 12 seconds respectively. This suggests that the order of the drum model can be reduced. However, as indicated in the previous section the dynamics of the steam-water mixture is essential for the non-minimum phase responses of drum level and cannot be neglected. Then it remains the state variables describing mean temperature

of riser steel masses and drum liquid temperature. It seems possible to neglect both these dynamics. The first one can be neglected without changing the structure of the drum model. Also in the previous chapter the eigenvalues of a state space model of the drum system adjusted to measurements was compared to those of an initial model obtained from construction data. It was found that the eigenvalue associated with the mean temperature of riser tubes was decreased with roughly a factor 10 and the corresponding time constant then equals 3 seconds. If drum liquid is assumed to be at saturation state this is a more drastic change and could affect the dynamics of the well behaving drum model analysed here.

The transfer function relating drum pressure to control valve position is also dominated by the modes 4 and 5 defined in Table 3.2. The gain of other modes maximally equals 5 % of the gain of these modes. The parameters of the maximum likelihood model were given in Table 3.5 in Chapter 5. This table shows that the gain of the fastest of the three modes is very small compared to the total gain and the order of dominating dynamics of both models coincide.

Table 3.1 shows that steady state gains of drum pressure loops, estimated from measurements and computed from physical equations, agree very well.

Active power

The third order transfer functions which relate active power to fuel flow and control valve position are both dominated by the modes 4, 5 and 2 where mode No. 2 is associated with the reheater of the boiler. According to measurements first and second order dynamics are sufficient and the parameters are given in Tables 3.8 and 3.10 in Chapter 5. The single time constant in Table 3.8 in Chapter 5 is of the expected order of magnitude.

The continuous equivalent of the maximum likelihood model with control valve position as input is

$$G_{ML}(s) = 1.1 + 0.7 \frac{1}{1 + 17s} - 3.4 \frac{1}{1 + 333s} \quad (3.3)$$

and the modal expansion of the ninth order construction data model gives

$$G_{CD}(s) = 1.9 + 1.0 \frac{1}{1 + 436s} - 2.9 \frac{1}{1 + 2\zeta Ts + T^2 s^2} \quad (3.4)$$

where

$$T = 178$$

$$\zeta = 0.856$$

and the other terms are neglected. The fast first order dynamics in the maximum likelihood model is due to the large steam volumes in reheater, feed and exhaust pipes for turbines. The dynamics of these volumes were neglected when deriving the construction data model. However, the sum of the gains of the first two terms in (3.3) agree well with the gain of the direct connection between input and output in (3.4).

The steady state gains of the maximum likelihood models differ considerably from those of the model from construction data. Theoretically the gains of the construction data models are expected and quite reliable. The gain estimates produced by the M. L. method is uncertain for two reasons. The dynamics include a large time constant, which means, that even rather small uncertainties in the coefficients of the A^* -polynomial of the M. L. model might give poor gain estimates. Further, the experiments were not specially designed to give accurate estimates of the steady state gain.

Drum level

Great difficulties were recognized when modelling the drum level loops with data from Exps. A and E. The origin of these difficulties is that the feedwater flow was changed only a couple of times and that the feedwater temperature varied according to the changing feedwater, fuel and steam flows.

The responses of the deterministic maximum likelihood models agree well with the responses of the deterministic state space model discussed in the previous chapter. Thus also the models adjusted to measurements give drum level responses with the same characteristics as those of the ninth order model from construction data. This clearly suggests, that the measured drum level responses cannot be explained by the phenomena included in the models. Using physical arguments presented in the previous section we conclude that drum level responses of the construction data model will be improved by including a dynamic model of the economiser.

The non-minimum phase characteristics of the drum system responses are improved after adjustment to measurements and agree well with measurements with respect to amplitude and duration. The physical cause for this behaviour is thus present in the model equations and will produce realistic constraints when designing the regulator.

Steam temperature before control valve

Among the steam temperatures available for comparison, the steam temperature before the control valve was chosen, since it is an essential controlled variable.

The figures given in Table 3.1 show that the superheaters, which are distributed parameter systems, are modelled with only second order models when using the maximum likelihood method. This strongly supports the earlier stated opinion that a higher order approximation of superheaters does not considerably improve model properties. The fourth order models are the dominating dynamics of the construction data model and are in all cases dominated by the modes 4, 5, 6 and 7 as defined in Table 3.2. The eigenvalues 6 and 7 are associated with the second and third superheaters.

The theoretically calculated gains and the gains estimated from measurements agree reasonably well except for the loop, steam temperature - attemperator flow 2. However, this loop is quite simple and the calculated gain is probably a good approximation.

3.2 One-Step Ahead Prediction Errors

For control purposes a possible measure of the goodness of the used models is the one-step ahead prediction error. In Table 3.3 the standard deviation of this error for some maximum likelihood models as well as for the construction data models is given. The prediction errors for the construction data model are computed using a reduced order model.

The standard deviations of the prediction errors of the two types of models differ generally with a factor 2-5. There are three exceptions which are the drum level errors and one steam temperature error.

The magnitude of drum level errors of the construction data model confirms the conclusion that feedwater temperature should be modelled. The large difference in steam temperature error is partly due to the fact that

| Input
Output | Fuel flow
[kg/s] | | Control
valve pos.
[%] | | Feedwater
flow
[kg/s] | | Attenuator
flow 2
[kg/s] | |
|--|---------------------|-------|------------------------------|-------|-----------------------------|-------|--------------------------------|-------|
| | M. L. | C. D. | M. L. | C. D. | M. L. | C. D. | M. L. | C. D. |
| Drum pressure
[bar] | 0.033 | 0.073 | 0.055 | 0.175 | | | | |
| Active power
[MW] | 0.373 | 1.135 | 0.58 | 3.33 | | | | |
| Drum level
[mm] | 1.2 | 11.6 | 1.31 | 13.8 | 2.91 | 6.67 | | |
| Steam temperature
before control
valve
[°C] | 0.075 | 1.39 | 0.055 | 0.27 | | | 0.083 | 0.356 |

Table 3.3 - Comparison of the standard deviation of one-step ahead prediction errors of maximum likelihood models (M. L.) and models from construction data (C. D.). The sampling rate is 10 seconds.

only the last 240 points were used in the maximum likelihood identification while the prediction error of the construction data model was based on the entire time series.

Compared to a model, where parameters have been determined in order to minimize the sum of prediction errors, with respect to the recorded data sequences, the errors of the construction data model are quite large. However, in most cases these errors are acceptable small, and in some cases even very small.

4. Conclusions and Recommendations

In this section we will use the discussion of good fit and discrepancies of the construction data model responses compared to measurements and results of identification to summarize the validity of different approximations. Also we will indicate possible extensions to improve on model properties.

The construction data model has only been applied and compared to one specific boiler in this work. This obviously limits the generality of the conclusions drawn. However, even if e.g. attemperators, number of superheaters, type of heat transfer, sensors, actuators and the geometric lay-out of the boiler may differ considerably from one drum type boiler to another the gross dynamics included in the derived model is governed by the same equations in all cases.

The discussion in previous sections shows that drum pressure loops behave very well in all respects. Active power loops perform reasonably well. Still active power heavily depends on how well steam flow responses are predicted. In this respect the construction data model does not show very good performance. Steam temperature loops are in most cases good and the behaviour can be accepted. The modelling of drum level dynamics is bad but the discussion above has clearly explained the reasons for this. However, the non-minimum phase responses to control valve position perturbations is a property of the model.

The following important assumptions have been verified and can be recommended as an initial set of approximations

- drum model structure is sufficient,
- a 1:st order approximation of superheaters and reheater is sufficient,

- steam dynamics can be neglected,
- static models are sufficient for turbines and attemperators.

The evaluation of the construction data model has also indicated that the model can be significantly improved by

- including a model of the economiser,
- a static calculation of gas temperature distribution along the combustion gas path,
- careful treatment of the pressure distribution along steam path and across turbines.

The first extension means the introduction of a new state variable namely a mean temperature for the economiser steel masses. The increased model complexity is well motivated. A more realistic treatment of combustion gas temperatures will probably improve steam temperature responses to fuel flow perturbations. The last recommendation above merely points out that model prediction of steam flow is very essential since it both affects steam temperatures and active power.

A possible further simplification of the presented model is

- neglect heat capacity of riser masses.

This has been indicated by both the maximum likelihood identification in Chapter 5 and the estimation of parameters in state space models in Chapter 6.

REFERENCES

- [1] Algorithm 46, The Computer Journal, Vol. 13, p. 111, 1970
- [2] Anderson, J.H., Dynamic Control of a Power Boiler, Report No. 27, April, 1968, University of Manchester Institute of Science & Technology, Control Systems Center.
- [3] Anderson, J.H., Kwan, H.W., Qualtrough, G.H., Dynamic Paper 66-WA/HT-57.
- [4] Anderson, J.H., Kwan, H.W., Qualtrough, G.H., Dynamic models for power station boilers. Paper presented at the Third U.K.A.C. Control Convention, April 1968.
- [5] Barker, H.A., Raeside, D., Linear Modelling of Multivariable Systems with Pseudo Random Binary Input Signals, Automatica, Vol. 4, 1968.
- [6] Becker, K.N., Jahnberg, S., Haga, I., Hansson, P.T., Mathisen, R.P., Hydrodynamic Instability and Dynamic Burnout in Natural Circulation Two-Phase Flow. An Experimental and Theoretical Study. AB Atomenergi Report no AE-156, Stockholm 1964.
- [7] Bellman, R., Åström, K.J., On Structural Identifiability, Mathematical Biosciences 7 (1970), 329-339.
- [8] Briggs, P.A.N., Godfrey, K.R., Hammond, P.H., Estimation of Process Dynamic Characteristics by Correlation Methods Using Pseudo Random Signal, IFAC, Prague 1967.
- [9] Caines, P.E., The Parameter Estimation of State Variable Models of Multivariable Linear Systems, Report No 146, April 1971, Control Systems Centre, University of Manchester, Institute of Science and Technology.
- [10] Chien, K.L., Ergin, E.I., Ling, C., Lee A., Dynamic analysis of a boiler. A.S.M.E. paper No. 58-IRD-4 presented at the Fourth Instrument and Regulating Division Conference, April 1958.
- [11] Dallas, H.G., Sauter, D.M., Field Testing for Verification of a Dynamic Model. A.S.M.E. Paper 61-SA-68, A.S.M.E. Summer Annual Meeting, 1961.

- [12] Daniels, J.H., Enns, M., Hottenstine, R.D., Dynamic Representation of a Large Boiler-Turbine Unit. Paper presented at the A.S.M.E. Summer Meeting, June 1961.
- [13] Deutsch, R., Estimation Theory. New York, Prentice-Hall, Inc., 1965.
- [14] Eaton, J., Identification for Control Purposes. Paper, IEEE Winter Meeting, N.Y., 1967.
- [15] Eklund, K., Multivariable Control of a Boiler. An Application of Linear Quadratic Control Theory. Report 6901, Jan., 1969, Lund Institute of Technology, Division of Automatic Control.
- [16] Eklund, K., Numerical model building. Int. J. Control, 1970, vol. 11, No. 6, 973-985.
- [17] Eklund, K., Linear Mathematical Models of the Drum-Downcomer-Riser Loop of a Drum Boiler. Report 6809, Nov., 1968, Lund Institute of Technology, Division of Automatic Control.
- [18] Engvald, J., Unpublished material, Lund Institute of Technology, Division of Telecommunication Theory.
- [19] Enns, M., Comparison of Dynamic Models of a Superheater, A.S.M.E. Journal of Heat Transfer, Nov 1962, p 375-385.
- [20] Eykhoff, P., van der Grinten, P.M.E.M., Kwakernaak, H., Veltman, B.P.Th., Systems Modelling and Identification, Survey Paper, IFAC, London 1966.
- [21] Fletcher, R., Powell, M.J.D., A Rapidly Convergent Descent Method for Minimization, The Computer Journal, Vol. 6, p. 163, 1963.
- [22] Gustafson, R.D. et al: Digital Control of a Steam Propulsion System of a Naval Vessel, 2-6 Quarterly Reports. Purdue University, Lafayette, Indiana, Purdue Energy Research and Education Center, PEREC Report No. 3, 27, 28, 39, 41, Oct. 1966 - Dec. 1967.
- [23] Gustavson, I., Comments on Identification Experiments - Especially the Choice of Input Signal, (in Swedish), Internal Report, March 1970, Lund Institute of Technology, Division of Automatic Control.
- [24] Gustavsson, I., Parametric Identification of Time Series, Report no. 6803, April 1968, Lund Institute of Technology, Division of Automatic Control.

- [25] Gustavsson, I., Parametric Identification of Multiple Input-Single Output Linear Dynamic Systems, Report no. 6907, July 1969, Lund Institute of Technology, Division of Automatic Control.
- [26] Gustavsson, I., Comparison of Different Methods for Identification of Industrial Processes. Accepted for publication in IFAC Journal-Automata.
- [27] Gustavsson, I., Choice of Sampling Interval for Parametric Identification. Report 7103, April, 1971, Lund Institute of Technology, Division of Automatic Control.
- [28] Isermann, R., Das regeldynamische Verhalten der Überhitzung bei Berücksichtigung der Koppelungen mit anderen Teilen eines Dampferzeugers. Abh. Dr.-Ing., Techn. Hochs. Stuttgart, 1965.
- [29] Isermann, R., Messung und Berechnung des regeldynamischen Verhaltens eines Überhitzers. VDI Zeitschrift. Fortschr.-Ber. VDI-Z., Reihe 6, Nr. 9, Okt. 1965.
- [30] Koenig, H. E., Tokad, Y., and Kesavan, H.K., Analysis of Discrete Physical Systems. New York, Mc Graw Hill 1967.
- [31] Kutateladze, S.S., Heat Transfer in Condensation and Boiling. Translation Series. AEC-tr-3770, United States Atomic Energy Commission, 1959.
- [32] Kwan, H.W., Anderson, J.H., A mathematical model of a 200 MW boiler. Int. J. Control, 1970, vol. 12, no. 6, 977-998.
- [33] Mc Donald, J.P., Kwatny, H.G., Modeling and simulation of a of a reheat boiler-turbine-generator system. Philadelphia Company, Report No. E-192. Sept. 1969.
- [34] Mc Donald, J.P., Kwatny, H.G., Spare, J.H., Nonlinear model of a reheat Boiler-turbine-generator system. Philadelphia Electric Company. Report No. E-196. Sept. 1970.
- [35] Nicholson, H., Dynamic Optimisation of a Boiler-Turboalternator Model. Proc. IEE, Vol. 113, No. 2, February 1966.
- [36] Operating Conditions of Thermal Power Plants. (In Swedish) Statens Vattenfallsverk. May, 1969.
- [37] Power Generation and Consumption during the 1970's. (In Swedish) Centrala Driftledning, Dec. 1967.
- [38] Profos, P., Die Regelung von Dampfanlagen. Springer-Verlag, Berlin, 1962.

- [39] Saaty, T. L., Brown, J., *Nonlinear Mathematics*, Mc Graw-Hill, New York, 1964.
- [40] Stuart III, G. W., A modification of Davidon Minimization Method to Accept Difference Approximations of Derivatives, *JACM*, Vol. 14, p. 72, 1967.
- [41] Symposium on Two-Phase Flow, Exeter 21-23 June 1965 Proceeding, Dept. of Chemical Engineering, University of Exeter.
- [42] Thal-Larsen, H., Dynamics of Heat Exchangers and their Models, *ASME Journal of Basic Engineering*, June 1960, p. 489-504.
- [43] Thompson, F. T., A Dynamic Model of Drum-Type Boiler System. *IEEE Trans. Power Appl. and Sys.*, Vol. PAS-86, No. 5, pp. 625-635, 1967.
- [44] Tyllered, G. O., Thermodynamics, (in Swedish) sept, 1970, Lund Institute of Technology, Division of Thermodynamics and Fluid Flow.
- [45] Walters, R. C., Williams, T. J., A Linearized Mathematical Model for the Dynamics and Control of the Propulsion System (Steam Boiler-Turbine) of a Naval Vessel. Paper No 2570 presented at the IFAC Symposium in Sydney, Aug. 1968, E.E.T., March 1969.
- [46] Williams, B. J., Clarke, D. W., Plant Modelling from P.R.B.S. Experiments, *Control*, Vol. 12, no 124-125, 1968.
- [47] Wpo, K. T., Maximum Likelihood Identification of Noisy Systems. Preprints of the 2nd Prague IFAC Symposium, Czechoslovakia, 15-20 June, 1970.
- [48] Åström, K. J., *Introduction to Stochastic Control Theory*, New York, Academic Press, 1970.
- [49] Åström, K. J., *Reglerteori*, Almqvist & Wiksell/Gebbers Förlag AB, Stockholm 1968.
- [50] Åström, K. J., Lectures given during the fall 1970. Lund Institute of Technology, Division of Automatic Control.
- [51] Åström, K. J., Bohlin, T., Numerical Identification of Linear Dynamic Systems from Normal Operating Records, *Proceedings of the IFAC Conference on Self-Adaptive Control Systems*, Teddington (1965).

- [52] Åström, K. J., Bohlin, T., Wensmark, S., Automatic Construction of Linear Stochastic Dynamic Models for Stationary Processes with Random Disturbances Using Operating Records, IBM Nordic Laboratory, Sweden, Report TP 18.150 (1965).
- [53] Åström, K. J., Eklund, K. E., A Simplified Nonlinear Model of a Drum Boiler-Turbine Unit, Report 7104, April 1971, Lund Institute of Technology, Division of Automatic Control. (Accepted for publication in Int. J. Control.)
- [54] Åström, K. J., Eykhoff, P., Identification and Process Parameter Estimation. Preprints of the 2nd Prague IFAC Symposium, Czechoslovakia, 15-20 June, 1970.
- [55] Öhbom, C., Larsson, U. C., A Mathematical Model of a Power Plant, (In Swedish), Report RE-55, July, 1969, Lund Institute of Technology, Division of Automatic Control.

APPENDIX A.

1* SUBROUTINE DR5M(DC,R,DM,TD,E,C,IPRINT,AA,SV,IA,Ib,IC,KUF)
 2* C
 3* C COMPUTES A 5TH ORDER LINEAR MODEL OF THE DRUM OF A DRUM
 4* C BOILER
 5* C REFERENCE:K EKLUND,LINEAR MATHEMATICAL MODELS OF THE
 6* C DRUM=DOWNCOMER=RISEK LOOP OF A DRUM BOILER.REPORT 6809
 7* C NOV 68,LTH:DIV OF AUT. CONTROL
 8* C AUTHOR:K EKLUND 25/4-69
 9* C
 10* C DC=DOWNCOMER DATA VECTOR.ELEMENTS
 11* C FRICTION COEFFICIENT (FD)
 12* C TOTAL LENGTH OF TUBES (ALD)
 13* C LENGTH OF ONE TUBE (ALD1)
 14* C TOTAL FLOW AREA (AD)
 15* C TOTAL TUBE DIAMETER (DD)
 16* C R=RISEK DATA VECTOR.ELEMENTS
 17* C FRICTION COEFFICIENT (FR)
 18* C TOTAL LENGTH OF TUBES (ALR)
 19* C LENGTH OF ONE TUBE (ALR1)
 20* C TOTAL FLOW AREA (AR)
 21* C TOTAL TUBE DIAMETER (DR)
 22* C MASS OF RISEK TUBES (RMASS)
 23* C HEAT INPUT RATE TO RISEK TUBES (QR)
 24* C DM=DRUM DATA VECTOR.ELEMENTS
 25* C MASS OF DRUM LIQUID (WMASS)
 26* C VOLUME OF VAPOR IN DRUM (VS)
 27* C LIQUID SURFACE AREA IN DRUM (ADR)
 28* C TD=TEMPERATURE-DENSITY DATA VECTOR.ELEMENTS
 29* C DENSITY OF SATURATED LIQUID (DEW)
 30* C DENSITY OF SATURATED VAPOR (DESS)
 31* C DRUM LIQUID TEMPERATURE (TW)
 32* C RISEK TUBE TEMPERATURE (TR)
 33* C SATURATION TEMPERATURE (TS)
 34* C E=ENTHALPY DATA VECTOR.ELEMENTS
 35* C ENTHALPY OF DRUM LIQUID (HW)
 36* C ENTHALPY OF FEED WATER (HFW)
 37* C ENTHALPY OF SATURATED LIQUID (HWS)
 38* C ENTHALPY OF SATURATED VAPOR (HSS)
 39* C ENTHALPY OF EVAPORATION (HE)
 40* C C=CONSTANT DATA VECTOR.ELEMENTS
 41* C TEMPERATURE-PRESSURE PROPORTIONAL CONSTANT AT SATU-
 42* C RATION STATE (PK1)
 43* C DENSITY-PRESSURE PROPORTIONAL CONSTANT AT SATURATION
 44* C STATE (PK2)
 45* C WATER ENTHALPY-PRESSURE PROPORTIONAL CONSTANT AT SATU-
 46* C RATION STATE (PK3)
 47* C HEAT CAPACITANCE OF DRUM LIQUID (PK6)
 48* C HEAT CAPACITANCE OF RISEK TUBES (PK8)
 49* C VAPOR ENTHALPY-PRESSURE PROPORTIONAL CONSTANT AT SATU-
 50* C RATION STATE (PK9)
 51* C STEAM DISTRIBUTION CONSTANT (BETA)
 52* C LOSS FACTOR (XSI)

```

53* C COEFFICIENT C1 OF THE LINEAR APPROXIMATION OF EQ.
54* C ( 3.10 ) (C1)
55* C COEFFICIENT C2 OF THE LINEAR APPROXIMATION OF EQ.
56* C ( 3.10 ) (C2)
57* C IPRINT-IF NO PRINTOUTS FROM THE SUBROUTINE IS DESIRED
58* C IPRINT IS SET EQUAL TO ZERO.ELSE IPRINT IS SET NOT EQUAL
59* C TO ZERO
60* C AA=MATRIX RETURNED CONTAINING THE COEFFICIENTS OF THE MODEL
61* C EQUATION: AA*Z=0 WHERE Z(TRANPOSE)=X(DOT X U V) WHERE
62* C X EQUALS
63* C DRUM PRESSURE
64* C DRUM LEVEL
65* C DRUM LIQUID TEMPERATURE
66* C RISER TUBE TEMPERATURE
67* C STEAM QUALITY
68* C U EQUALS
69* C HEAT FLOW TO RISER TUBES
70* C FEED WATER FLOW
71* C STEAM OUTLET FLOW
72* C V EQUALS
73* C MASS FLOW OF RISER OUTLET
74* C DOWNCOMER MASS FLOW
75* C EVAPORATION MASS FLOW
76* C HEAT FLOW TO RISER STEAM-WATER MIXTURE
77* C MINIMUM DIMENSION OF AA IS 9*17
78* C SV=STATIONARY VALUE VECTOR RETURNED CONTAINING
79* C MEAN VALUE OF STEAM QUALITY (XM)
80* C TOTAL MASS FLOW (W)
81* C OUTLET DENSITY OF STEAM-WATER MIXTURE (DE)
82* C MEAN DENSITY OF STEAM-WATER MIXTURE (DEM)
83* C CONSTANT OF EVAPORATION (PK4)
84* C EVAPORATION MASS FLOW (WE)
85* C OUTLET STEAM FLOW
86* C HEAT TRANSFER COEFFICIENT RISER TUBES-STEAM WATER
87* C MIXTURE (PK5)
88* C OUTLET ENTHALPY OF MIXTURE (HM)
89* C MEAN ENTHALPY OF MIXTURE (HMM)
90* C MINIMUM DIMENSION IO
91* C IA-DIMENSION PARAMETER
92* C IB-DIMENSION PARAMETER
93* C IC-DIMENSION PARAMETER
94* C KUF=ERROR PARAMETER
95* C KUF=4 UNABLE TO DETERMINE ROOT OF THE STEAM QUALITY
96* C POLYNOMIAL WITH 500 ITERATIONS ON 5 STARTING VALUES
97* C KUF=5 HIGH ORDER COEFFICIENT OF STEAM QUALITY POLY
98* C NOMIAL IS ZERO
99* C KUF=0 THERE IS NO POSITIVE REAL ROOT OF THE STEAM
100* C QUALITY POLYNOMIAL
101* C
102* C SUBROUTINE REQUIRED
103* C PULRT
104* C
105* C DIMENSION AA(IA,IB),SV(IC),DC(IC),R(IC),DM(IC),TD(IC),E(IC),C(IC)
106* C DIMENSION ALFA(5),ROOTR(5),ROOTI(5),XROOT(5),XROOTR(5)
107* C FD=DC(1)
108* C ALD=DC(2)
109* C ALD1=DC(3)
110* C AD=DC(4)

```



```

111*      UU=DU(4)
112*      FR=FR(1)
113*      ALR=FR(2)
114*      ALR1=FR(3)
115*      AR=FR(4)
116*      UR=FR(5)
117*      RMMASS=FR(6)
118*      WR=FR(7)
119*      RMMASS=UM(1)
120*      VS=L.M(2)
121*      AUK=UM(3)
122*      UE=TL(1)
123*      DESS=TL(2)
124*      TA=TL(3)
125*      TR=TL(4)
126*      TS=TL(5)
127*      HE=E(1)
128*      HF=E(2)
129*      HWS=L(3)
130*      HSS=L(4)
131*      HE=E(5)
132*      PK1=C(1)
133*      PK2=C(2)
134*      PK3=C(3)
135*      PK4=C(4)
136*      PK5=C(5)
137*      PK9=C(6)
138*      BETA=C(7)
139*      XSI=C(8)
140*      C1=C(9)
141*      C2=C(10)
142*      IF(IPRINT) 300,305,300
143*      C
144*      C      PRINT INPUT DATA
145*      C
146*      300 PRINT 1051
147*      1051 FORMAT(1H1)
148*      PRINT 1009
149*      1009 FORMAT(1H1,2(/),5H DRUM,2(/))
150*      PRINT 1011
151*      1011 FORMAT(/,15H DOWNLOMER DATA,/)
152*      PRINT 1012,FD
153*      1012 FORMAT(21H FRICTION COEFFICIENT,14X,F11.5)
154*      PRINT 1013,ALD
155*      1013 FORMAT(22H TOTAL LENGTH OF TUBES,13X,F11.5)
156*      PRINT 1014,ALD1
157*      1014 FORMAT(19H LENGTH OF ONE TUBE,16X,F11.5)
158*      PRINT 1015,AU
159*      1015 FORMAT(16H TOTAL FLOW AREA,19X,F11.5)
160*      PRINT 1016,LJ
161*      1016 FORMAT(20H TOTAL TUBE DIAMETER,15X,F11.5)
162*      PRINT 1017
163*      1017 FORMAT(2(/),11H RISER DATA,/)
164*      PRINT 1012,FR
165*      PRINT 1013,ALR
166*      PRINT 1014,ALR1
167*      PRINT 1015,AR
168*      PRINT 1016,DR

```

109* PRINT 1010,LE#
170* 1018 FORMAT(2(/),23H DENSITY OF SATURATED LIQUID,7X,F11.5)
171* PRINT 1019,DESS
172* 1019 FORMAT(27H DENSITY OF SATURATED VAPOR,8X,F11.5)
173* PRINT 1020,TW
174* 1020 FORMAT(24H DRUM LIQUID TEMPERATURE,11X,F11.5)
175* PRINT 1021,TR
176* 1021 FORMAT(23H RISER TUBE TEMPERATURE,12X,F11.5)
177* PRINT 1050,RMASS
178* 1050 FORMAT(20H MASS OF RISER TUBES,13X,F13.5)
179* PRINT 1022,TS
180* 1022 FORMAT(23H SATURATION TEMPERATURE,12X,F11.5)
181* PRINT 1023,HW
182* 1023 FORMAT(24H ENTHALPY OF DRUM LIQUID,11X,F11.5)
183* PRINT 1024,HF#
184* 1024 FORMAT(22H ENTHALPY OF FLEEWATER,13X,F11.5)
185* PRINT 1025,HWS
186* 1025 FORMAT(29H ENTHALPY OF SATURATED LIQUID,6X,F11.5)
187* PRINT 1026,HVS
188* 1026 FORMAT(28H ENTHALPY OF SATURATED VAPOR,7X,F11.5)
189* PRINT 1027,HE
190* 1027 FORMAT(24H ENTHALPY OF EVAPORATION,11X,F11.5)
191* PRINT 1028
192* 1028 FORMAT(2(/),10H DRUM DATA,/))
193* PRINT 1029,WMASS
194* 1029 FORMAT(21H MASS OF DRUM LIQUID,15X,F11.5)
195* PRINT 1030,VS
196* 1030 FORMAT(24H VOLUME OF VAPOR IN DRUM,11X,F11.5)
197* PRINT 1031,ADK
198* 1031 FORMAT(20H LIQUID SURFACE AREA IN DRUM,7X,F11.5)
199* PRINT 1032,QR
200* 1032 FORMAT(/,31H HEAT INPUT RATE TO RISER TUBES,3X,F12.5)
201* PRINT 1033
202* 1033 FORMAT(2(/),10H CONSTANTS,/))
203* PRINT 1034,PK1
204* 1034 FORMAT(9H PK1 (KT),26X,F11.5)
205* PRINT 1035,PK2
206* 1035 FORMAT(9H PK2 (KD),26X,F11.5)
207* PRINT 1036,PK3
208* 1036 FORMAT(9H PK3 (KH),26X,F11.5)
209* PRINT 1037,PK6
210* 1037 FORMAT(10H PK6 (CP#),25X,F11.5)
211* PRINT 1039,PK8
212* 1039 FORMAT(9H PK8 (CR),26X,F11.5)
213* PRINT 1040,PK9
214* 1040 FORMAT(9H PK9 (KS),26X,F11.5)
215* PRINT 1070,BETA
216* 1070 FORMAT(5H BETA,30X,F11.5)
217* PRINT 1071,XSI
218* 1071 FORMAT(4H XSI,31X,F11.5)
219* PRINT 1072,C1
220* 1072 FORMAT(3H C1,32X,F11.5)
221* PRINT 1073,C2
222* 1073 FORMAT(3H C2,32X,F11.5)
223* 305 GA=9.81
224* C
225* C FACTORS OF COEFFICIENTS OF POLYNOMIAL IN STEAMQUALITY IS
226* C CALCULATED

```

227*
228*      AV1=GA*AD*AL
229*      AV2=GA*AN*AL
230*      AV3=GM*GN
231*      A1=(FD*ALD/ED+3.)/(2.*AV1*DEW)
232*      A2=ALL1*UEY
233*      B1=(FK*ALN/LN+1.)/(2.*AV2)
234*      U2=U.9/(AV2*UEY)
235*      U3=U.1/AV2
236*      U4=X51/(2.*AV1*E.*F/EM)
237*      U5=ALM1
238*      J1=HELM*(1./DES5=1./DEW)
239*      U2=1./DF
240*      L1=HW=HWS
241*      L2=DELTA*HE
242*
243*      C
244*      C
245*      C
246*      ALFA(4)=C1*(AV3*B1*U2*U2+U5*E2*E2)
247*      ALFA(5)=AV3*B1*U1*(C2*U1+2.*C1*U2)+B5*E2*(C2*E2=2.*C1*E1)-A2*E2*E2
248*      ALFA(2)=AV3*(B1*U2*(C1*U2+2.*C2*U1)+B3*U1-B4*C1)+U5*E1*(C1*E1-2.*C
249*      12*E2)*2.*A2*E1*E2
250*      ALFA(1)=AV3*(B1*C2*U2+C2+U2+B3*U2-B4*C2+A1)+E1*E1*(B5*C2-A2)
251*
252*      C
253*      C
254*      C
255*      KUF=IER+1
256*      GO TO(39,39,41,41),KUF
257*      41 GO TO 999
258*      39 IF(IPRINT) 42,47,42
259*      42 PRINT 40
260*      40 FORMAT(/'ROOTS OF STEAM QUALITY POLYNOMIAL'/)
261*      PRINT 220
262*      220 FORMAT(5X,'REAL PART',11X,'IMAGINARY PART'/)
263*      DO 221 I=1,3
264*      221 PRINT 222,ROOTR(I),ROOTI(I)
265*      222 FORMAT(2L20.8)
266*
267*      C
268*      C
269*      47 J=
270*      DO 60 I=1,3
271*      IF(ABS(ROOTI(I))-1.E-06) 65,60,60
272*      65 J=J+1
273*      XROOTR(J)=ROOTR(I)
274*      60 CONTINUE
275*      K=0
276*      DO 70 I=1,J
277*      IF(XROOTR(I)) 70,70,75
278*      75 K=K+1
279*      XROOT(K)=XROOTR(I)
280*      70 CONTINUE
281*      IF(K=1) 80,85,80
282*      80 KUF=6
283*      GO TO 999
284*      85 CONTINUE

```

```

205* C
206* C COMPUTE AND PRINT STEADY STATE VALUES
207* C
208* W=H/(F2*XROOT(1)-E1)
209* UE=1./(F1*XROOT(1)+D2)
210* UE=UE1*XROOT(1)+C2
211* WVS=TS-Tn
212* PK4=H*(BETA*XROOT(1)*(HWS-HFW)/AVS-(HWS-HW)/AVB)/(HSS-HFW)
213* AE=PK4*AV3
214* NS=WE+ETA*XROOT(1)*W
215* WFA=NS
216* PK5=WV/(TR-TS)**3
217* HME=H*5+BETA*XROOT(1)*Ht
218* HMY=H*5+XROOT(1)*Ht
219* SV(1)=XROOT(1)
220* SV(2)=W
221* SV(3)=UE
222* SV(4)=UEM
223* SV(5)=PK4
224* SV(6)=WE
225* SV(7)=WS
226* SV(8)=PK5
227* SV(9)=HME
228* SV(10)=HMY
229* IF(IPRINT) B1.46+E1
230* B1 PRINT 86,XROOT(1)
231* B6 FORMAT(//,2BH MEAN VALUE OF STEAM QUALITY,15.5,/)
232* PRINT 90,W
233* 90 FORMAT(10H TOTAL MASS FLOW,15X,E15.5)
234* PRINT 101,UE
235* 101 FORMAT(10H OUTLET DENSITY OF STEAM-WATER,/,8H MIXTURE,23X,E15.5)
236* PRINT 102,UEM
237* 102 FORMAT(10H MEAN DENSITY OF STEAM-WATER,/,8H MIXTURE,23X,E15.5)
238* PRINT 95,PK4
239* 95 FORMAT(24H CONSTA.T OF EVAPORATION,17X,E15.5)
240* PRINT 100,WE
241* 100 FORMAT(22H EVAPORATION MASS FLOW,9X,E15.5)
242* PRINT 105,WS
243* 105 FORMAT(10H OUTLET STEAM FLOW,13X,E15.5)
244* PRINT 91,PK5
245* 91 FORMAT(31H HEAT TRANSFER COEFFICIENT FROM,/,27H RISER TUBES TO STE
246* 1AM-WATER,/,8H MIXTURE,23X,E15.5)
247* PRINT 92,HME
248* 92 FORMAT(27H OUTLET ENTHALPY OF MIXTURE,/,15H IN RISER TUBES,16X,E15
249* 1.5)
250* PRINT 103,HMY
251* 103 FORMAT(25H MEAN ENTHALPY OF MIXTURE,/,15H IN RISER TUBES,16X,E15.5
252* 1)
253* C
254* C ALL STEADY STATE VALUES KNOWN.
255* C
256* C
257* C THE ELEMENTS OF MATRIX AA IS CALCULATED
258* C
259* 46 DO 200 I=1,9
260* DO 200 J=1,17
261* 200 AA(I,J)=0.0
262* AV4=UEW=UESS

```

```

343. AV5=1.+PI*TA*AV4*X. OUT(1)/LESS
344. AV6=ALOG(AV5)
345. AV7=1./AV5
346. AV9=DEW*DEW
347. AV10=AR*ALR1*DEW
348. AV11=1.-DETA*XRCOT(1)
349. AV15=BETA*XROOT(1)*AV4
350. AA(1,1)=(AV9*AV6/(BETA*XROOT(1)*AV4*AV4)-AV9*AV7/(DESS*AV4))*PK2
351. AA(1,5)=DEW*AV7/XROOT(1)-LEW*DESS*AV6/(BETA*XROOT(1)*XROOT(1)*AV4)
352. AA(1,14)=1./(AR*ALR1)
353. AA(1,15)=-AA(1,14)
354. AA(2,6)=(((B1*W*W)/(DE*DE)-(XSI*W*W)/(2.*AV1*AV9)+ALR1)*AA(1,1)/PK
355. 12-(((FK*ALR)/LR+0.1)*(W*W*BETA*XRCOT(1))/(AV2*DESS*DESS))*PK2
356. AA(2,10)=(B1*W*W/(DE*DE)-XSI*W*W/(2.*AV1*AV9)+ALR1)*AA(1,5)+(B1*DE
357. 1M*2./DE+0.1/AV2)*W*W*U1
358. AA(2,14)=(B1*2.*DEW/DE+0.2/AV2)*W/LE
359. AA(2,15)=((1.d/.V2-XSI*DEW/(AV1*DEW))/(DEW*112.))*#
360. AA(3,17)=-1./(AR*ALR1*DEW*HE)
361. AA(3,18)=(PK3-XROOT(1)*(PK3-PK9))/LE
362. AA(3,5)=1.
363. AA(3,6)=-AA(3,17)*#*(PK3-BETA*XROOT(1)*(PK3-PK9))
364. AA(3,8)=AA(3,17)*#*PK6
365. AA(3,10)=BETA*W/AV10
366. AA(3,14)=-((1.-BETA)*XRCOT(1)/AV10
367. AA(3,15)=AA(3,17)*(HW-HMM)
368. AA(4,9)=-3.*PK5*(IR-TS)**2
369. AA(4,6)=-AA(4,9)*PK1
370. AA(4,17)=1.
371. AA(5,4)=1.
372. AA(5,11)=-1./(RMASS*PK8)
373. AA(5,17)=-AA(5,11)
374. AA(6,2)=ADR*DEW
375. AA(6,3)=MASS*PK6/HW
376. AA(6,6)=-((AV11*#*PK3-WE*PK9)/HW
377. AA(6,8)=#*PK6/HW
378. AA(6,10)=W*HWS*BETA/HW
379. AA(6,12)=-HF#/#W
380. AA(6,14)=-AV11*HWS/HW
381. AA(6,15)=1.
382. AA(6,16)=HSS/HW
383. AA(7,2)=AA(6,2)
384. AA(7,10)=#*BETA
385. AA(7,12)=-1.
386. AA(7,14)=-AV11
387. AA(7,15)=1.
388. AA(7,16)=1.
389. AA(8,1)=1.
390. AA(8,13)=1./(VS*P+2)
391. AA(8,2)=-ADR*DESS*AA(8,13)
392. AA(8,10)=-BETA*W*AA(8,13)
393. AA(8,14)=-BETA*XROOT(1)*AA(8,13)
394. AA(8,16)=-AA(8,13)
395. AA(9,6)=PK4*PK1
396. AA(9,8)=-PK4
397. AA(9,16)=1.
398. IF(IPRINT) 205,210,205
399. 205 PRINT 211
400. 211 FORMAT(2(/),10H MATRIX AA//)

```

```
401*      DO 201 I=1,9
402* 201 PRINT 202,(AA(I,J),J=1,6)
403*      PRINT 170
404* 170 FORMAT(/)
405*      DO 203 I=1,9
406* 203 PRINT 202,(AA(I,J),J=7,12)
407*      PRINT 170
408*      DO 175 I=1,9
409* 175 PRINT 202,(AA(I,J),J=13,17)
410* 202 FORMAT(6E20.8)
411* 210 CONTINUE
412* 999 RETURN
413*      END
```

APPENDIX B.

Drum System

Reasonable numerical values of the constant ζ_1, \dots, ζ_4 are used in the expressions for the coefficients.

$$a_1 = \left[\frac{\rho_w^2}{\beta x_m (\rho_w - \rho_s)^2} \ln \left(1 + \frac{\beta (\rho_w - \rho_s)}{\rho_s} x_m \right) - \frac{\rho_w^2}{\rho_s (\rho_w - \rho_s)} \cdot \frac{1}{1 + \frac{\beta (\rho_w - \rho_s)}{\rho_s} x_m} \right] k_d$$

$$a_2 = \frac{\rho_w}{x_m} \cdot \frac{1}{1 + \frac{\beta (\rho_w - \rho_s)}{\rho_s} x_m} - \frac{\rho_w \rho_s}{\beta x_m^2 (\rho_w - \rho_s)} \ln \left(1 + \frac{\beta (\rho_w - \rho_s)}{\rho_s} x_m \right)$$

$$a_3 = \frac{1}{A_r L r_1}$$

$$a_4 = -a_3$$

$$a_5 = \frac{\rho_m L r_1}{\rho A_r g}$$

$$a_6 = \frac{L d_1}{A_d g}$$

$$a_7 = (b_1 b_2 - b_3 b_4) k_d$$

where

$$b_1 = \left(f_r \frac{L_r}{D_r} + 1 \right) \frac{m_o^2}{2gA_r \rho_o^2} - \xi \frac{m_w^2}{3gA_d \rho_w^2} + L_{r1}$$

$$b_2 = a_1 / k_d$$

$$b_3 = \left(f_r \frac{L_r}{D_r} + 1 \right) \frac{m_o^2 \rho_m}{gA_r \rho_o^2} + 0.1 \frac{m_o^2}{gA_r \rho_o^2}$$

$$b_4 = \frac{\beta x m_o^2}{2 \rho_s}$$

$$a_8 = b_1 a_2 + b_3 b_5$$

where

$$b_5 = \beta \left(\frac{1}{\rho_s} - \frac{1}{\rho_w} \right) \rho^2$$

$$a_9 = \left(f_r \frac{L_r}{D_r} + 1 \right) \frac{m_o \rho_m}{gA_r \rho_o^2} + 0.2 \frac{m_o}{gA_r \rho_o}$$

$$a_{10} = b_6 + b_7$$

where

$$b_6 = 1.8 \frac{m_o}{gA_r \rho_w} - \xi \frac{m_o \rho_m}{gA_d \rho_w}$$

$$b_7 = (f_d \frac{L_d}{D_d} + 3) \frac{m_o}{gA_d \rho_w}$$

$$a_{11} = \frac{k_h - x_m (k_h - k_s)}{h_e}$$

$$a_{12} = 1$$

$$a_{13} = \frac{m_o \{k_h - \beta x_m (k_h - k_s)\}}{A_r L_r \rho_m h_e}$$

$$a_{14} = - \frac{m_o c_{pw}}{A_r L_r \rho_m h_e}$$

$$a_{15} = \frac{\beta m_o}{A_r L_r \rho_m}$$

$$a_{16} = \frac{(1-\beta)x_m}{A_r L_r \rho_m}$$

$$a_{17} = - \frac{h_w - h_m}{A_r L_r \rho_m h_e}$$

$$a_{18} = - \frac{1}{A_r L_r \rho_m h_e}$$

$$a_{19} = 3k_r (T_r - T_s)^2 k_T$$

$$a_{20} = - 3k_r (T_r - T_s)^2$$

$$a_{21} = 1$$

$$a_{22} = 1$$

$$a_{23} = - \frac{1}{M_r c_r}$$

$$a_{24} = \frac{1}{M_r c_r}$$

$$a_{25} = A \rho_w$$

$$a_{26} = \frac{M_w c_{pw}}{h_w}$$

$$a_{27} = - \frac{(1-\beta x_m) m_o k_h - m_e k_s}{h_w}$$

$$a_{28} = \frac{m_o c_{pw}}{h_w}$$

$$a_{29} = \frac{m_o h_w \beta}{h_w}$$

$$a_{30} = - \frac{h_{fw}}{h_w}$$

$$a_{31} = - \frac{(1-\beta x_m) h_w s}{h_w}$$

$$a_{41} = - \frac{\rho_s A}{V_s k_d}$$

$$a_{32} = 1$$

$$a_{42} = \frac{\beta m_o}{V_s k_d}$$

$$a_{33} = \frac{h_{ss}}{h_w}$$

$$a_{43} = \frac{1}{V_s k_d}$$

$$a_{34} = a_{25}$$

$$a_{44} = - \frac{\beta x_m}{V_s k_d}$$

$$a_{35} = m_o \beta$$

$$a_{36} = -1$$

$$a_{45} = - \frac{1}{V_s k_d}$$

$$a_{37} = - (1-\beta x_m)$$

$$a_{46} = k_e k_T$$

$$a_{38} = 1$$

$$a_{47} = - k_e$$

$$a_{39} = 1$$

$$a_{48} = 1$$

$$a_{40} = 1$$

Superheater

$$a_1 = M_{mn}^c p_m$$

$$a_2 = k_f$$

$$a_3 = \frac{0.8k_{spn}}{m_s 0.2} (T_{mn} - T_{sn})$$

$$a_4 = k_{spn} m_s^{0.8}$$

$$a_5 = -a_4$$

$$a_6 = \frac{0.8k_{spn}}{m_s} (T_{mn} - T_{sn}) - c_{psn} (T_{sn} - T_{sn-1}) + 2m_s^2 c_{Tsn} k_{p1n}$$

$$a_7 = k_{spn} m_s^{0.8}$$

$$a_8 = -k_{spn} m_s^{0.8} - m_s c_{psn}$$

$$a_9 = m_s c_{ps, n-1}$$

$$a_{10} = m_s (c_{Ts, n-1} - c_{Tsn})$$

Attemperator

Indices 1 and 2 refer to the inlet and outlet of the attemperator.

$$a_1 = m_{s2} c_{p2}$$

$$a_7 = -h_c$$

$$a_8 = 1$$

$$a_2 = m_{s2} c_{T2}$$

$$a_9 = -1$$

$$a_3 = -h_{s1}$$

$$a_{10} = 1$$

$$a_4 = -m_{s1} c_{p1}$$

$$a_{11} = 1$$

$$a_{12} = -1$$

$$a_5 = -m_{s1} c_{T1}$$

$$a_{13} = 2k_{a2} m_{s2}$$

$$a_6 = h_{s2}$$

Control Valve

Indices 1 and 2 refer to the inlet and outlet of the control valve.

$$a_1 = - \frac{k (p_{s1} - p_{s2}) A_v f'(u)}{m_s}$$

$$a_5 = - c_{Ts1}$$

$$a_2 = - \frac{k A_v^2}{2m_s}$$

$$a_6 = c_{Ts2}$$

$$a_3 = - a_2$$

$$a_7 = - c_{ps1}$$

$$a_4 = c_{ps2}$$

$$a_8 = - k p_{s1} f'(u)$$

$$a_9 = - k \frac{A_v}{v}$$

Turbine

High pressure turbine.

$$a_1 = m_s \eta_t^c \frac{p_{s1}}{T_1} - m_s \eta_t^c \frac{p_{s2}}{T_{s2}} - \frac{m_s \eta_t^c p_{s2} p_{s1}}{p_{s2}}$$

$$a_2 = - 1$$

$$a_3 = m_s \eta_t^c \frac{p_{s1}}{T_{s1}} - m_s \eta_t^c \frac{p_{s2}}{T_{s2}} + \frac{m_s \eta_t^c p_{s2}^3 C}{p_{s2}^2 C_t^2}$$

$$a_4 = h_{s1} - h_{s2} + \frac{c_{s2} C_{T_{s1}} \eta_t^c m_s^2}{p_{s2}^2 C_t^2}$$

$$a_5 = - 1$$

$$a_6 = \frac{c_{Ts1}}{c_{ps2}} - \eta_t \frac{c_{Ts1}}{c_{ps1}} + \eta_t^d \frac{c_{sp2}}{c_{ps2}} + \frac{\eta_t^c s_2^D s_1}{p_{s2}^c c_{ps2}}$$

$$a_7 = - \frac{c_{Ts2}}{c_{ps2}}$$

$$a_8 = \frac{c_{ps1}}{c_{ps2}} - \eta_t \frac{c_{ps1}}{c_{ps2}} + \eta_t^d \frac{c_{sp2}}{c_{ps2}} - \frac{\eta_t^c s_2^2 C_m^2}{2 p_{s2}^c c_{ps2} C_t^2}$$

$$a_9 = - \frac{\eta_t^c s_2^{CT} s_1^m s}{p_{s2}^c c_{ps2} C_t^2}$$

$$a_{10} = - 2p_{s1}$$

$$a_{12} = \frac{C_m^2}{C_t^2}$$

$$a_{11} = 2p_{s2}$$

$$a_{13} = \frac{2CT s_1^m s}{C_t^2}$$

Low pressure turbine.

$$a_1 = - 1$$

$$a_5 = - 1$$

$$a_2 = \eta_t^c c_{Ts1}^m s - \eta_t^c s_{p2}^d c_{Ts1}^m s$$

$$a_6 = K$$

$$a_3 = \eta_t^c c_{ps}^m s - \eta_t^c s_{p2}^d c_{ps1}^m s$$

$$a_4 = h_{s1} - h_{s2}$$

APPENDIX C

Numerical values of the matrices A, B, C and D of the linearized boiler-turbine model. The matrices are valid for 90 % of full load of the Öresundsverket power plant unit P16-G16. Steady state values of state variables are

| | |
|-------|-----------|
| x_1 | 142,5 bar |
| x_2 | 0 m |
| x_3 | 320 °C |
| x_4 | 450 °C |
| x_5 | 0.115 |
| x_6 | 480 °C |
| x_7 | 515 °C |
| x_8 | 570 °C |
| x_9 | 570 °C |

and steady state values of inputs are

| | |
|-------|---|
| u_1 | 9.55 kg/s |
| u_2 | 119.96 kg/s (equals drum outlet steam flow) |
| u_3 | 3.94 kg/s |
| u_4 | 0.84 kg/s |
| u_5 | 100 % |

MATRIX J

| | | | | |
|-----------|-----------|---------------|---------------|---------------|
| .00000000 | .00000000 | .43451546+01 | .38986706-01 | -.60159342-02 |
| .00000000 | .00000000 | -.46626365+01 | -.86010905-01 | .13272034-01 |
| .00000000 | .00000000 | -.92805266+00 | -.83269111+00 | .12849033+00 |
| .00000000 | .00000000 | -.20426576+01 | -.46613856-02 | .71927410-03 |
| .00000000 | .00000000 | -.19767113+01 | -.57444108+01 | .5522872-02 |
| .00000000 | .00000000 | .71947340-01 | -.83269108+00 | .12849033+00 |
| .00000000 | .00000000 | -.62718869+00 | -.18189851+01 | -.27677470-02 |
| .00000000 | .00000000 | .71947336-01 | .16730891+00 | .12849033+00 |
| .00000000 | .00000000 | -.46422790+00 | -.13443328+01 | .53654145-01 |
| .00000000 | .00000000 | .27153821-01 | .38931265-01 | .12354069+00 |
| .00000000 | .00000000 | -.40187908+02 | -.12278435+03 | .19134434+02 |
| .00000000 | .00000000 | -.67396999-01 | -.19506953+00 | -.13662318-02 |
| .00000000 | .00000000 | .25099963-01 | .58368355-01 | .44825880-01 |
| .00000000 | .00000000 | .85921506+02 | .19546372+03 | .16690201+03 |

APPENDIX D.

Symbols used in Chapter 4

| | |
|----------|---|
| L_d | total length of downcomer tubes [m] |
| L_{di} | length of one downcomer tube [m] |
| L_r | total length of riser tubes [m] |
| L_{ri} | length of one riser tube [m] |
| A_d | total flow area of downcomer tubes [m^2] |
| A_r | total flow area of riser tubes [m^2] |
| A_v | opening area of control valve [m^2] |
| D_d | total diameter of downcomer tubes [m] |
| D_r | total diameter of riser tubes [m] |
| M_r | mass of riser tubes [kg] |
| M_w | mass of drum liquid [kg] |
| M_m | mass of superheater tubes [kg] |
| M_s | mass of steam in superheaters [kg] |
| V_s | volume of vapor phase in drum [m^3] |
| Q_g | heat flow from gases to riser walls [kJ/s] |
| Q_r | heat flow from riser walls to steam-water mixture in riser tubes [kJ/s] |
| Q_{gm} | heat flow from gases to superheater tubes [kJ/s] |
| Q_{ms} | heat flow from superheater tubes to steam [kJ/s] |
| ρ_w | density of drum liquid [kg/m^3] |
| ρ_s | density of saturated steam [kg/m^3] |
| ρ_m | mean density of steam-water mixture in the riser tubes [kg/m^3] |
| ρ_o | density of steam-water mixture at the outlet of the risers [kg/m^3] |
| R | constant of ideal gas law |

| | |
|----------|---|
| T_w | drum liquid temperature [$^{\circ}\text{C}$] |
| T_r | riser tube temperature [$^{\circ}\text{C}$] |
| T_s | saturation temperature [$^{\circ}\text{C}$] |
| T_m | superheater tube temperature [$^{\circ}\text{C}$] |
| h_w | drum liquid enthalphy [$\text{kJ}/\text{kg}^{\circ}$] |
| h_{ws} | saturated liquid enthalpy [$\text{kJ}/\text{kg}^{\circ}$] |
| h_{ss} | saturated steam enthalpy [kJ/kg] |
| h_e | enthalpy of evaporation [kJ/kg] |
| h_{fw} | feedwater enthalpy [kJ/kg] |
| h_m | mean enthalpy of steam-water mixture in risers [kJ/kg] |
| h_s | steam enthalpy [kJ/kg] |
| h_c | coolant water enthalpy [kJ/kg] |
| h_o | enthalpy of steam-water mixture at the outlet of the risers [kJ/kg] |
| m_w | downcomer mass flow [kg/s] |
| m_o | mass flow at the outlet of risers [kg/s] |
| m_s | steam flow [kg/s] |
| m_e | evaporation mass flow [kg/s] |
| m_{fw} | feedwater flow [kg/s] |
| m_c | coolant flow in attemperator [kg/s] |
| m_f | fuel flow [kg/s] |
| p_d | drum pressure [bar] |
| p_{md} | mud drum pressure [bar] |
| p_s | steam pressure [bar] |
| P_{HT} | active power of H. P. turbine [kW] |
| P_{LT} | active power of L. P. turbine [kW] |
| c_w | downcomer flow velocity [m/s] |
| c_o | riser flow velocity at the outlet of risers [m/s] |
| s | enthropy [kJ/kg] |
| v_s | specific volume of steam [m^3/kg] |
| y | drum liquid level [m] |

z length coordinate
 x_o steam quality at the outlet of risers
 x_m mean value of steam quality

Constants

g acceleration due to gravity [m/s^2]
 k_t temperature-pressure proportional constant at saturation state
 k_d density-pressure proportional constant at saturation state
 k_h water enthalpy-pressure proportional constant at saturation state
 k_e evaporation constant
 k_r heat transfer coefficient from riser walls to steam-water mixture
 k_{p1}, k_{p2} pressure drop proportional constants
 k_{sp} heat transfer coefficient from superheater tubes to steam
 k_f proportional constant relating heat flow to fuel flow
 k_s vapor enthalpy-pressure proportional constant of saturation state
 k_v pressure drop proportional constant for valve equation
 K pressure drop proportional constant for turbine
 c_{pw} heat capacitance for drum liquid [$kJ/kg^\circ C$]
 c_r heat capacitance for riser tubes [$kJ/kg^\circ C$]
 c_m heat capacitance for superheater tubes [$kJ/kg^\circ C$]
 c_p, c_T partial derivatives of $h(p, T)$
 c_s, c_{sp} partial derivatives of $h(s, p)$
 d_p, d_T partial derivatives of $s(p, T)$
 f_d energy loss coefficient for downcomer flow
 f_r energy loss coefficient for riser flow
 ζ_i energy loss coefficient for entrance and exit losses

| | |
|----------|--|
| ξ | loss factor |
| η_t | turbine efficiency |
| C_t | constant in turbine mass flow equation |

Index

| | |
|-----|------------------------|
| c | coolant |
| d | drum or downcomer |
| e | evaporation |
| fw | feedwater |
| m | superheater material |
| md | mud drum |
| n | section number n |
| o | riser exit |
| r | riser |
| s | steam or saturated |
| t | turbine or temperature |
| v | valve |
| w | water |
| 1,2 | inlet, outlet |

